Copyright Warning & Restrictions

The copyright law of the United States (Title 17, United States Code) governs the making of photocopies or other reproductions of copyrighted material.

Under certain conditions specified in the law, libraries and archives are authorized to furnish a photocopy or other reproduction. One of these specified conditions is that the photocopy or reproduction is not to be "used for any purpose other than private study, scholarship, or research." If a, user makes a request for, or later uses, a photocopy or reproduction for purposes in excess of "fair use" that user may be liable for copyright infringement,

This institution reserves the right to refuse to accept a copying order if, in its judgment, fulfillment of the order would involve violation of copyright law.

Please Note: The author retains the copyright while the New Jersey Institute of Technology reserves the right to distribute this thesis or dissertation

Printing note: If you do not wish to print this page, then select "Pages from: first page # to: last page #" on the print dialog screen

NJIT
New Jersey's Science &
Technology University

The Van Houten library has removed some of the personal information and all signatures from the approval page and biographical sketches of theses and dissertations in order to protect the identity of NJIT graduates and faculty.

GALLIUM NITRIDE FILM DEPOSITION BY IONIZED CLUSTER BEAM EPITAXY

BY

GHULUM BAKIRI

This thesis is being submitted in partial fulfillment of the requirements, outlined by the Electrical Engineering Department, to the faculty of New Jersey Institute of Technology for the degree of Master of Science in Electrical Engineering, 1983.

APPROVAL SHEET

Title of Thesis: Gallium Nitride Film Deposition by Ionized Cluster Beam Epitaxy

Name of Candidate: Ghulum Bakiri

Master of Science in Electrical Engineering, 1983

Thesis and Abstract Approved:

Dr. Roy Cornely
Associate Professor
Dept. of Electrical Engineering

Dr. Lawrence Suchow
Professor
Dept. of Chemical Engineering and Chemistry

Dr. Warren H. Ball
Associate Chairman
Dept. of Electrical Engineering

VITA

Name: GHULUM BAKIRI

Degree and date to be conferred : M.S.E.E. 1983

Collegiate Institute Attended:	Date	Degree	Dates of Degree
N. J. Institute of Technology	82-83	M.S.E.E.	1983
University of Texas, Austin	75-76	B.S.E.E.	1976
American University of Beirut	71-74	--	--

Position Held: Senior Application Engineer,

Worthington Group Int'l.

P. O. Box 5893

MANAMA,

BAHRAIN.

ABSTRACT

Title of Thesis: Gallium Nitride Film Deposition by Ionized Cluster Beam Epitaxy

Ghulum Bakiri, Master of Science in Electrical Engineering, 1982.

Thesis Directed by: Roy H. Cornely, Associate Professor of Electrical Engineering.

An experimental Ionized Cluster Beam System similar in design to the one developed at Kyoto University in Japan was designed and constructed in the Microelectronics Laboratory at NJIT. This involved making the working drawings, having the parts machined and then assembling the system in a vacuum system together with the necessary variable power supplies, meters, controls, gas inlets, cooling water connections, etc.

Eleven deposition runs were then attempted to grow gallium nitride utilizing the system constructed. In a typical deposition run, gallium was vaporized from a boron nitride crucible at $1000^{o}C$ and allowed to expand through a 0.5mm nozzle into a low pressure region containing nitrogen at $1\text{-}5 \times 10^{-4}$ torr in order to form clusters of about 1000 atoms each. The gallium clusters were ionized by an electron source (300 mA) and deposited on heated quartz substrates ($550^{o}C$) for reactive growth with nitrogen.

For the above deposition conditions, the film growth rate was only 1 Å/min and the films were highly insulating. Photoluminescence measurements and surface analysis of the grown films revealed boron contaimination which was then traced to water vapor contamination of the boron nitride crucible and heater. The water vapor, if not driven out by pre-heating the crucible in an oven, caused the boron nitride to decompose at elevated temperatures introducing reactive contaminants at the substrate surface. Further experiments showed that for GaN

deposition rates greater than 1 Å/min (and up to 1 Å/sec) the crucible temperature should be at least 1100°C but preferably around 1400°C.

Blank Page

A C K N O W L E D G E M E N T

I wish to express my sincere appreciation to all those who contributed to the work culminating in the writing of this thesis. Special thanks are due to Dr. Roy Cornely for a great deal of his time spent in reviewing my work and for his most valuable suggestions which resulted in many important improvements in this thesis. Sincere gratitude is also due to Dr. Lawrence Suchow for his advice.

I must express my indebtedness to Dr. Jack Pankove of RCA Laboratories (Princeton) for performing/supervising many of the tests and measurements on the deposited films and for many enlightening conversations. Similar gratitude is also due to Mr. Tony Emmanuele the NJIT machine shop supervisor, for his full cooperation in making the necessary parts for the ICB system.

I am also grateful to my fellow students Chetan Mehta, Fred Solomon, Young Shin Pyun and many other students whose help made this work possible.

Finally, I must thank my sister, Sharifa, for her patience in typing and retyping of material as necessitated by corrections and changes.

TO MY WIFE

TABLE OF CONTENTS

CHAPTER		PAGE
ACKNOWLEDGEMENT		i
I.	INTRODUCTION	1
	1.1 About This Work	5
II.	I C B DEPOSITION	7
	2.1 General Overview	7
	2.2 Cluster Formation Mechanism	9
	- Simple View	9
	- Representative Curve of the Expansion	10
	- Simple Classical Formation	11
	- Nucleation Region	13
	- Growth Region	14
	2.3 Effects of the Expansion Parameters on Cluster Formation	16
	- Variation of Nozzle Diameter	16
	- Effects of Source Pressure and Temperature	17
	2.4 Size Distribution of the Clusters	18
	2.5 Deposition Rate	18
	- Nozzle Diameter	18
	- Crucible Temperature	20
	- Chamber Pressure	20

2.6 Ionizing the Clusters: 22

- The Electron Current for Ionization, I_e. 22
- Electron Accelerating Voltage, V_e 22
- The Cluster Cross Section for Ionization 24

2.7 Accelerating the Clusters and Energy Distribution 26

2.8 Film Growth Mechanism 27

2.9 Effects of Kinetic Energy 29

- Sputtering and Implantation Effects 29
- Thermal Effects 31
- Migration Effects 31

2.10 Effects of Presence of Ions 33

2.11 Effect on Substrate Temperature Required for Epitaxial Growth 35

III. CONSTRUCTION OF THE ICB SYSTEM 38

3.1 Complete System 38

3.2 The Nozzle Assembly 40

3.3 The Ionization Assembly 43

3.4 The accelerating Electrode and the Substrate Holder 45

3.5 Electrical (Power Supplies and Meters) 47

3.6 Accessories 47

- Substrate Heater 47

- Temperature Sensors 50

- Power Inlet (Vacuum Leadthrough) Terminals 50

- Nitrogen Gas Supply 50

- Cooling Water Inlet / Outlet 52

3.7 Setting the Electron Current for Ionization 52

3.8 Typical Start Up Procedure 55

3.9 Typical Shut Down Procedure 56

3.10 Practical Difficulties 57

IV. GROWTH OF GaN FILMS BY RICBD 60

A. Gallium Nitride:- 60

4.1 Why Choose GaN? 60

4.2 Material Synthesis 61

4.3 GaN by R-ICB Deposition 62

4.4 Important Properties of GaN Films 62

- Electroluminescence 63

B. Experimental Details:- 66

4.5 Introduction 66

4.6 Run No. 1 67

4.7 Run No. 2 68

4.8 Run No. 3 70

4.9 Run No. 4 71

4.10 Run No. 5 72

4.11 Run No. 6 72

4.12 Potential Problems 78

4.13 Solution Employed 78

- Low Substrate Temperature 79
- Residual Oxygen in the Vacuum Chamber 79
  1. Small Leaks 79
  2. Oxygen Contamination from the Nitrogen Tank 81
  3. Insufficient Pumpdown and Outgassing 81

4.14 Start-Up Procedure Adopted for Runs No. 7 Onwards 81

A. System Preparation 81

B. Start Up Procedure 82

4.15 Shut Down Procedure Adopted for Run No. 7 Onwards 85

4.16 Runs No. 7 and 8 86

4.17 Run No. 9 87

4.18 Run No. 10 88

4.19 Run No. 11 90

4.20 Conclusions and Suggestions for Further Work 91

A. With Regard to the ICBD System

B. With Regard to the Deposition of GaN Films By R-ICBD 92

C. The Contamination Problem 95

D. Final Remarks 96

V. APPENDICES 98

Appendix A 98

Appendix B 112

VI. REFERENCES 115

LIST OF FIGURES

FIGURES

1.1 Schematic diagram of the ICB system used by Takagi Research Group.

2.1 Conceptual illustration of the ICB system.

2.2 Representative curve of the "expansion with condensation" in the log P - log T diagram.

2.3 Size distribution of the clusters at the end of the nucleation region (before their growth).

2.4 Size distribution of Ag clusters deposited at P_o = 1 Torr for 30 seconds.

2.5 Dependence of the deposition rate of silicon on the crucible temperature.

2.6 Conceptual schematic diagram of the ionization part of the ICB system.

2.7 Dependence of the ion current collected at the substrate on the ionization voltage, V_e, and the ionization current, I_e.

2.8 Film formation process by the ICBD technique.

2.9 Adhesion strength of Cu films deposited on glass as a function of acceleration voltages.

2.10 a. Set up for investigating the migration effects.

LIST OF FIGURES (CONTINUED)

FIGURES

2.10 b. Electron micrographs of films form by migrated deposits.

2.11 RHEED patterns showing the influence of the electron current for ionization, I_e, on the crystallinity of ZnO films deposited by the R-ICBD technique.
(a) $I_e = 0$, (b) $I_e = 150$ mA, (c) $I_e = 300$ mA.

2.12 Mass deposited vs. reciprocal substrate temperature, and the change of transition temperature for different acceleration voltages.

3.1 General Assembly drawing of the ICB system.

3.2 Detailed section of the nozzle assembly.

3.3 Drawing of the crucible supported inside the crucible heater.

3.4 Top and side view of the ionization assembly of the ICB system.

3.5 Three dimensional view of the Anode of the Ionization Assembly.

3.6 Complete Electrical Wiring Diagram of the ICB system(Superimposed on the outline of the system for easier identification).

LIST OF FIGURES (CONTINUED)

FIGURES

3.7 Substrate heating arrangement used in runs No. 2 through No.6 .

3.8 Type 6D (Edward Scientific) vacuum leadthrough used for supplying power to the ICB system.

3.9 a. Output characteristics (voltage versus output current) for the power supply used for V_e.
b. Typical I_e versus V_e characteristics for the ICB system for different values of filament voltage, V_F.

4.1 Structure of the GaN, MIS LED (Metal - Insulator - Semiconductor Light Emitting Diode).

4.2 a. Fowler - Nordheim - like plot of the I-V characteristics for a typical Zn-doped GaN diode with the metal (m) biased positively.
b. Band diagram for the GaN diode under the m-positive bias condition.

4.3 Section of the crucible inside the crucible heater showing the accumulation of gallium metal after the first deposition run.

4.4 Photoluminescence spectra of various samples of GaN at room temperature.

LIST OF FIGURES (CONTINUED)

FIGURES

4.5 Photoluminescence spectra of various samples of GaN at liquid Nitrogen temperature.

4.6 Photoluminescence spectra of the quartz substrates at liquid Nitrogen temperature.

4.7 Structure of the substrate heater used for runs No. 7 onwards.

4.8 Mounting arrangement of the substrate and the substrate heater on the substrate holder.

4.9 Vapour Pressure chart of selected metals vs. temperature.

A.1 Machine shop drawing of the system base.

A.2 Machine shop drawing of the Nozzle Assembly Baseplate.

A.3 Machine shop drawing of the Heat Shield.

A.4 Machine shop drawing of the Nozzle Assembly Top Plate.

A.5 Machine shop drawing of the Ionization Assembly Baseplate.

A.6 Machine shop drawing of the Anode Upper Plate.

A.7 Machine shop drawing of the Anode lower Plate.

LIST OF FIGURES (CONTINUED)

FIGURES

A.8 Machine shop drawing of the Anode holder, the substrate holder and the acceleration electrode.

A.9 Machine shop drawing of the Crucible Heater.

A.10 Machine shop drawing of the Crucible.

A.11 Machine shop drawing of the rotating plate of the rotating substrate holder.

A.12 Machine shop drawing of the stationary plate of the rotating substrate holder.

A.13 Machine shop drawing of the parts for the shield (shutter).

B.1 Internal wiring diagram for the DC variable power supply used for V_e.

B.2 Internal wiring diagram for the DC variable, high voltage power supply used for V_a.

CHAPTER I

I N T R O D U C T I O N

Ionized cluster beam deposition (ICBD),first reported by T. Takagi et. al. of Kyoto University in 1972, is now emerging from laboratory development and is promising to become an important competing technique for the fabrication of various kinds of solid state devices and materials[936,37,51)]. It combines a relatively high deposition rate with several additional advantages over conventional vacuum deposition methods such as molecular beam epitaxy, thermal evaporation, the various sputtering techniques (magnetron, triode, diode) and alternative ion transport methods[40,57].

A schematic diagram of the system used in Takagi's experiments is shown in fig. 1.1. For ICB epitaxy, metal or semiconductor material to be deposited is placed in a confined crucible and heated to a high temperature so that an optimum pressure (usually between 0.01 and several torr) is maintained in the crucible. Vapour is ejected from the crucible through a small nozzle into a high vacuum chamber (pressure usually in the 10^{-6} range). As the temperature of the expanding vapour is reduced due to the adiabatic expansion, a point of supersaturation is reached, condensation occurs, and clusters are formed. Clusters are groups of 500 - 2000 atoms, loosely coupled together by

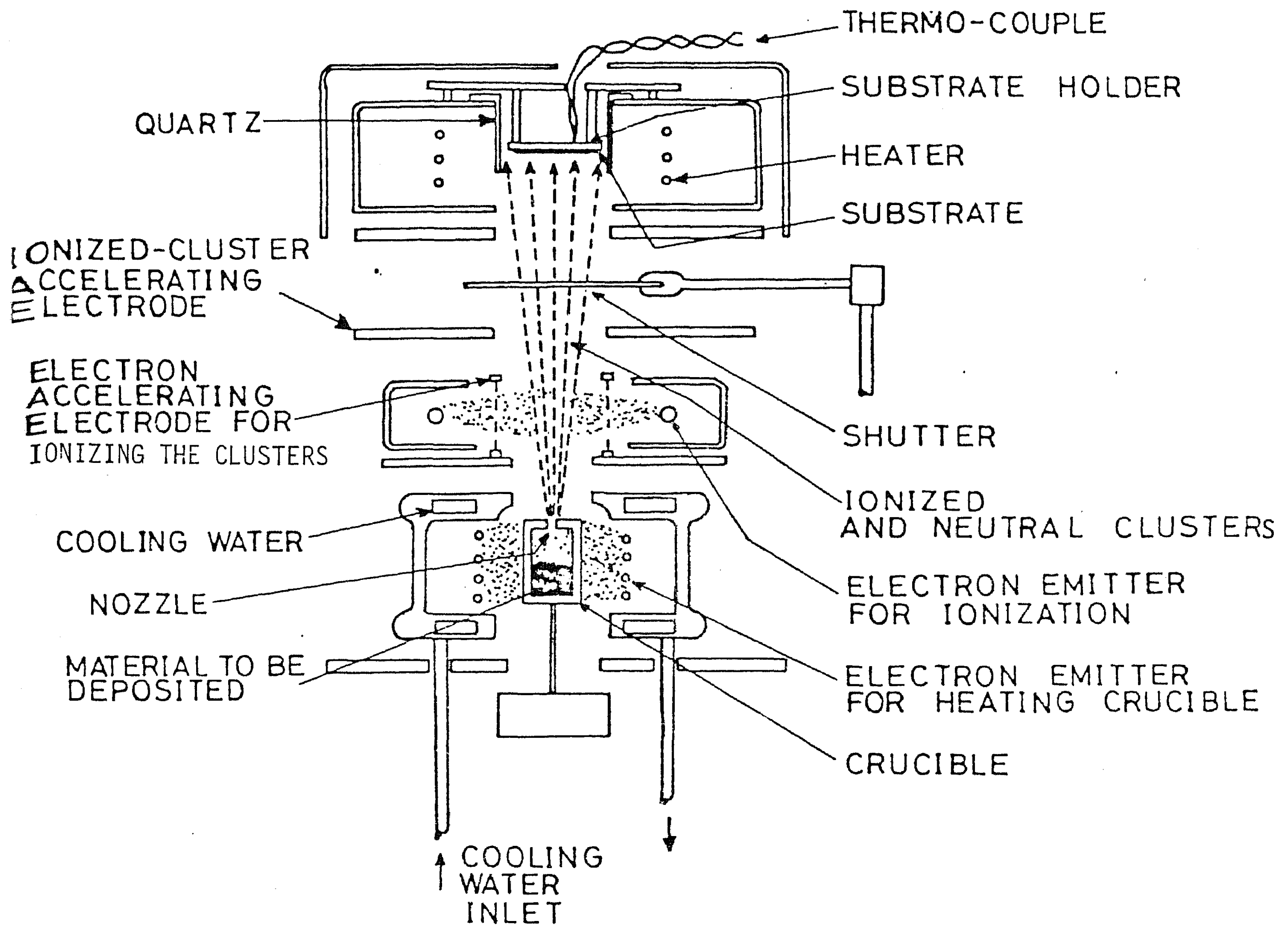

fig. 1.1 Schematic diagram of the ICB system used by Takagi Research Group.(41,46)

weak van der Waals forces. The clusters are ionized by electron impact in the ionization section located above the crucible. The cluster ions are accelerated toward the substrate by a high negative potential applied to the accelerating electrode. Ionized clusters typically comprise a few % to 40% of the total flux arriving at the substrate, the rest being neutral clusters which move toward the substrate by their ejection velocity alone.

In the reactive ion cluster beam deposition (R-ICBD), the same technique described above is used, and in addition a reactive gas is supplied from a gas nozzle through a controlled leak valve to maintain the desired gas pressure in the chamber (usually 10^{-4} to 10^{-5} torr). Some of the gas molecules are ionized along with the clusters, and are accelerated toward the substrate, where neutral and ionized gas atoms react with neutral and ionized particles of the vaporized metal clusters to form the desired compound film.

One important advantage of ICBD is the enhancement of surface migration of adatoms on the substrate surface during film formation, as the kinetic energy of the impinging clusters are converted to lateral movement of the individual atoms of the broken up clusters. Also, as the ionized cluster beam has an extremely small charge to mass ratio (e/m), problems due to the space charge effects in high current beam transportation (with a low voltage) and

problems encountered in depositing onto an insulating substrate can be eliminated. A third advantage is the controllability of the ICBD technique, where the dependence of the film properties on the ionization content (ratio), the acceleration voltage, source material temperature, and substrate temperature allows the optimization of deposition and enhancing the properties of the deposited film. There are also inherent advantages in the presence of even a small percentage of ions in the system, not only for accelerating these ions by the application of an electric field, but also to influence the critical parameters of initial film formation such as nucleation, coalescence, removing (scrubbing) of adsorbed impurities from the substrate surface, and chemical reactivity.

A large number of elemental and compound films deposited by the ICB process have been demonstrated. Examples have included metals such as Cu, Au, Ag, and Pb, and oxides such as BeO, PbO, and ZnO [55]. Crystallographic structures and physical characteristics of these films, such as adhesion strength, density, thin layer continuity, and absence of contaminants, have been extraordinary. Very important applications of the ICB technique involve active semiconductor films. It has been shown that undoped and doped crystalline silicon films can be grown epitaxially on silicon substrates at substrate temperatures as low as 620°C.

Thermally-stable amorphous silicon-hydrogen alloy semiconductor films suitable for solar cell use have been achieved. Compound semiconductor films such as CdTe, GaAs, GaP, GaN, and ZnS with excellent physical, optical and electrical characteristics have been deposited. Reference 55 includes a summary table listing the various films deposited so far by ICBD or by R-ICBD along with references which the reader may consult for further details of the results obtained in each case.

1.1 About This Work:-

The work reported in this thesis was carried out in two steps:-

1. The first step was to design and construct an experimental ICB system in the Microelectronics Laboratory at NJIT. This was done by the writer with the help of Fred Solomon and Chetan Mehta, two undergraduate E.E. students at NJIT.

Chapters II and III deal with this part of the work. Chapter II discusses the ionized cluster beam deposition method from the theoretical standpoint. The discussion includes cluster formation mechanism and the effects that varying the expansion parameters have on cluster formation. Characteristics of the ionized cluster beam, film formation mechanism, and the effects of the various control parameters on the properties of films obtained by the ICBD technique are also discussed.

Chapter III is devoted to a detailed description of the ICB system constructed at NJIT.

2. The next step was to use the ICB system thus constructed for GaN film deposition. Eleven deposition runs were attempted. The results obtained in each of these runs are described in chapter IV along with details of the experimental procedure followed in these runs.

Chapter IV also deals briefly with gallium nitride material including material synthesis by chemical vapour transport methods and by the R-ICB technique, GaN optical properties and the structure of GaN light-emitting diodes. Conclusions and suggestions for future work are the subject of the last section of chapter IV (section 4.20).

CHAPTER II

I.C.B. DEPOSITION

2.1 General Overview

The Ion Cluster Beam (ICB) technique is a superior method for the deposition of thin films which offers controls over fundamental characteristics of film growth not possible by conventional thin-film production processes. The basic ICB deposition process is suggested in fig. 2.1 . Material to be deposited is vaporized from a confinement crucible at high temperatures into a high-vacuum chamber. Crucible nozzle configuration and operating temperatures are such that the emerging vapour undergoes supercondensation following adiabatic expansion through the nozzle, and atomic aggregate clusters, each of about 500 to 2000 loosely coupled atoms, are formed. A fraction of the clusters are then caused to become singly charged by electron impact ionization and these positively charged clusters can be accelerated toward the substrate by a high negative potential. Both neutral and ionized clusters contribute to film growth. Clusters arriving at the growth surface are broken up into individual atoms upon impact. Energy per atom is small in the case of the neutral clusters but averages eV_a/N for the ionized clusters of N atoms accelerated through potential V_a. In this chapter, cluster formation and growth will be investigated theoritically together with the characteristics of the ionized cluster beam. Film formation mechanism by the ICB deposition is then discussed taking into

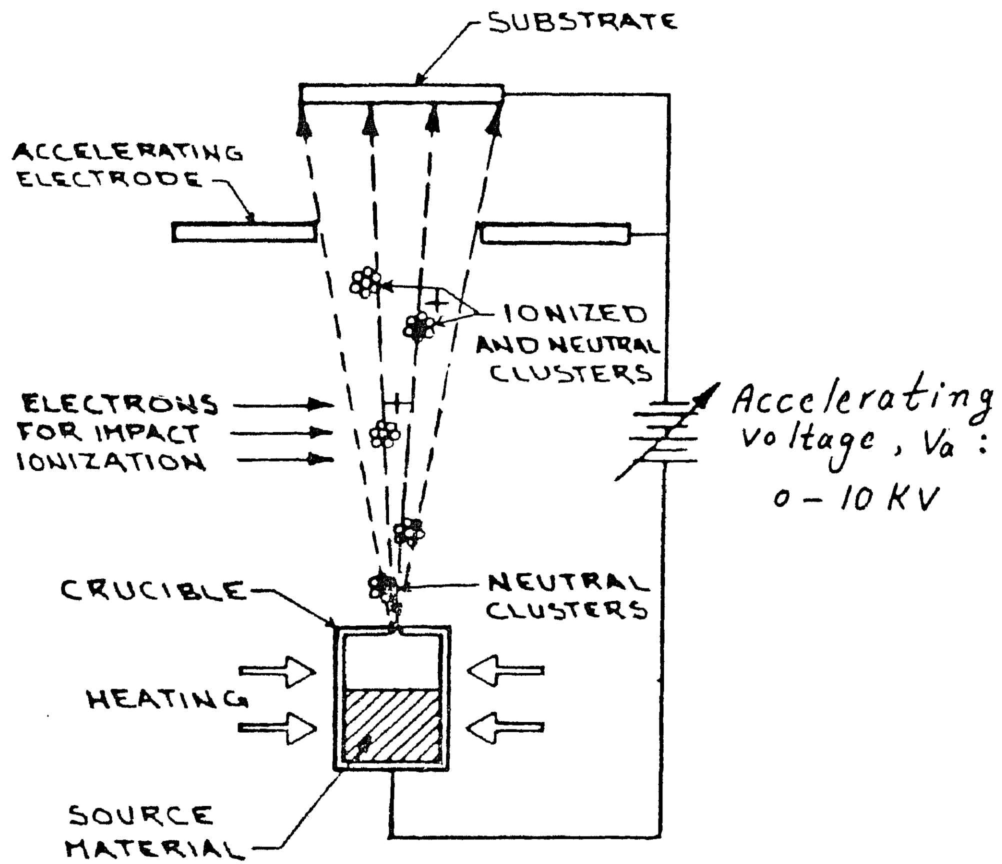

fig. 2.1 Conceptual illustration of the ICB system.

account the effects of the kinetic energy and the presence of ions for film formation. Experimental results already published are cited, where appropriate, to support the theoritical discussion.

2.2 Cluster Formation Mechanism

Simple View [52]

When a gas leaves a source (Temperature T_o, Pressure P_o) and expands into a vacuum chamber (Pressure P_1 in the beam), its temperature, with the assumption of adiabatic expansion, drops to a value T_1 given by the relation: [3,14]

$$\frac{T_1}{T_o} = \frac{P_1}{P_o}^{(\gamma-1)/\gamma} \quad \dots\dots\dots\dots \quad (1)$$

where γ is the ratio between specific heats at constant pressure and constant volume:

$$\gamma = \frac{C_p}{C_v} = 1 + \frac{2}{f} \quad \dots\dots\dots\dots \quad (2)$$

f is the number of degrees of freedom of one molecule of the gas. ($\gamma = \frac{5}{3}$ for monoatomic gases). From (1) it is seen that if the aperture between the source and vacuum chamber is small enough to allow a pressure ratio, P_1/P_o, of the order of 10^{-3} or less, the temperature ratio, T_1/T_o, will be of the order of 10^{-1} or less. If we start from the vapour of a metal just above its boiling point, i.e. $T_o = T_{boiling}$, it is clear that $T_1 = 10^{-1} \times T_{boiling}$ will carry the vapour to a supersaturated state. The jet expansion then becomes an efficient process for nucleating clusters. Once the critical nuclei have been produced, they continue to grow as long as the pressure of their surrounding

gas (vapour) remains high enough for frequent collisions to occur. In practice, this applies along the first few millimeters away from the nozzle source. Further downstream, the pressure would have dropped close to the high vacuum range (10^{-4} to 10^{-7} torr), at which point there are virtually no further collisions between the clusters formed and the vapour molecules, so the clusters keep their sizes constant.

A more "in depth" description of the condensation and clustering process can be given by carrying the analogy even further between metal vapour expansion into a high vacuum chamber and the expansion of a gas in a free jet. The description also requires the use of the classical theory of nucleation and condensation in the supersaturated state.

Representative curve of the expansion

Assuming the gas(vapour) leaves the source, passing through a nozzle of diameter D, then expands as a free jet into a vacuum chamber where there is a pressure P_1, we may consider this expansion to be adiabatic and isentropic[8]. For a perfect gas, it is then possible to calculate the Mach number, M, numerically for every point of the jet[33]. In particular, along the axis, one obtains the function $M = f(x/D)$, where x is the distance from the point on the axis to the orifice[21].

The temperature and pressure are then given by[2]:-

$$T = T_o . \left[1 + \frac{1}{2} (\gamma - 1) M^2 \right]^{-1}$$

$$P = P_o . (T/T_o)^{\gamma/(\gamma - 1)}$$

$$= P_o . \left[1 - \frac{1}{2} (\gamma - 1) M^2 \right]^{- \gamma/(\gamma - 1)}$$

from which we can write

$$\log P - \log P_o = [\gamma/(\gamma-1)] (\log T - \log T_o),$$

which is a straight line with constant slope as shown in fig. 2.2 . If the expansion starts at point A (P_o , T_o), it will follow the line marked isentrope as far as point B where the isentrope meets the coexistence curve, xy, of the two phases. If there were equilibrium between the phases, the expansion would continue following BY. However, if the density is high enough beyond point B (as is the case normally when $\frac{P_o}{P_1}$ is larger than 10^3), the expansion will continue along the so called "dry isentrope", BZ, into regions where the gas is in a supersaturated state. The saturation ratio, $S = \frac{P}{P_e}$, where P_e is the equilibrium solid vapour pressure at the temperature under consideration, rises from unity at point B, to a maximum value of S_D at point D, where the presence of clusters in the gas becomes noticeable. Further along the curve, the effect of condensation is to draw the representative point of the expansion towards the equilibrium curve.

<u>Simple Classical Formulation</u> (8)

According to the classical theory of nucleation (1) a cluster, which is assumed to be spherical, is in equilibrium with its vapour if it has a critical radius r^*, and contains n^* number of molecules given by:-

$$r^* = 2\, Q\, V/KT \log S$$

$$n^* = 4\, \pi\, r^{*3}/3V$$

where K = the Boltzmann constant, Q = the surface tension,

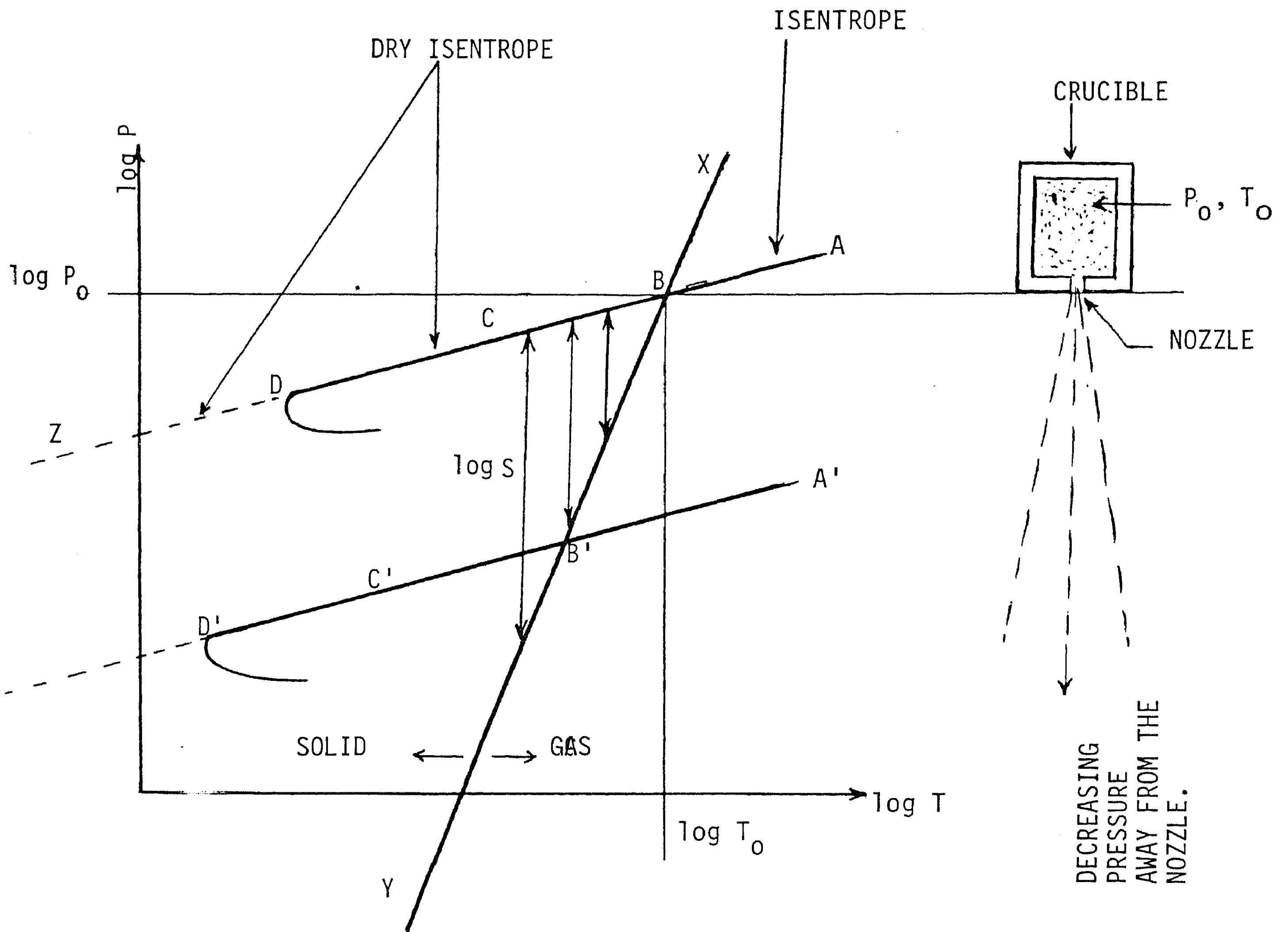

fig. 2.2 Representative curve of the " Expansion with Condensation" in the log P - log T diagram.[8]

V = the average volume of one molecule in the cluster, T = the vapour temperature, and S = the saturation ratio defined earlier. Clusters of smaller size than critical are unstable and tend to break up and diminish in radius. On the other hand, a cluster of the critical radius will continue to grow very rapidly if it receives additional molecules through collisions.

A cluster of size n (i.e. having n molecules, where n can be less than or equal to n*, the critical size) can come into existence simply as a result of density fluctuations in the vapour though its free energy of formation ΔG_n is positive and rises with n. Assuming that the probability of finding a cluster of n molecules is proportional to the Boltzmann factor $\exp(-\Delta G_n/KT)$, we see that the number, N_{n*}, of clusters per cm^3 which reach the critical size rises rapidly as n* gets smaller, which occurs when the saturation ratio rises:

$$(S\uparrow \longrightarrow r^*\downarrow \longrightarrow n^*\downarrow \longrightarrow \Delta G_{n*}\downarrow)$$

The nucleation rate, J, represents the number of clusters which pass the critical size per cm^3 per second. J is proportional to N_{n*}. Therefore it is apparant that the nucleation rate rises extremely rapidly with S, the saturation ratio.

Nucleation Region

Starting from point A (fig. 2.2), the gas expands following the line BZ as described earlier. Beyond point B, S continues to rise; the critical size gets smaller and the nucleation rate starts to increase. A point is reached (C in fig. 2.2) where J is sufficiently large that it becomes

probable for a critical nucleus to be formed within a small volume (of the order of D^3 around the axis) during the characteristic time of the expansion. Once formed, the critical nuclei continue to grow at the expense of the surrounding vapour molecules. Point C then can be considered as the onset of nucleation. Beyond that point, the nucleation rate rises extremely rapidly. This continues until the amount of vapour condensed in the jet is no longer negligible as a fraction of the total (point D). At this point, the rate of nucleation reaches its maximum value. If it were possible to measure the number of clusters as a function of their size at point D, one would find a rapidly decreasing function as shown in fig. 2.3 . The largest clusters are less numerous since they were formed further upstream where the nucleation rate is smaller.

Growth Region

Downstream from D, the condensation of the gas causes the pressure to drop, while the temperature remains roughly constant and then rises as result of the release of the latent heat of vaporization. The saturation ratio diminishes and with it the nucleation rate. The production of critical nuclei ceases fairly quickly but the condensation continues allowing the clusters already formed to continue to grow until they reach the high-vacuum regions where the gas density is low and collisions are minimal.

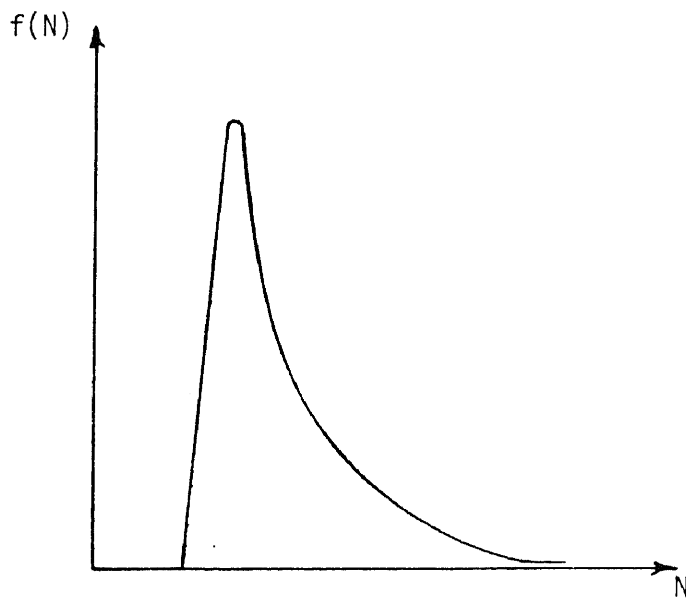

fig. 2.3 Size distribution of the clusters at the end of the nucleation region (before their growth).[8]

2.3 Effects of the Expansion Parameters on Cluster Formation [11]

Although the classical theory of homogeneous nucleation is not quantitatively applicable to small clusters[55], it is possible to use the theory to understand qualitatively the effects that varying the expansion parameters will have on the clusters.

Variation of Nozzle Diameter

A reduction in the nozzle diameter results in increasing the speed of the expanding vapour, and hence the gas stays a shorter time in the nucleation and growth regions. The shorter time for growth means that the clusters formed will be smaller. Therefore a reduction of the diameter of the nozzle causes a reduction in the size of the clusters formed. In ICB experiments reported by T. Takagi group[56,52,44], nozzle diameters of up to 2 mm were shown to be adequate for cluster formation with 2 mm being the most effective. For larger nozzle sizes the intensity of the cluster beam starts to drop until it completely disappears with nozzle diameters greater than 5 mm. This is due to the pressure difference between the inside and the outside of the crucible being insufficient. Under these conditions, the vapour consists of atoms, molecules and/or small clusters comprising several atoms instead of larger clusters[55].

Effect of Source Pressure and Temperature

In considering the effect of source pressure and temperature on cluster formation, one cannot continue using the analogy between free gas expansion and metal vapour expansion, because in the case of the free gas both T_o and P_o are usually controlled independently, while in the case of metal evaporation, the source usually contains metal vapour at pressure P_o in equilibrium with the solid, so P_o and T_o are related. This means that in fig. 2.2, our starting point (P_o , T_o) is not point A, but rather point B. For the expansion of gas in a free jet, the effect of an increase in T_o opposes and in effect balances the effects of an increase in P_o [11]. Since an increase in P_o is almost always achieved by increasing T_o in ICB experiments, one would expect no dependence of cluster size (and hence energy) on P_o. There is however the requirement that P_o (and hence T_o) be high enough to produce a high saturation ratio as discussed earlier. In practice, it is found that $P_o = 10^3 \cdot P_{chamber}$ is sufficient for cluster formation. In Takagi's experiments, it was found that there is an optimum pressure $P_{o,opt}$ for each nozzle diameter D, that resulted in the highest intensity of the cluster beam. Taking the values of $P_{o,opt}$ for different nozzle diameters, D, the product $P_{o,opt} \cdot D$ was approximately constant. Since the mean free path, λ, is inversely proportional to P_o, we conclude that D/λ is constant.

This means that the intensity of the cluster beam is maximum for a specific ratio of (D/λ) which depends on the other parameters of the system.

2.4 Size Distribution of the Clusters

Fig. 2.3 for the size distribution of clusters at point D (beginning of the growth region) undergoes a change as the clusters pass through the growth region. Larger clusters grow faster than smaller ones because of their larger capture cross section[8]. This has the effect of broadening the distribution curve, which will then correspond more closely to the curves obtained in ICB experiments as shown in fig. 2.4 . The average diameter of clusters ranges from 50 Å[56] to 150 Å[52], and the size between 500 to 2000 atoms[55].

2.5 Deposition Rate:-

The deposition rate in the ICB system is primarily dependent on the source nozzle diameter, the vapour pressure inside the crucible (P_o) and the pressure outside the crucible ($P_{chamber}$).

Nozzle Diameter

The deposition rate is proportional to the area of the nozzle opening, which for a circular hole is proportional to the square of the nozzle diameter. If, for example, a deposition rate of 0.4 Å /sec is obtainable at certain conditions with a 1 mm diameter nozzle*, the deposition rate can

* See page 20.

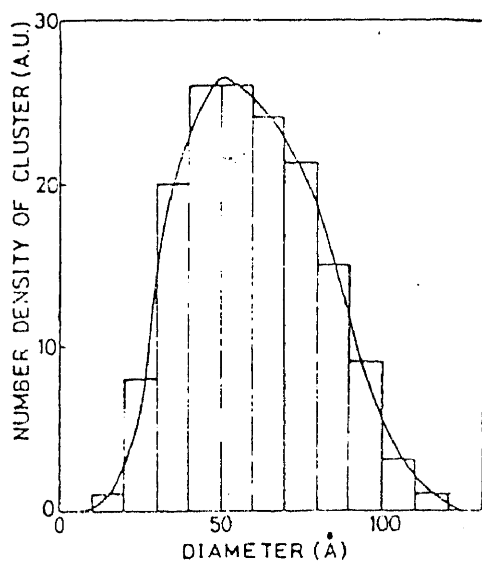

Fig. 2.4 Size distribution of Ag clusters deposited at P_o = 1 torr for 30 seconds. (56)

be increased to about 1Å /sec* by increasing the nozzle diameter to 1.5 mm.

Crucible Temperature:-

This determines the vapour pressure inside the crucible, P_o, and must be made high enough to achieve a pressure ratio, $P_o/P_{chamber}$, of at least $10^4 - 10^5$ to achieve satisfactory deposition rates.

Fig. 2.5 shows the relation between the deposition rate and the source (crucible) temperature for silicon deposition using a 1.5 mm diameter nozzle and a chamber pressure in the 10^{-7} torr range. A "threshold" temperature of about 1900°C is observed below which the deposition rate is rather low, but it increases rapidly beyond this threshold temperature.

Chamber Pressure:-

Increasing the chamber pressure has the same effect on the deposition rate as lowering the crucible temperature, and vice versa.

---

*These values are typical for silicon deposition using a crucible temperature of about 2050°C (corresponding to a vapour pressure in the crucible of 1 torr) and a chamber pressure of 10^{-7} torr (Source: Nova, Corp. Boston, Mass. Private Communication with Mr. Allen Kirkpatrick.)

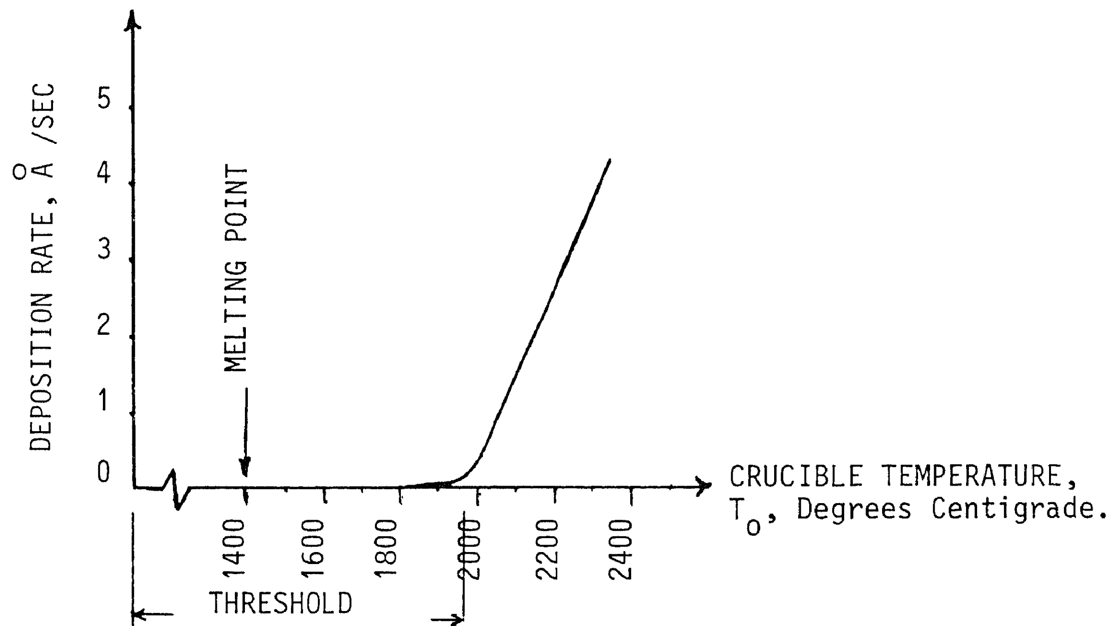

fig. 2.5 Dependence of the deposition rate of silicon on the crucible temperature.

2.6 Ionizing the Clusters

A proportion of the cluster flux is ionized by crossing it with an electron beam as shown schematically in fig. 2.6. The mechanism of ionization is by elctron bombardment, which knock off electrons from the cluster, rather than by electron capture, so the ionized clusters are expected to have a positive charge.

The ionization ratio (ratio of the ionized clusters' flux to the total flux) depends on: (1) the electron current for ionization, I_e; (2) the voltage applied to accelerate the electrons, V_e; and (3) the cluster cross section for ionization.

The Electron Current for Ionization, I_e

The ionization ratio can be increased from zero to about 50% by increasing the electron current for ionization from zero to 500 mA.[38,55]

I_e can be increased by increasing the current through the electron emitter (filament), thereby increasing its temperature. This can be achieved by increasing V_F. I_e can also be increased by increasing the electron accelerating voltage V_e.

Electron Accelerating Voltage, V_e

V_e must be high enough to accelerate the electrons to energies well above the ionization energy of the clusters. This is necessary to insure that a cluster will be ionized

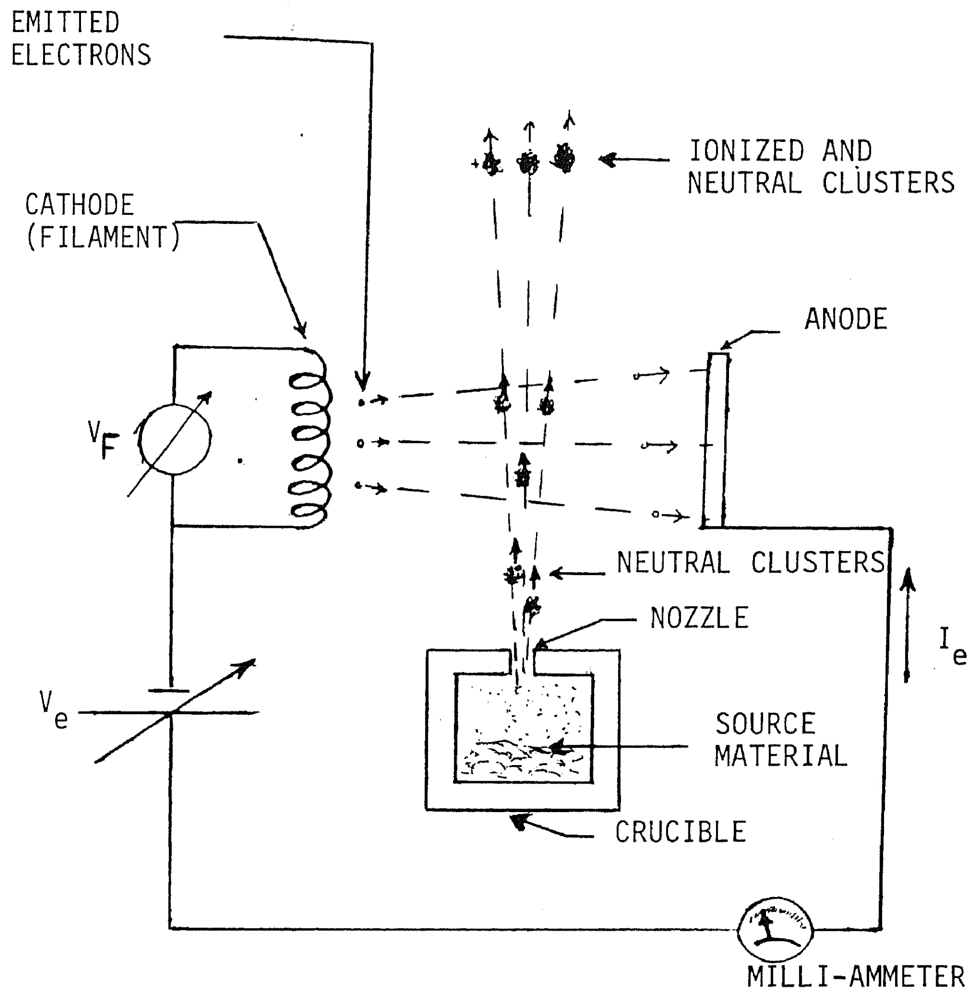

fig. 2.6 Conceptual schematic diagram of the ionization part of the ICB system.

once it is in the path of an accelerated electron.

Fig. 2.7 shows the dependence of ion current collected at the substrate as a function of ionization voltage, V_e, and ionization current, I_e[49]. The figure shows that a minimum voltage of approximately 50 volts is typically required for accelerating the electrons, and that an accelerating voltage of 100 volts is an optimum value at which the ion current (and therefore the ionization ratio) is maximum.

The Cluster Cross Section for Ionization

The cross section for ionization is a function of both cluster size (radius) and its ionization energy (i.e., the energy required to free an electron). A smaller ionization energy and a larger cluster radius result in a larger ionization cross section. The ionization energy of a cluster is somewhat lower than the ionization energy of its individual atoms and is usually in the range 5 - 10 eV [49]. The radius of a cluster is obviously much larger than that of an individual atom. Therefore the clusters have a much larger cross section for ionization, which make them much easier to ionize compared to individual atoms. This is an advantage compared to ion plating deposition technology.

The ionized clusters are invariably singly charged for two reasons:-

(1) The probability of multiple electron impact with the same cluster is very low.

(2) The cluster atoms are only weakly bound together by

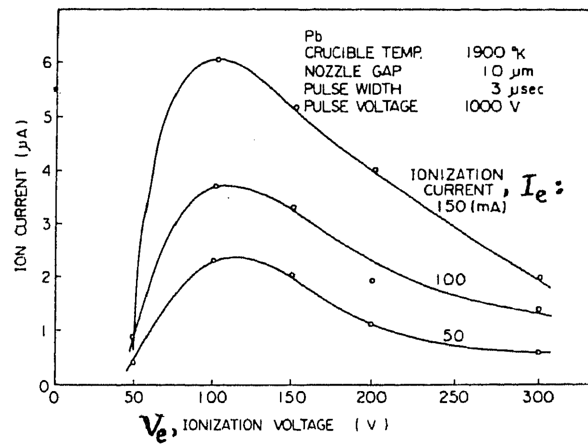

Fig. 2.7 Dependence of the ion current collected at the substrate on the ionization voltage, V_e, and the ionization current, I_e.[49]

van der Waals forces; therefore even if a second charge is created, the strong electrostatic repulsion forces between the two charges will either break up the cluster or result in a charged atom leaving, and hence restoring the singly charged status of the cluster.

2.7 Accelerating the Clusters and Energy Distribution

The positively charged clusters can be accelerated towards the substrate by the application of a negative bias, V_a, as shown in fig. 2.1 . Although high values of several kilovolts are normally used for V_a, the energy imparted to each atom in the cluster is small and averages eV_a/N (*), which is typically in the range of a fraction of an electron volt to a few electron volts. It is within this energy range that an optimum value of energy per atom can be achieved which should be high enough for surface diffusion, but not sufficient for inducing defects in the film layer ($E \leq 5$ eV)[52,55].

The neutral clusters are not affected by the acceleration voltage and travel to the substrate by their ejection speed alone. It can be assumed[52,55] that the expansion through the nozzle provides every atom in the vapour with a kinetic energy of the order of $k\ T_o$, where k is the

---

* e = the electron charge, V_a = the cluster accelaration voltage and N = the average Number of atoms per cluster.

Boltzmann constant and T_o is the crucible temperature. Therefore the energy per atom in the case of neutral clusters is in the range 0.1 to 0.2 eV depending on the crucible temperature (usually 1200^oK to 2500^oK).

2.8 Film Growth Mechanism

Upon impact with the substrate (or film surface), the clusters break up into their constituent atoms. The velocity direction of the atoms changes from the bombardment direction to directions along the substrate surface as a result of multiple collisions as the cluster impacts the surface. The change in the direction of motion of the atoms increases the migration of atoms and their diffusion along the substrate surface. The long migration distance is one of the important characteristics of ICBD. Other effects are also present: implantation, sputtering of the substrate material and sputtering of freshly deposited material on the substrate. These effects are shown in fig. 2.8[41].

In discussing factors that influence film growth in the ICB technique, it is convenient to consider separately the effects of:

(1) The kinetic energy of the clusters, which is easily controlled by the acceleration voltage.

(2) The presence of ions, which can be controlled from a few percent to about 50% by varying the electron current for ionization from zero to 500 mA.

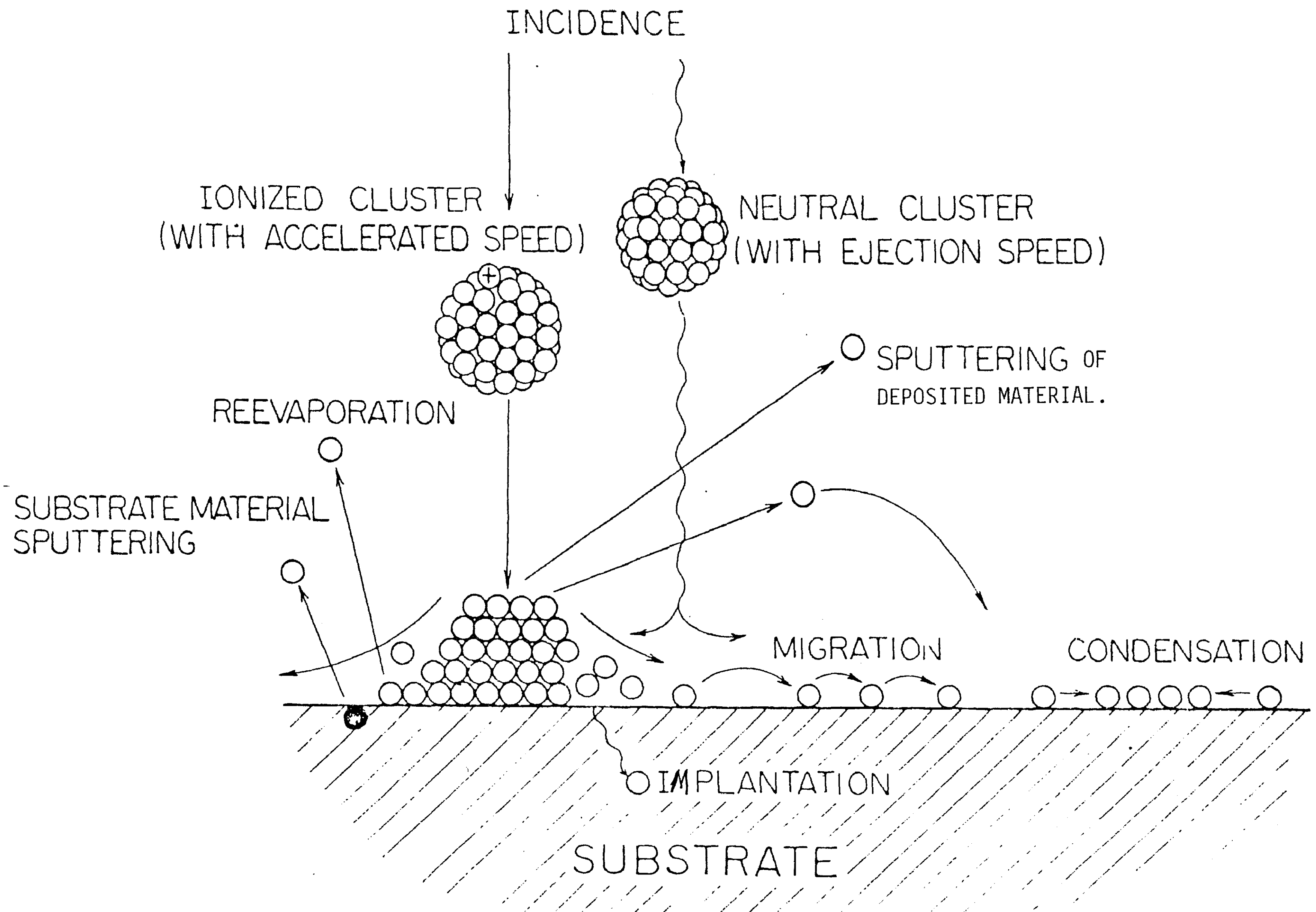

Fig. 2.8 Film Formation Process By The ICBD Technique.[41]

2.9 Effects of Kinetic Energy [56]

The kinetic energy of the accelerated clusters are converted upon impact to:-

(1) sputtering energy, (2) implantation energy,

(3) hermal energy(surface heating), and (4) migration energy of adatoms.

Sputtering and Implantation Effects

These are caused by the high energy tail of the energy spectrum of the flux arriving at the substrate, and result in surface cleaning and deep etching, thereby improving the adhesion strength of the deposited film. The sputtering effect can also enhance the creation of activated centers such as defects and displacement of surface atoms. These act as centers of nucleus formation during the initial stages of film formation[40]. Furthermore, ion implantation and the blending of sputtered substrate material with the deposited material enhance the formation of an interfacial layer, which also contributes to strong adhesion of the deposited film.

Fig. 2.9 shows the adhesion strength of Cu films deposited on glass substrates with different values of acceleration voltage [45,46,50,57]. It is clear that the adhesion strength is improved by more than an order of magnitude as the acceleration voltage is increased up to

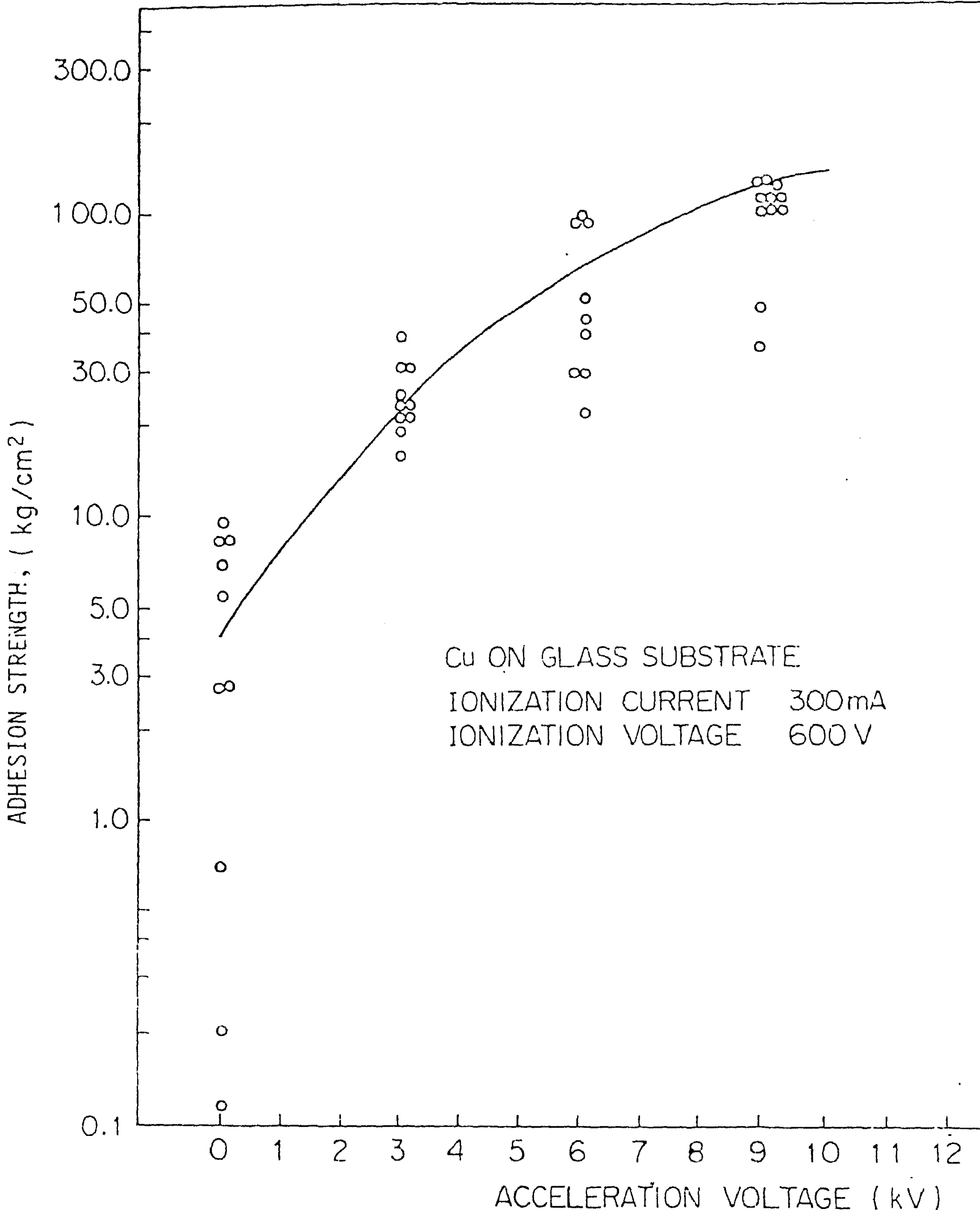

Fig. 2.9 Adhesion strength of Cu films deposited on glass as a function of acceleration voltage. (45,46,50,57)

10 kv, and is improved by a factor of 100 over that obtained by conventional vacuum deposition (about 0.5 kg/cm^2).

Thermal Effects

Thermal energy converted from the kinetic energy of the bombarding particles is available at the surface of the substrate and the deposited layer. This allows a high surface temperature to be obtained with relatively lower bulk heating as compared to that required for conventional vacuum deposition. The increased temperature can bring about a change in morphology, and, in the case of R-ICB, an increase in the chemical reaction rates.

Migration Effects

The increase of migration of deposited particles with acceleration voltage was demonstrated and reported by T. Takagi's research group in 1976[50]. Gold was deposited onto silicon oxide substrates both by ICBD and by conventional vacuum deposition. The substrate surface was partially covered with a cleaved NaCl mask as shown in fig. 2.10a. The time of the deposition run was made short enough to observe the initial stages of the deposit (island formation). Electron micrographs of the resulting films near the edge of the mask are reproduced in fig. 2.10b. The results clearly demonstrate the increase of migration distance along the surface with increasing acceleration voltage. It was also found that even with zero accelerating

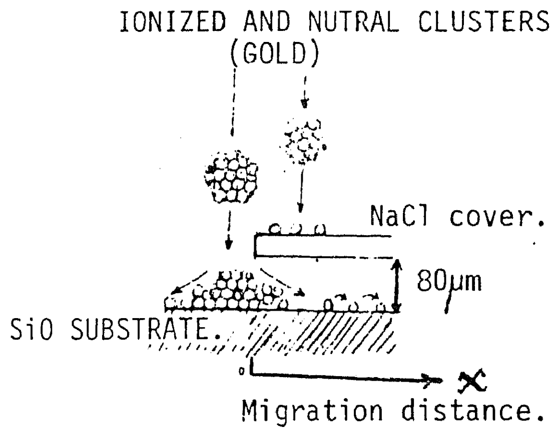

(a)

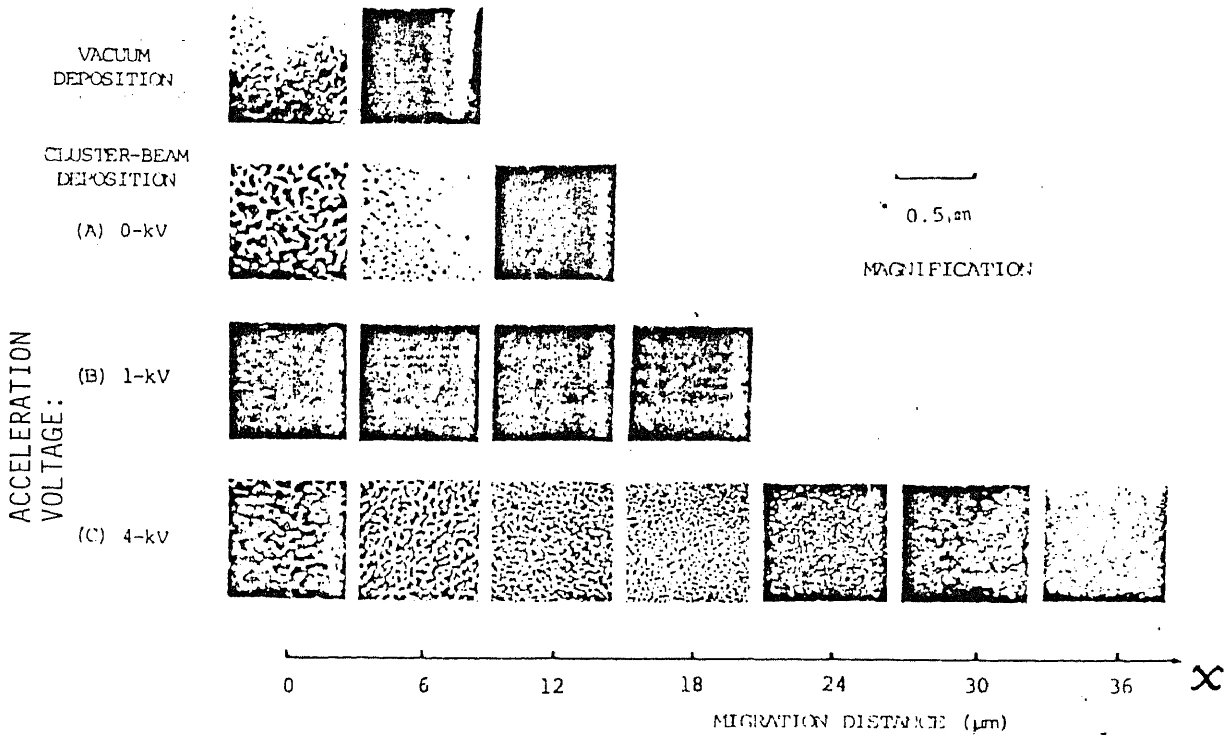

(b)

Fig. 2.10 (a) Set up for investigating the migration effects.
(b) Electron micrographs of films formed by migrated deposits.

voltage, the migration distance is greater for ICBD than that for vacuum deposition by thermal evaporation. This can be attributed to the fact that the kinetic energy of atoms is greater in the ICB technique as a result of the ejection speed at the end of the adiabatic expansion process. The extra kinetic energy of adatoms promotes chemical reaction at the substrate surface, which is important in the case of Reactive ICB deposition.

2.10 Effect of Presence of Ions

The presence of ions, even in small proportion compared to the total flux, has been found to have a profound effect on the quality of films produced by ICBD, independently of the effects of kinetic energy of the clusters. Attempts to explain how the presence of ions influence the critical condensation process in terms of the nucleation, growth of nuclei and coalescence have been made by K.L. Chopra[4,5]. For our purposes, it is instructive to consider here the results reported by T.Takagi's group[43] on the deposition of ZnO films onto glass substrates using the R-ICB method. Figure 2.11 shows RHEED patterns of the films deposited at different electron currents for ionization of zero, 150 mA, and 300 mA. At these levels, the percentages of ionized clusters in the total flux are 0, 8 - 10%, and 25 - 30% respectively. Other operating conditions were kept constant as follows: Acceleration voltage, zero volts; P_o (vapour

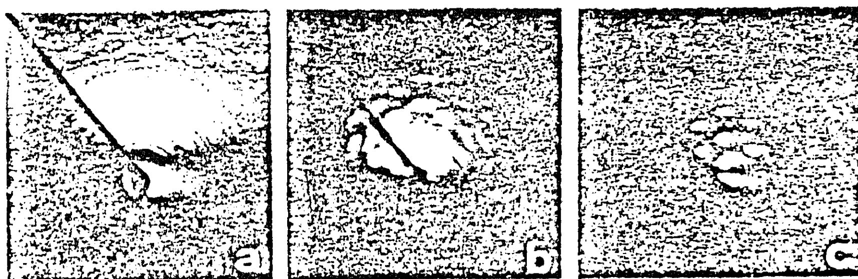

Fig. 2.11 RHEED patterns showing the infuence of the electron current for ionization, I_e, on the crystallinity of ZnO films deposited by the R-ICBD technique.[43]

(a) I_e = 0, (b) I_e = 150 mA, (c) I_e = 300 mA

pressure of zinc in the crucible), 0.1 torr; and P(chamber, oxygen), 5×10^{-4} torr. It was observed that a good quality film - having a preferred orientation, with the wurtzite c-axis perpendicular to the substrate surface - develops as the ionization current is increased.

Y. Namba and M. Toshio investigated the epitaxial growth of ZnTe on NaCl by ion beam techniques[20]. They found that the epitaxial growth was notably favoured by the presence of ions in the particle flux for deposition, while no distinct dependence on the ion energy could be observed. They also found that once the first few hundred Angstroms or so are deposited, the epitaxial growth continues even when the ion content of the particles is reduced to zero. This indicates that the presence of ions plays its most important role in the initial stages of heteroepitaxial growth.

Enhanced chemical reaction activity resulting from the presence of ions is one of the principal reasons for the effectiveness of the reactive ion cluster beam method for film formation. The method has been successfully used for preparing films of compound materials such as ZnO, BeO, SnO_2[55] and nitrides such as GaN[17,18].

2.11 Effect on Substrate Temperature Required for Epitaxial Growth

Epitaxial growth of films deposited by ICB has been reported to be possible at lower substrate temperatures than

that required by alternative methods[39,56]. Fig. 2.12 shows the mass of Si deposited as a function of the reciprocal substrate temperature for different values of acceleration voltage and keeping the other variables constant as indicated on the graph. Superimposed on these curves are lines for $T_{(s \leftarrow p)}$, the transition temperature from polycrystalline to single crystal state, and $T_{(p \leftarrow a)}$, the transition temperature from the amorphous to the polycrystalline state. Two effects are evident in this graph:

(1) The increase in substrate temperature with the mass deposited is greater as the voltage is increased. This is obviously due to the increased kinetic energy of the clusters, part of which is converted to thermal energy upon impact with the substrate as discussed earlier.

(2) $T_{(s \leftarrow p)}$ and $T_{(p \leftarrow a)}$ decrease as the acceleration voltage is increased. This is due to the fact that the substrate temperature required for epitaxial growth is lower for higher acceleration voltages. This suggests the possibility of growing epitaxial films at low substrate temperatures, resulting in films with reduced amounts of strain, and hence, improved quality[12].

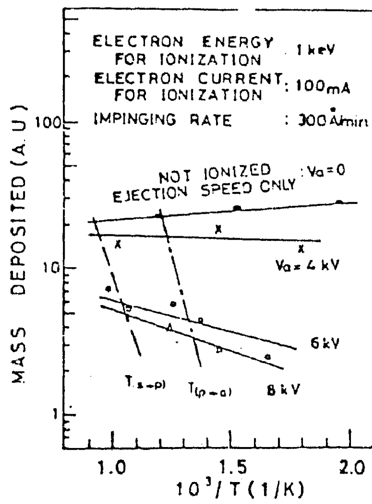

Fig. 2.12 Mass deposited vs. reciprocal substrate temperature, and the change of transition temperature for different acceleration voltages. (39,56)

CHAPTER III

CONSTRUCTION OF THE ICB SYSTEM

An experimental ICB system similar to the one used by Takagi research group was designed and constructed in the Microelectronics Laboratory at NJIT. Machine shop drawings were made by Fred Solomon, an undergraduate E.E. student, and the parts were made locally in the NJIT machine shop. The complete machine shop drawings are included in Appendix A.

The system was then assembled by the writer in the chamber of a Veeco Instrument Inc. oil diffusion pump vacuum system. Variable power supplies required (minimum of 4) were arranged as well as cooling water connections, thermocouple temperature monitors, voltmeters, ammeters and nitrogen gas inlet and accessories. In the following paragraphs a detailed description of the ICB system constructed will be given.

3.1 Complete System

The complete ICB system is shown in fig. 3.1 . Source material vapour is generated in the nozzle assembly (a_1) and ejected into the ionization region (a_2). The vapour condenses in the process of adiabatic expansion and clusters are formed. The clusters are ionized by electron bombardment in the ionization region. The ionized clusters are accelerated by

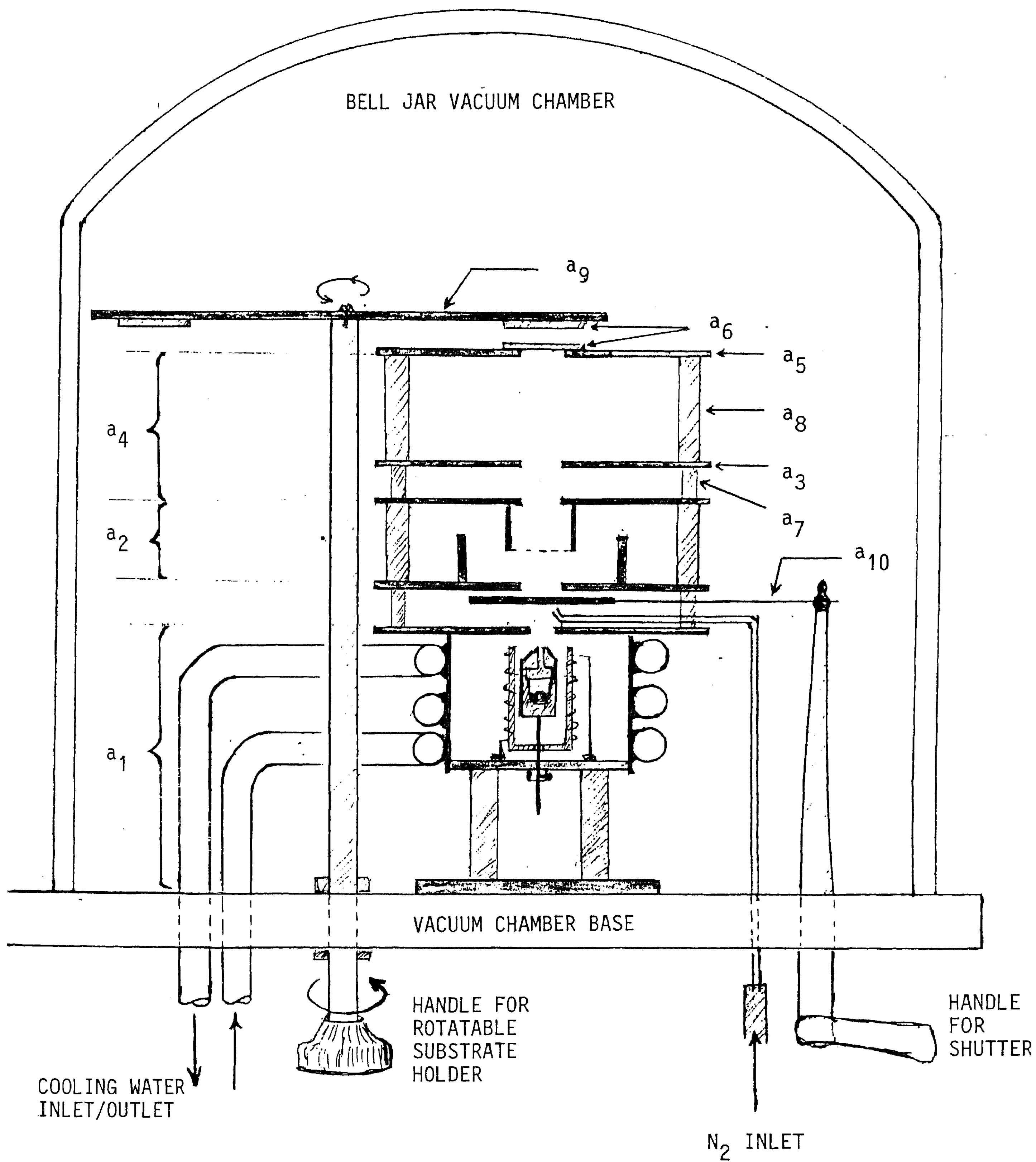

Fig. 3.1 General Assembly Drawing of the Ionized Cluster Beam (ICB) System.

the accelerating electrode (a_3) in the acceleration region (a_4) and land on the substrate (a_6) together with the neutral clusters.

3.2 The Nozzle Assembly

The cluster beam generation part of the system is shown in fig. 3.2 . Material to be deposited is placed in the crucible(1) and confined by the lid(2) which is designed to push-fit tightly on the crucible. The lid has a 0.5 mm diameter nozzle(3) at the center to allow source material vapour to be ejected into the high vacuum region at a high velocity, but at the same time allow the pressure in the crucible, P_o, to be at least 10^3 times the pressure outside the crucible. The crucible is heated by placing it in a heater (4) which in turn is directly heated by a filament(5) wrappedaround it as shown in fig. 3.3 . The crucible is supported in the heater by a thin tungsten rod(6) fitted to its base. The supporting rod passes through a hole in the base of the heater and is fixed against the stainless steel baseplate by screw(7), thus allowing for the adjustment of the vertical position of the crucible inside the heater. Both the crucible and the heater are made of boron nitride material, and a 0.023" diameter tungsten wire is used as the filament material. A 0 - 130 volt, 45 Amps Powerstat*

---

*This rating for the powerstat is used because of its availability. Actually, a 0 - 80 volts, 30 Amps powerstat would suffice.

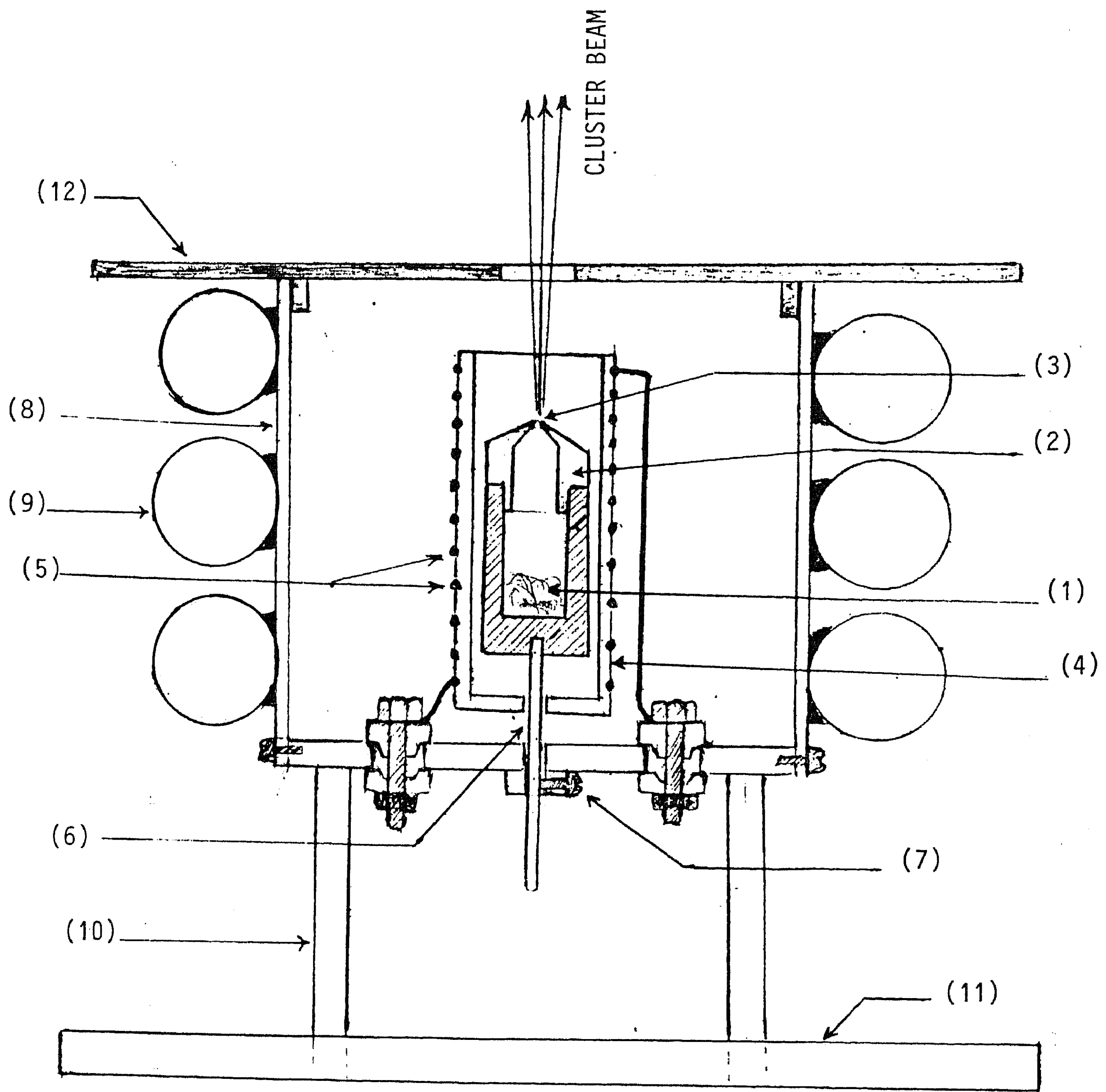

fig. 3.2 Detailed section of the Nozzle Assembly.

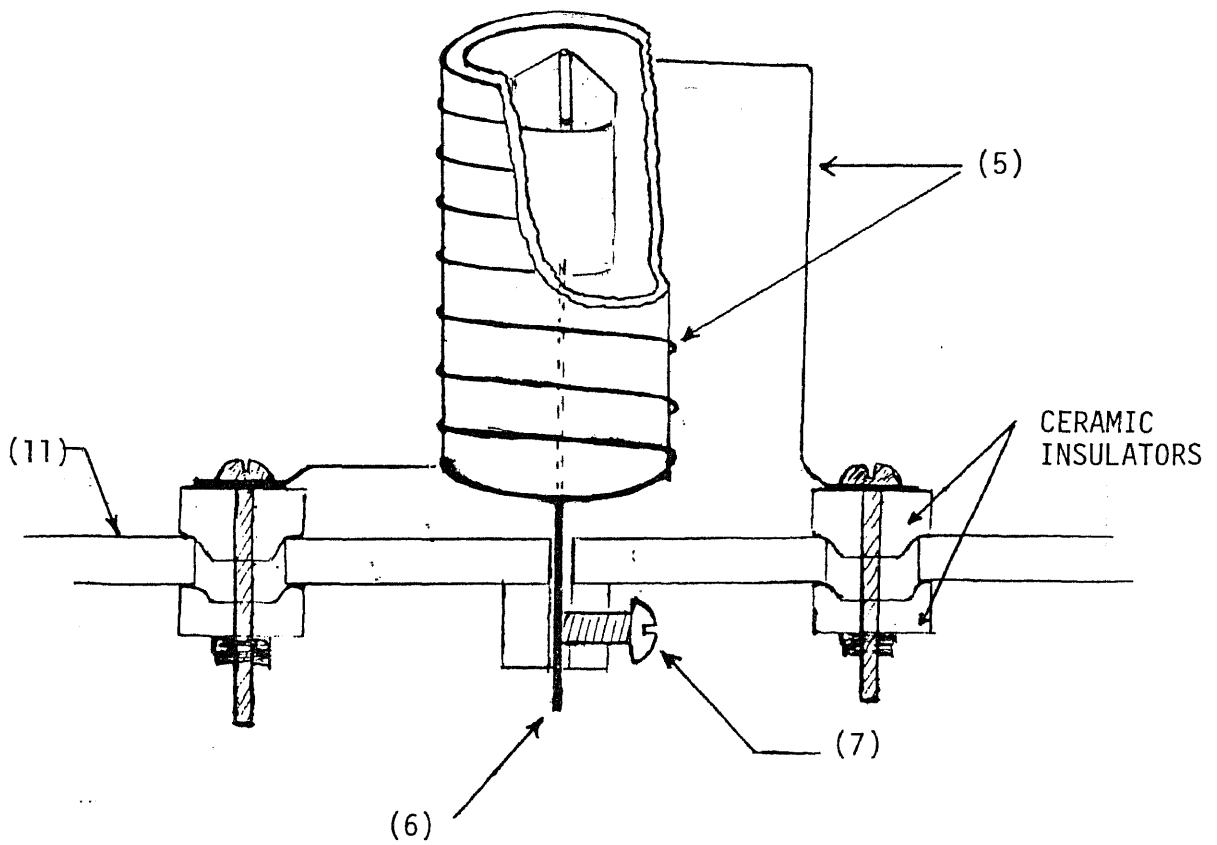

fig. 3.3 Drawing of the crucible supported inside the crucible heater.

(variable autotransformer) is used to drive a high ac current through the filament, and by controlling this current, the crucible temperature can be controlled.

The assembly is surrounded by a stainless steel "box" which acts as a heat shield(8). Cooling water is circulated through copper cooling coils(9) welded on around the heat shield. The generation part of the system is supported by four 63-mm long ceramic insulators(10) fixed to the system baseplate(11). The top plate(12) acts as a baseplate to support the next stage of the ICB system, namely the ionization assembly.

3.3 The Ionization Assembly

The ionizing electrode assembly is shown in fig. 3.4 . It rests on the top plate of the nozzle assembly supported by three 25-mm ceramic insulators(13). The electron emitter (cathode) consists of a square loop of 0.019" tungsten wire (14) supported by four hook shaped thicker tungsten wire(15) fixed to the cathode supporting plate(16) by stainless steel screws(17) through ceramic insulators(18). The cathode leads are also terminated around stainless steel screws(19), which are brought out through ceramic insulators(20) for power connections. The cathode is heated for thermionic emission of electrons by passing a high current through it. A 0 - 130 volt, 45 Amps powerstat* is used to supply this

---

*This rating for the owerstat is used because of availability. Actually a 0 - 30 volt, 30 Amps powerstat would suffice.

(14) (21)

(a) Top view.

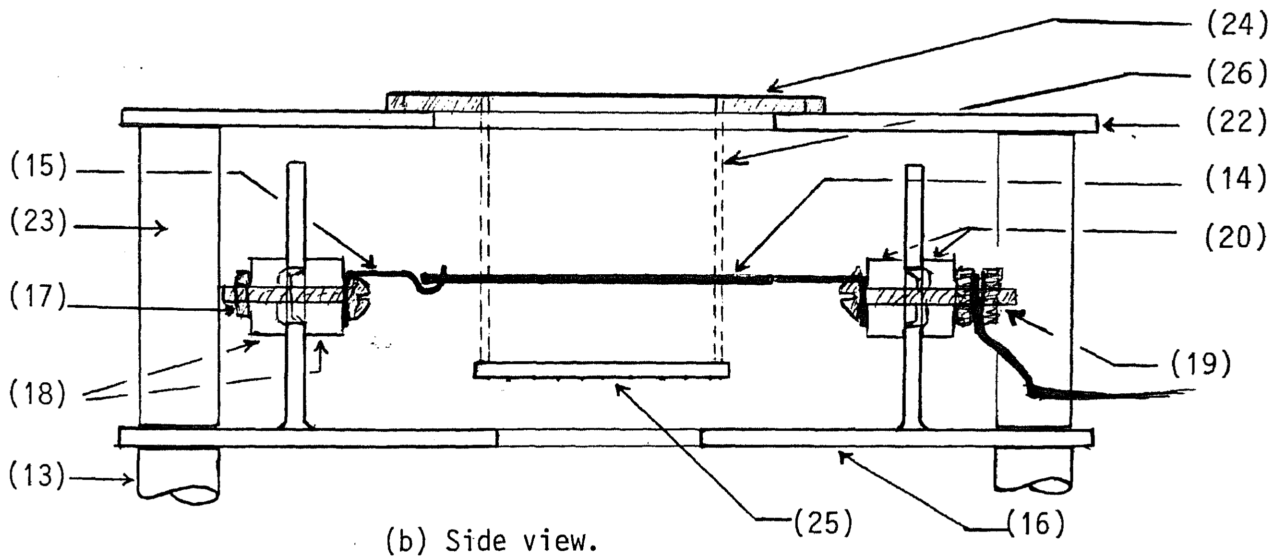

(b) Side view.

Fig. 3.4 Top and side view of the Ionization Assembly of the ICB system.

current.

The anode (fig. 3.5) is made of two stainless steel plates (24),(25) connected by 0.019" tantalum wire mesh(26) shaped like a hollow parallelopiped (21 in fig. 3.4) with a square cross section that fits at the center of the square-shaped cathode filament. The anode assembly is suspended from the anode supporting plate(22) which in turn rests on the cathode supporting plate(16), supported by three 50-mm ceramic insulators(23). The anode is biased positively with respect to the cathode to accelerate the thermally emitted electrons towards the center, where the clusters are passing. The wiring diagram for the ICB system is shown in fig. 3.6 .

3.4 The Accelerating Electrode and the Substrate Holder

The accelerating electrode (a_3 in fig. 3.1) rests on the ionization assembly(a_2) supported by three 25-mm ceramic insulators(a_7). The fixed substrate holder(a_5) rests in turn on the accelerating electrode supported by three 63-mm ceramic insulators (a_8). An alternative rotatable substrate holder (a_9) was also made, that could hold up to six substrates arranged in a circle, and any one substrate could be rotated externally into position to receive the cluster beam. In this manner, it would be possible (at least theoretically) to deposit on six substrates under six different sets of deposition parameters in the same pumpdown. A shutter (a_{10}) was also included that could be controlled externally to block or allow the deposited material flux to reach the substrate.

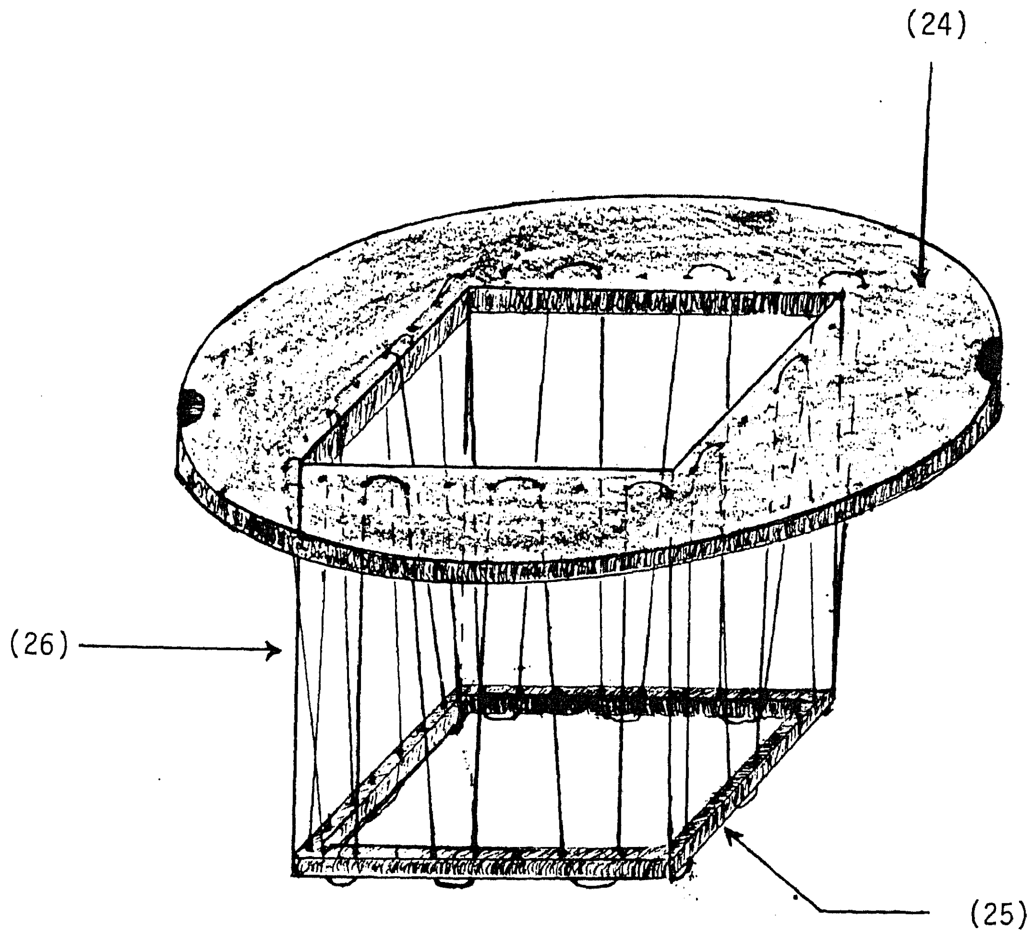

Fig 3.5 Three dimensional view of the Anode of the Ionization Assembly.

3.5 Electrical (Power Supplies and Meters)

The complete wiring diagram for the system is shown in fig. 3.6 . Three AC variable power supplies are used for supplying 0 -30 Amp currents through the crucible heater, the substrate heater and the ionization assembly cathode, as indicated on the diagram. Two high voltage DC supplies are also needed: V_e, the electron accelerating voltage (zero to 1000 volts), and V_a, the ion cluster accelerating voltage (0 - 10 kV). A simple autotransformer (0 - 130 volts, 45 Amps) is used for V_H, but isolating transformers I.T.1 and I.T.2 are necessary for V_F and V_s respectively to provide DC isolation between the high voltage biases (V_e and V_a) and the mains power supplies. The range of variation for each power supply and meter as well as ratings for the components used are all indicated on the wiring diagram(fig. 3.6). Internal wiring diagrams for the variable DC power supplies (V_a and V_e) are included in Appendix B.

3.6 Accessories

Substrate Heater

Originally, two tungsten filaments mounted on the substrate holder (at the back of the substrate) were used for substrate heating as shown in fig. 3.7 . However, as this arrangement was not capable of raising the substrate temperature beyond 350°C, alternative substrate heaters were developed and used as described in chapter 4.

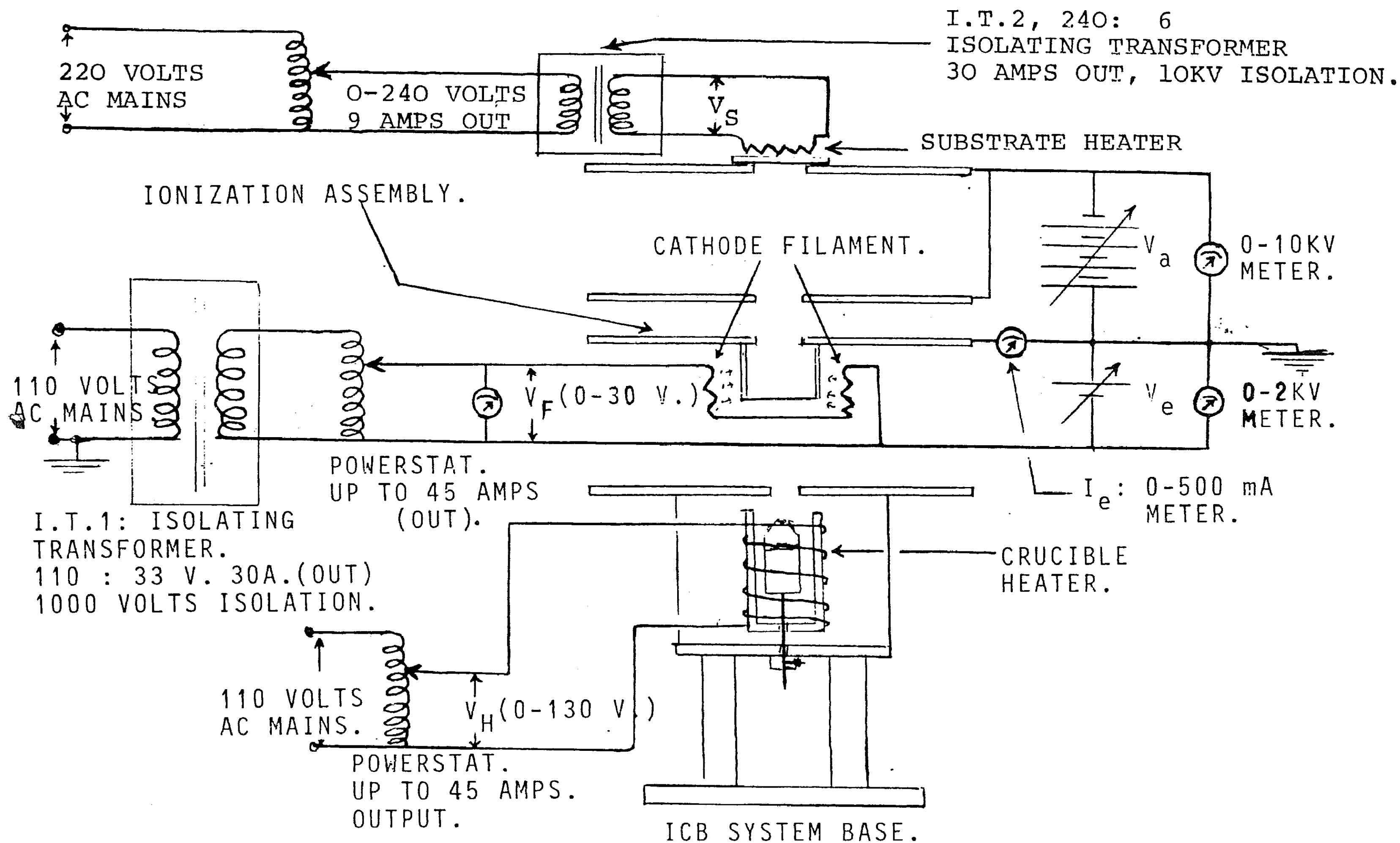

Fig. 3.6 Complete electrical wiring diagram of the ICB system. (Super-imposed on the outline of the system for easier identification).

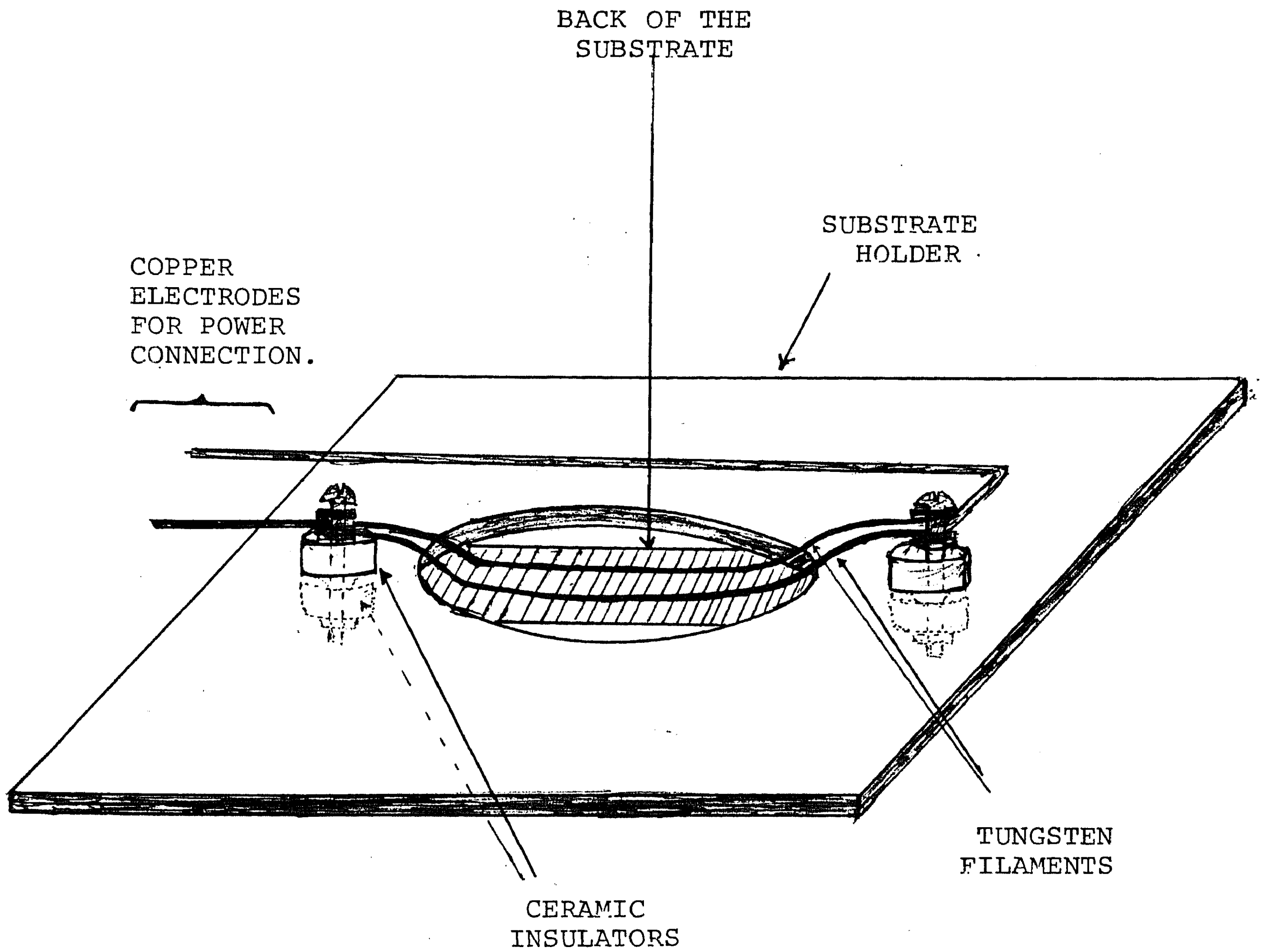

Fig. 3.7 Substrate heating arrangement used in runs No. 2 through No.6.

Temperature Sensors

Two type-K thermocouple sensors were included for monitoring the crucible and the substrate temperatures,respectively These were used in conjuction with a model 871 digital thermometer made Omega Engineering Inc., Stamford, Conn., which could read temperatures ranging from -40°C to 1,370°C with 1°C resolution. A battery-operated unit were used and the thermocouple leads were brought out through a high-voltage vacuum lead-through (properly insulated from the vacuum chamber base) to have the option of allowing the thermocouples near (or touching) the substrate, even when it is biased at a high potential of several kilovolts.

Power Inlet(VacuumLead-through) Terminals

Eight vacuumlead-throughs were used for providing a vacuum-tight means of conveying the electrical power to the system through the base of the vacuum chamber. These were type 6D made by Edward Scientific (fig. 3.8a) with a rating of 10 kV, up to 150 Amps, and up to 150°C operating temperature. The diameter of thelead.throughs had to be machined down to 0.992" at one point (fig. 3.8b) to fit the 1" diameter standard openings of the vacuum chamber base.

Nitrogen Gas Supply

A source of nitrogen supply to the vacuum chamber was needed for two reasons.

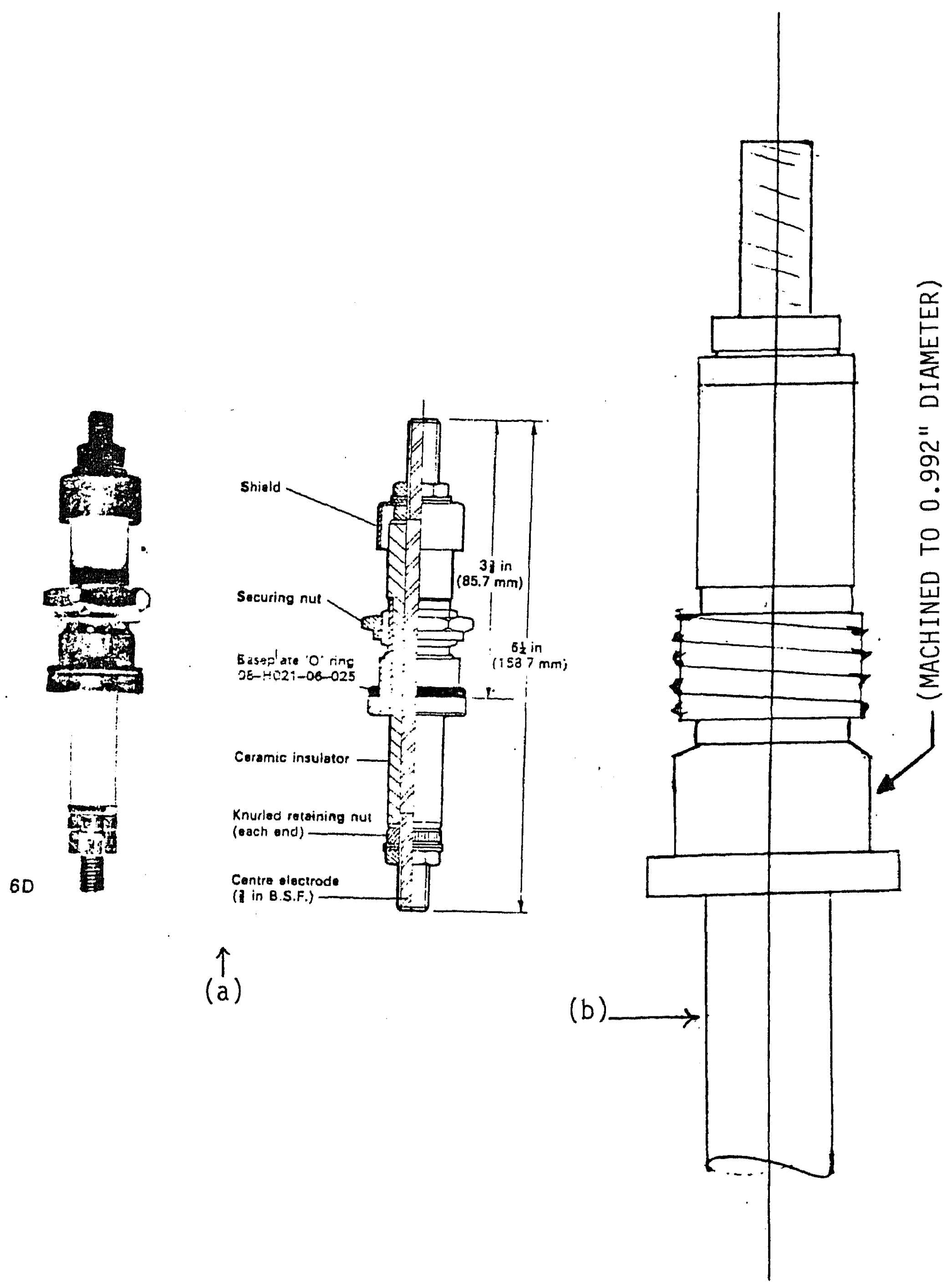

fig. 3.8 Type 6D (Edward Scientific) vacuum leadthrough used for supplying power to the ICB system.

(1). For the system in general, to fill the vacuum chamber with N_2 after shutdown and thus allow the system to cool in an inert atmosphere.

(2). For GaN deposition in particular, to maintain a nitrogen atmosphere of $1\text{-}5 \times 10^{-4}$ torr during gallium deposition and thus form gallium nitride by the Reactive Ion Cluster Beam Deposition (R-ICBD) technique.

Nitrogen was piped from the N_2 tank through a regulator and then a leak valve to the vacuum chamber, and was terminated with a 1/8" stainless steel tube at a point (fig. 3.1) midway between the nozzle assembly and the ionization assembly. The N_2 outlet nozzle was made pointing upwards and as close to the crucible nozzle opening as possible without obstructing the path of the flux coming out of the crucible.

Cooling Water Inlet/Outlet

A twin pipe, 1" vacuum feedthrough was used for providing a vacuum tight means of connecting the cooling water in and out of the vacuum chamber. The 3/8" steel tubes of the vacuum feedthrough were connected to the heat-shield cooling tubes inside the vacuum chamber using brass compression fittings. Rubber hoses were used outside the vacuum chamber for connecting the feedthrough tubes to the water supply and drain lines respectively.

3.7 Setting The Electron Current For Ionization

Normally, in an Ion Cluster Beam System, to set the

electron current for ionization, I_e, at a desired level (say 300 mA) at a certain value of electron accelerating voltage, V_e, (say 500 volts), one would normally increase V_e to 500 volts and then raise the cathode filament voltage, V_F, until the required I_e of 300mA is reached. However, since the DC power supply used in our system for V_e has a sharp drop in output voltage(V_e) as the output current (I_e) is increased, one has to set V_e at a much higher value initially, so that it drops at the specified load of 300 mA to the desired value of 500 volts.

Fig. 3.9a shows the dependence of the supply voltage output (V_e) on the output current (I_e) for different values of no-load voltage setting. Fig. 3.9b shows typical I_e versus V_e characteristics for the ICB system for different values of filament voltage, V_F. The 45° lines (V_e vs. V_e and I_e vs. I_e) are added to facilitate reflecting points between the two curves. The procedure for setting I_e at 300 mA with V_e at 500 volts is then as follows:-

A - Increase V_e to a higher value, say 600 volts.

B - Increase the filament voltage, V_F. I_e will start to increase and V_e decreases.

C - Repeat A and B above until the desired value of I_e and V_e is reached.

It should be noted that although it is possible (theor tically) to plot the values of I_e and V_e on fig. 3.9a and determine the no-load setting for V_e from the same figure and

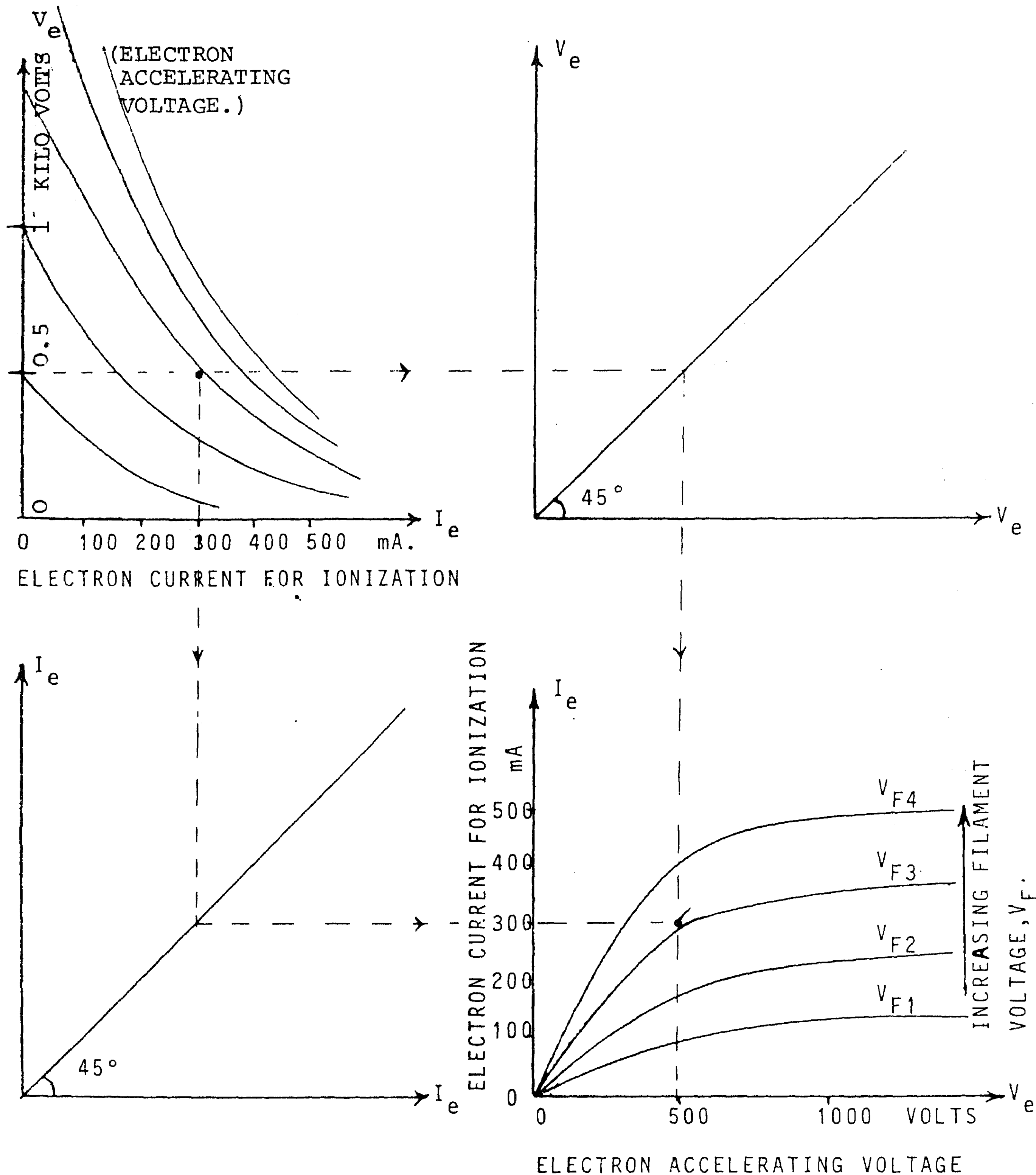

Fig. 3.9 (a)(Top left) Output characteristics (voltage vs. output current) for the power supply used for V_e .
(b)(Bottom right) Typical I_e vs. V_e characteristics for the ICB system for different values of filament voltage, V_F.

then reflect the operating point onto fig. 3.9b and determine the filament voltage, V_F, required this procedure is not followed for two reason.

(1) The characteristics of the ICB system shown in fig. 3.9b) are only typical and depend on many additional parameters such as time, whether V_F is being increased or decreased, and the temperature of the nearby crucible and substrate heaters which influence the cathode filament temperature by radiation.

(2) The no-load value of V_e required for initial setting is considerably higher than the actual operating value for V_e and might be high enough to cause breakdown between the cathode and anode especially in the presence of small amounts of residual gas as is the case in the Reactive Ion Cluster Beam Deposition (R-ICBD).

These problems are avoided by following the iterative procedure described above.

3.8 Typical Start Up Procedure

1. Charge the crucible with the source material to be deposited, put the substrate(s) in, and assemble the complete ICB system in the vacuum chamber.
2. Turn on the cooling water lines.
3. Pump down for at least one hour in the 10^{-6} torr range.
4. Raise the crucible temperature (with the shutter in place) up to the required value and stabilize the temperature to within a few degrees for at least 15 minutes.

5. Raise the substrate temperature to the desired value.

6. Set the ionization current at the desired level by, following the procedure described in the previous section.

7. Apply the desired ion accelerating voltage, V_a.

8. Move the shutter aside to start depositing.

3.9 Typical Shut Down Procedure:-

1. Move the shutter back in place.

2. Reduce the ion accelerating voltage, V_a, to zero.

3. Reduce the electron accelerating voltage, V_e, to zero.

4. Reduce the cathode filament voltage, V_F, to zero.

5. Reduce the substrate heater and the crucible heater voltages to zero.

6. Introduce nitrogen in the vacuum chamber and allow the system to cool down for at least two hours before opening up the vacuum chamber.

7. Turn off the cooling water lines.

In addition to the above, the normal steps for start up and shut-down of standard bell jar vacuum systems should of course be followed. A detailed description of the procedure adopted in our experiments for the deposition of GaN by R-ICB is given in section 4.14 .

3.10 <u>Practical Difficulties</u>

In any experimental work - such as that reported in this thesis - many practical problems arise during the course of the experiments. In this section, a few of the more important difficulties encountered are cited, along with the solutions employed (or proposed) for each case:-

1. Substrate heating presented many problems. It necessitated abandoning the multiple substrate holder as discussed in section 4.7 . Modified substrate heaters had to be constructed to meet the higher temperatures ($\gtrsim 450^{O}C$) required as discussed in sections 4.13 and 4.16 .
2. After every deposition run, the crucible lid would seal tightly on the crucible. Removing the lid to charge the crucible required heating the crucible - e.g. using a blower or a hair dryer - to melt the gallium inside it. Then the crucible would be held in a three-jaw grid(in the NJIT machine shop) and the lid turned slowly with pliers cushioned with a clean napkin or tissue paper.
3. After every deposition run, the top plate of the nozzle assembly (part 12 in fig. 3.2) would wrap, due to the inevitable uneven heating of the plate. This resulted in breaking of the tips of the three insulators

resting on this plate and supporting the ionization stage. The problem was partially solved by using larger diameter insulators supported by bigger screws. This eliminated the breakage problem, but the warping of the plate still resulted in tilting the top part of the ICB system slightly as the temperature was increased. To eliminate this problem in a second generation system, water cooling of this plate should be considered.

4. The screws feeding current to the crucible heater filament (fig. 3.3) were getting extremely hot and on occasions have been observed to melt where they touch the tungsten filament. This can be attributed to the very high temperature of the filament coupled with the relatively high thermal resistance of the stainless steel screws used. The problem could have been solved by using larger diameter screws having a lower thermal resistance. However, since larger screws required other modifications to accomodate them, it was suggested[25] doubling up the tungsten filament a short length near the screws. This lowered the equivalent resistance of this section of the filament touching the screws and hence reduced the heat generated nearer to the screws. This way the temperature of the screws was lowered and melting avoided.

5. After each of the first few runs, it was observed that the various tungsten filaments in the system were becoming brittle and difficult to handle. This was caused by the rapid cooling of the filaments after shutdown. To avoid this, a more elaborate shutdown procedure was adopted (section 4.15) which incorporated among other things slowly reducing the filament temperature instead of abruptly switching the supplies off.
6. In addition to the above, water vapour contamination presented a major difficulty. This is fully discussed in part C of section 4.20 at the end of Chapter IV .

CHAPTER IV

GROWTH OF GaN FILMS BY R-ICBD

The ICB system constructed at the NJIT Micro-electronics Laboratory was used to grow GaN films. In this chapter, the details of the experiments performed are given along with discussions of the results obtained.

A. Gallium Nitride

4.1 Why Choose GaN?

Gallium Nitride is a wide bandgap material which can be an efficient light emitter over a wide a spectral range including the visible (10,22,26) and the ultraviolet (24,27). It has also been made to lase in the ultraviolet region (7), and has exhibited negative electron affinity (15,23). In particular, blue-green luminescence has been observed at 5190Å with a power efficiency of 0.1% and a quantum efficiency of 1%, with no evidence of degradation over extended periods of continuous operation (28). Therefore, GaN promises a new class of numeric displays generating previously unattainable colors with highly acceptable brightness, and several additional advantages:-

(1) The luminous area is determined by the shape of the metalization, and all the electrodes are attached at the rear surface of the crystal.

(2) GaN is perfectly transparent throughout the visible range so that the emitted radiation can be viewed through

the crystal. Furthermore, the crystal can be a convenient support and window for LED's emitting other colors, thus permitting the fabrication of a multicolor display [29].

Thus far, the major stumbling block to the widespread use of GaN LED's has been the difficulty in growing large, homogeneous, strain free, single crystals.

4.2 Material Synthesis [27]

Several growth techniques have been described in the leterature for the preparation of GaN. One technique involves the flow of ammonia over gallium at a temperature greater than $800^{\circ}C$ as follows:

$$Ga + NH_3 \longrightarrow GaN + \frac{3}{2}H_2$$

Some of the small crystallites formed by the above reaction can be made to grow at the expense of decomposing neighboring ones by heating in flowing ammonia, and thus millimeter-size crystals can be obtained.

Another technique which has enjoyed the greatest favor among researchers is a vapour transport method known as the Maruska and Tietjen method [16,28]. $GaCl_3$ is produced by passing HCl over Ga in an open flow furnace. $GaCl_3$ (vapour) is then mixed with ammonia gas, near the surface of a sapphire substrate (at around $1000^{\circ}C$) on which GaN forms as a single crystal:

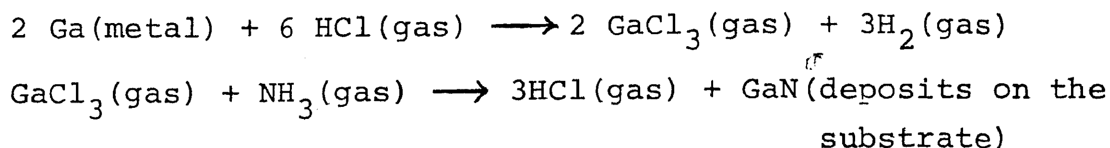

$$2\ Ga(metal) + 6\ HCl(gas) \longrightarrow 2\ GaCl_3(gas) + 3H_2(gas)$$

$$GaCl_3(gas) + NH_3(gas) \longrightarrow 3HCl(gas) + GaN(\text{deposits on the substrate})$$

A third method for growing an extended area of thin GaN film is reacting Ga vapour with ionized itrogen[13]. This method is the one being investigated in the present work and will be described in greater detail in the following section.

4.3 GaN By R-ICB Deposition

K. Matsubara and T. Takagi recently (1980) reported successful results in their attempts to grow GaN films using R-ICBD[17,18]. Pure Gallium was vapourized from a crucible with a nozzle diameter of 1 mm, in a Nitrogen atmosphere. The substrate used was hexagonal ZnO film on glass. Other conditions of the deposition were reported to be as follows:

- Crucible (Gallium) Temperature: About $900^{o}C$
- Electron Current for Ionization: 300 mA.
  (At this current level, the ionization ratio of the clusters is about 25 - 30%).
- Chamber (Nitrogen) pressure: 5×10^{-4} torr.
- Substrate temperature: $450^{o}C$.
- Acceleration voltage: Zero.

Under these conditions, it was reported that n type GaN was grown epitaxially on a ZnO-film surface.

4.4 Important Properties of GaN Films

GaN is almost always n-type when undoped, with the free electron concentration usually about 2×10^{18} electrons/cm^3 and an electron carrier mobility of about 130 $cm^2/V.sec$. The donors (which are believed to be native donors, i.e.

Nitrogen vacancies) can be compensated by the addition of Zn, Mg, Li or Be. When the material is compensated, it becomes semi-insulating, but not p-type. So far, it has not been possible to make the material p-type. The energy band gap of GaN is direct, about 3.4 eV at room temperature. Reference 26 is an excellent summary of the known properties of GaN including detailed band structure, absorption and reflectance spectra as well as their temperature-dependence.

Electroluminescence [27]

GaN light-emitting diodes have been fabricated using the MIS (metal - insulator - semiconductor) structure shown in fig. 4.1 . An undoped n type conduction layer is grown on a transparant substrate, usually sapphire. Then a Zn-doped insulating layer is grown on the n-type layer. The wafer is cut into 1-mm diameter discs which are then soldered with indium to a ceramic support. This peripheral solder makes an ohmic connection to the n-type layer. A small indium dot soldered at the center of the insulating layer forms a 10^{-3} cm^3 area of non-ohmic connection. Such a diode can, depending on the degree of doping, emit blue, green, yellow or red light. The light is emitted at the negative electrode (cathode). I - V characteristics have been observed to exhibit a linear relationship between ln(I/V) and $1/\sqrt{V}$. This suggests that tunneling rather than space charge limitation is the mechanism controlling the current as shown in fig. 4.2[30]. On the

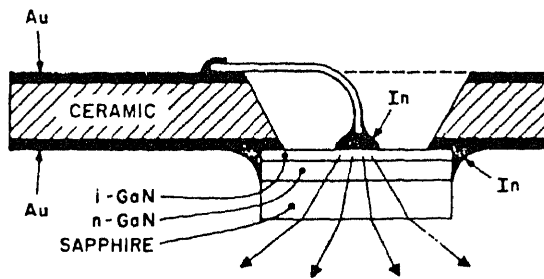

fig. 4.1 Structure of the GaN, MIS(Metal - Insulator - Semiconductor) Light Emitting Diode (LED).(27)

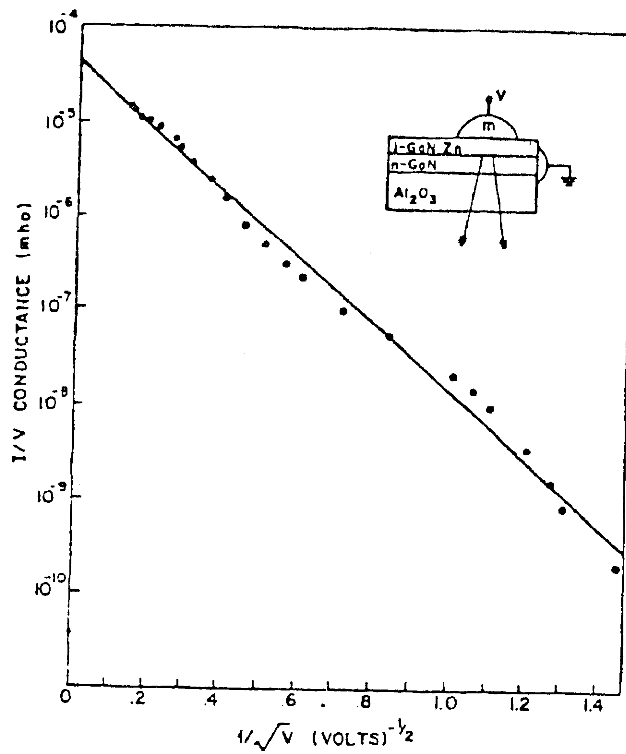

(a)

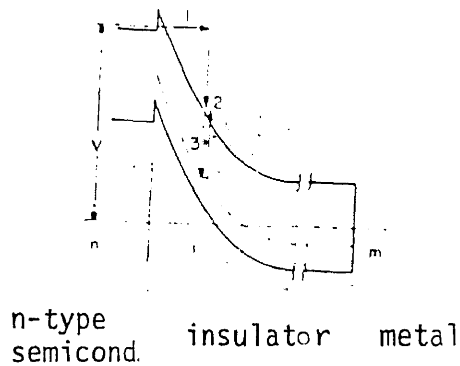

fig. 4.2 (a) Fowler - Nordheim - like plot of the I-V characteristics for a typical Zn-doped GaN diode with the metal (m) biased positively.

(b) Band diagram for the GaN diode under the m-positive bias condition. The proposed model for the process is: (1) Tunneling; (2) Impact excitation (direct case); (3) Radiative recombination.[30]

other hand, Matsubara and Takagi[18] reported that I-V characteristics of GaN LED's made by ICBD follow the relation ($I \propto V^n$) with n ranging from 1 to 3. These characteristics suggested space charge limitations as the current limiting mechanism. It was also reported that the light was emitted near the positive biased contact, in direct contradiction with the results reported by J.I.Pankove[30]

B. EXPERIMENTAL DETAILS

4.5. INTRODUCTION

As a first step in exploring the prospects of growing GaN films by R-ICBD, it was decided to attempt to reproduce the results reported by the Takagi research group in 1i80 (section 4.3)[17,18]. This decision might have been premature, considering that the ICB system constructed had not been tested yet with straightforward metal deposition; and that R-ICB deposition poses additional problems. These problems include among other things:

(1) The increased possiblility of creating a plasma, and hence destroying the clusters due to plasma heating.

(2) Sensitivity to the parameters of the deposition due to the requirement that a chemical reaction occur at the surface of the substrate in addition to the requirement that favorable conditions for film formation be attained.

Rather than discuss the best results obtained, it is instructive to scan through the runs made in sequence and

see how the results of each brought about changes in the conditions of the next run. This is necessary because the runs can be viewed as part of a learning curve.

4.6 Run No. 1

The first run was made using glass slides at room temperature as substrates. Deposition was made on 5 slides using the multiple substrate holder described earlier. Except for the substrate temperature, other parameters of the deposition run were adjusted to correspond to the optimum results reported the Takagi research group[17,18] as follows:

- Electron Current for Ionization: 300 mA.
- Accelerating Voltage: Zero.
- Nitrogen Pressure: $1 - 2 \times 10^{-4}$ torr.

The crucible temperature was 900°C for deposition on the first three slides while the deposition time was made progressively greater for each slide. This meant that theoretically speaking, we should have obtained a thicker film on slide No. 2 than on slide No. 1. Similarly, we should have obtained a thicker film on slide No. 3 than on slide No. 2. This was not the case. The film obtained on slide No. 2 clearly appeared, upon visual examination, to be the thickest of all films, even counting the other slides (No. 4 and No. 5), which were deposited at the higher crucible temperature of 950°C instead of 900°C. It was also observed (when the system was inspected after the run) that gallium

metal had accumulated in the heater and along the rod supporting the crucible as shown in fig. 4.3 . It was therefore suspected that the supporting tungsten rod might have punched through the crucible wall, and made a tiny hole in the base which allowed gallium to leak out. To avoid this problem, a new crucible was made to be used for the following runs, and extra care was taken to mount it gently on the tungsten rod without applying any unnecessary force.

4.7 Run No. 2

The conditions for the second run were similar to the first, except that substrate-heating was introduced. To do this, the multiple substrate-holder had to be abandoned in favor of a smaller, single substrate holder. This was necessary for several reasons. The large mass and area of the multiple substrate holder would require massive amounts of power to heat the entire plate. The large area would give rise to considerable radiation heat loss, and intolerable outgassing that might affect the performance of the small pumping system being used. There was also the practical difficulty of monitoring the temperature of movable substrates using a stationary thermocouple. For this (and subsequent) runs, quartz substrates were used. After 18 minutes from the start of the deposition, an opaque film started accumulating on the walls of the bell jar. The system was immediately shut down and allowed to cool. After the system was opened

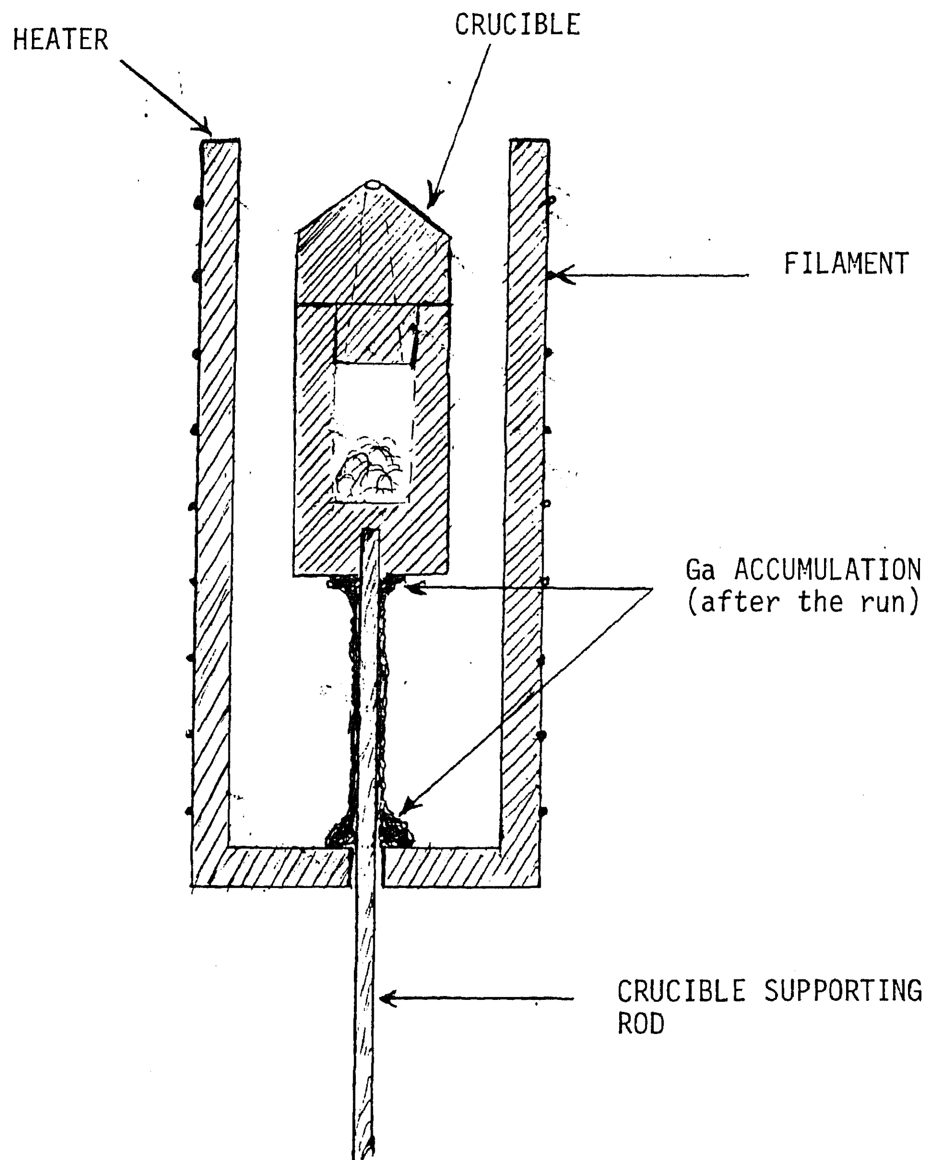

Fig. 4.3 Section of the crucible inside the crucible heater showing the accumulation of Ga after the first deposition run.

and examined, it was observed that the silver solder between the heat shield and the water cooling coils had melted. This could happen only if: (1) The cooling water was lost, e.g. accidentally shut off; or, (2) The pressure of the cooling water was so low that the cooling rate could not catch up with the rate of heat generation. The film obtained was not clean, and not uniform, and it was not carried any further to the measurements stage. The system including the bell jar and its base was thoroughly cleaned with HCl, and then trichloroethylene to remove any silver film that might have contaminated it.

4.8 Run No. 3:-

The conditions for this deposition run were set as follows:-

- Crucible Temperature: 1,000°C
- Electron Current for Ionization: 350 mA.
- Nitrogen Pressure in the Chamber: 1 - 2 x 10^{-4} torr.
- Substrate Temperature:-
  - initial: 300°C.
  - final: 330°C.

The deposition run was continued for 60 minutes after which the system was shut down and allowed to cool before it was opened. The film obtained was observed to have the following properties:-

(1) Transparent: although it could easily be distinguished from the quartz substrate by its "cloudy" appearance.

(2) Film growth was not uniform over the substrate surface. There were areas of the surface where film growth appeared inhibited.

(3) The film was soft and could be scratched off the surface of the substrate rather easily.

(4) Film thickness was estimated to be less than 200 Å, meaning that a deposition rate of only $\approx$ 3 Å/min was achieved. This is rather low for ICBD.

(5) Photoluminescence tests made at RCA Labs. in Princeton, N.J. showed no indication of the peaks normally associated with gallium nitride. (These tests will be discussed in greater detail for the film obtained in run No. 6). At this stage, the failure of the photoluminescence tests to reveal a GaN signature was attributed to any one or a combination of the following reasons:

(a) The film was not GaN, i.e. the substrate temperature was not high enough to enhance the reaction between Ga and N_2.

(b) The film was amorphous possibly because of the low substrate temperature.

(c) The film was too thin to show any photoluminescence peaks.

4.9 Run No. 4

The conditions for this run were set similar to that for run No. 3, except that the crucible temperature was raised to 1,080°C, in an attempt to achieve a higher deposition rate. The deposition was allowed for 30 minutes, but no observable

film resulted on the substrate. At this point, it was considered that the crucible temperature was still too low to give a reasonably high deposition rate so it was decided to raise the crucible temperature even higher for the next run.

4.10 Run No. 5:

An attempt was made to achieve a crucible temperature of 1,300^{o}C; but as the voltage applied to the crucible heater was increased, the power supply circuit breaker tripped although it was rated for 30 Amps. The run had to be abandoned. When the system was dismantled, it was observed that the screws carrying current to the filament of the crucible heater had melted, although stainless steel screws were used. It was also observed that the thermocouple tip had fused. These could have been caused by too rapid an increase in the voltage applied to the crucible heater, which did not allow sufficient time for heat conduction to establish equilibrium temperatures. Obviously, no film resulted. The system was dismantled, cleaned with HCl and then with trichloroethylene, then put together using a new filament for the crucible heater and new screws instead of the damaged ones.

4.11 Run No. 6

The deposition parameters for this run were set as follows:

- Average crucible temperature: 1,120^{o}C.
- Nitrogen Pressure: $2 - 3 \times 10^{-4}$ torr.

- Electron Current for Ionization: 360 mA.
- Acceleration Voltage: Zero.
- Substrate Temperature:
  - initial: $340^{o}C$.
  - final: $371^{o}C$.
- Deposition Time: 90 minutes.

Two samples were obtained from this run: R_{61} and R_{62}. The films were transparent, and moderately hard to scratch, in line with the properties of known samples of GaN. Conductivity measurements showed that the films were insulating. The films were then sent to RCA laboratories in Princeton for photoluminescence and absorption edge tests. In the photoluminescence tests setup of Dr. J.I.Pankove at RCA labs, the films are optically excited by a 325 nm, 2.2 mW laser beam. In optical excitation, a photon is absorbed by the semiconductor, creating an electron-hole pair which then recombines emitting one or more photons(31). Therefore by observing the emission spectra, peaks corresponding to the fundamental transition energy (band to band) as well as peaks corresponding to transitions between impurity levels, from the conduction band to impurity levels, and from impurity levels to the valence band, can be observed.

Results of such photoluminescence tests are shown in fig. 4.4 for room temperature and fig. 4.5 for liquid nitrogen temperature. These are shown for samples R_{61} and R_{62}, as

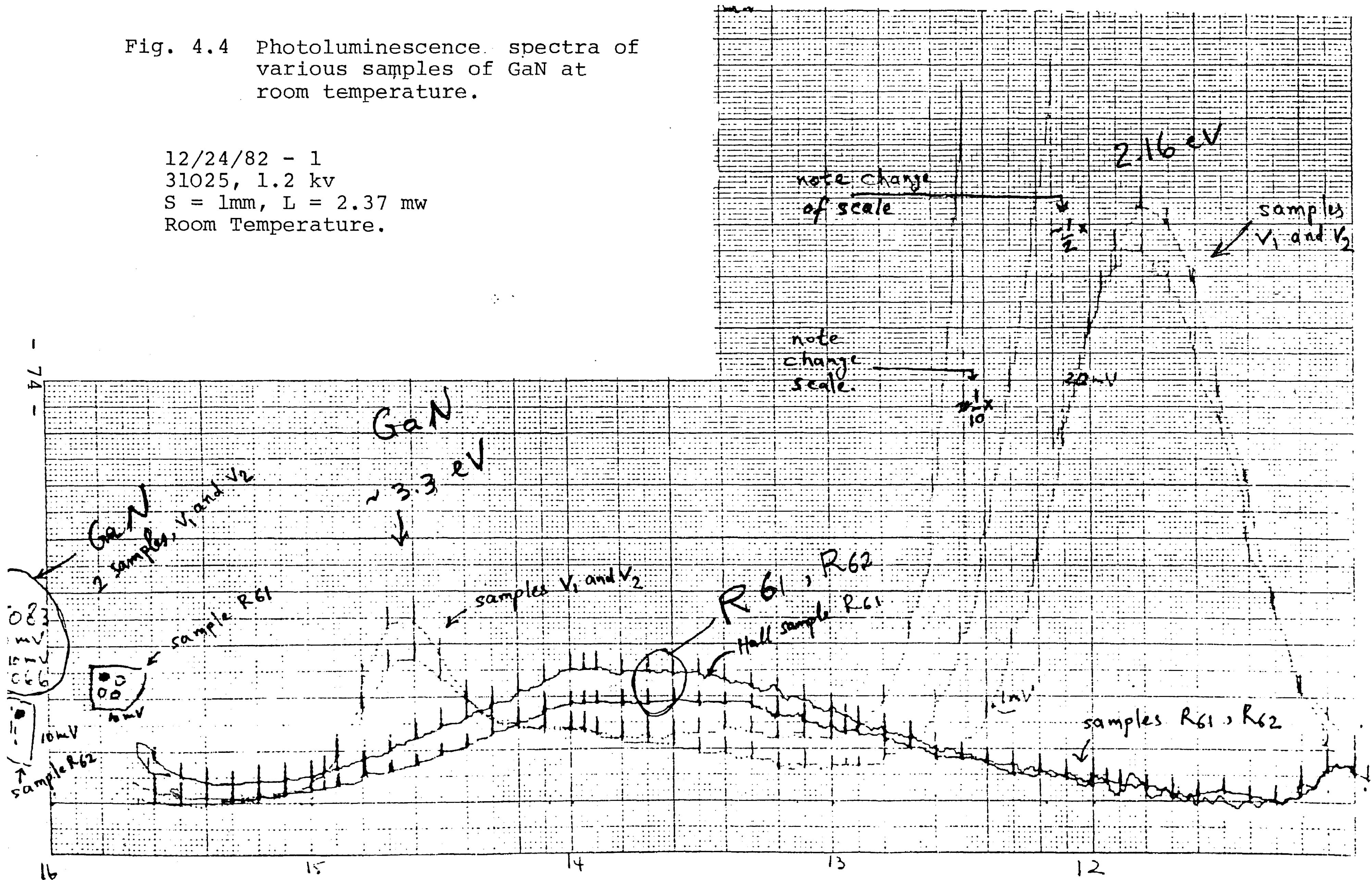

Fig. 4.4 Photoluminescence spectra of various samples of GaN at room temperature.

12/24/82 - 1
31025, 1.2 kv
S = 1mm, L = 2.37 mw
Room Temperature.

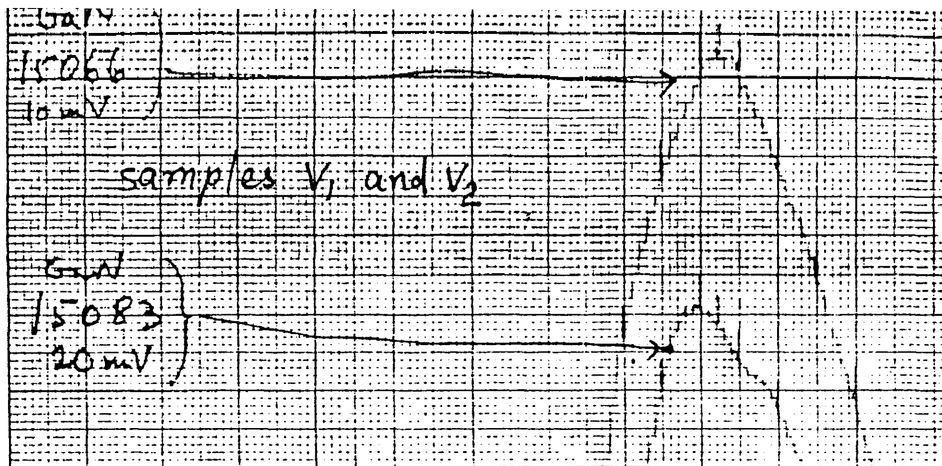

Fig. 4.5 Photoluminescence spectra of various samples of GaN at liquid nitrogen temperature.

12/24/82 - 2
S = 200 μm
31025, 1.2 kv
82 °K

well as for two other samples of GaN, V_1 and V_2, grown by the chemical vapour transport deposition method described in section 4.2 .

Examination of these two figures revealed that two peaks were present for samples V_1 and V_2 at room temperature:-

- One at a photon energy of approximately 3.3 eV.
- The other, a much higher peak, at a photon energy of approximately 2.16 eV.

At liquid nitrogen temperature (fig. 4.5), a low peak at 3.4 eV was observed, followed by a much higher peak at 3.15 eV and then the peak at 2.16eV, which was now a relatively smaller peak compared to the one at 3.15 eV. Samples R_{61} and R_{62} did not show these characteristics. Instead, a broad spectrum was obtained at room temperature. At liquid nitrogen temperature, a broad spectrum was similarly observed, but a peak at 1.7 eV was also present. This last peak was suspected to be due to the quartz substrate so another photoluminescence test was carried out on the substrate alone(at a point which was masked during the deposition of the film). The results of this test, shown in fig. 4.6, confirmed that the peak obtained at 1.7 eV could be attributed to the substrate since the peak was present in the spectra for the film/substrate as well as for the substrate alone. Since the photoluminescence spectra for the films (samples R_{61} and R_{62}) were the same for room temperature and liquid nitrogen temperature, and they did not

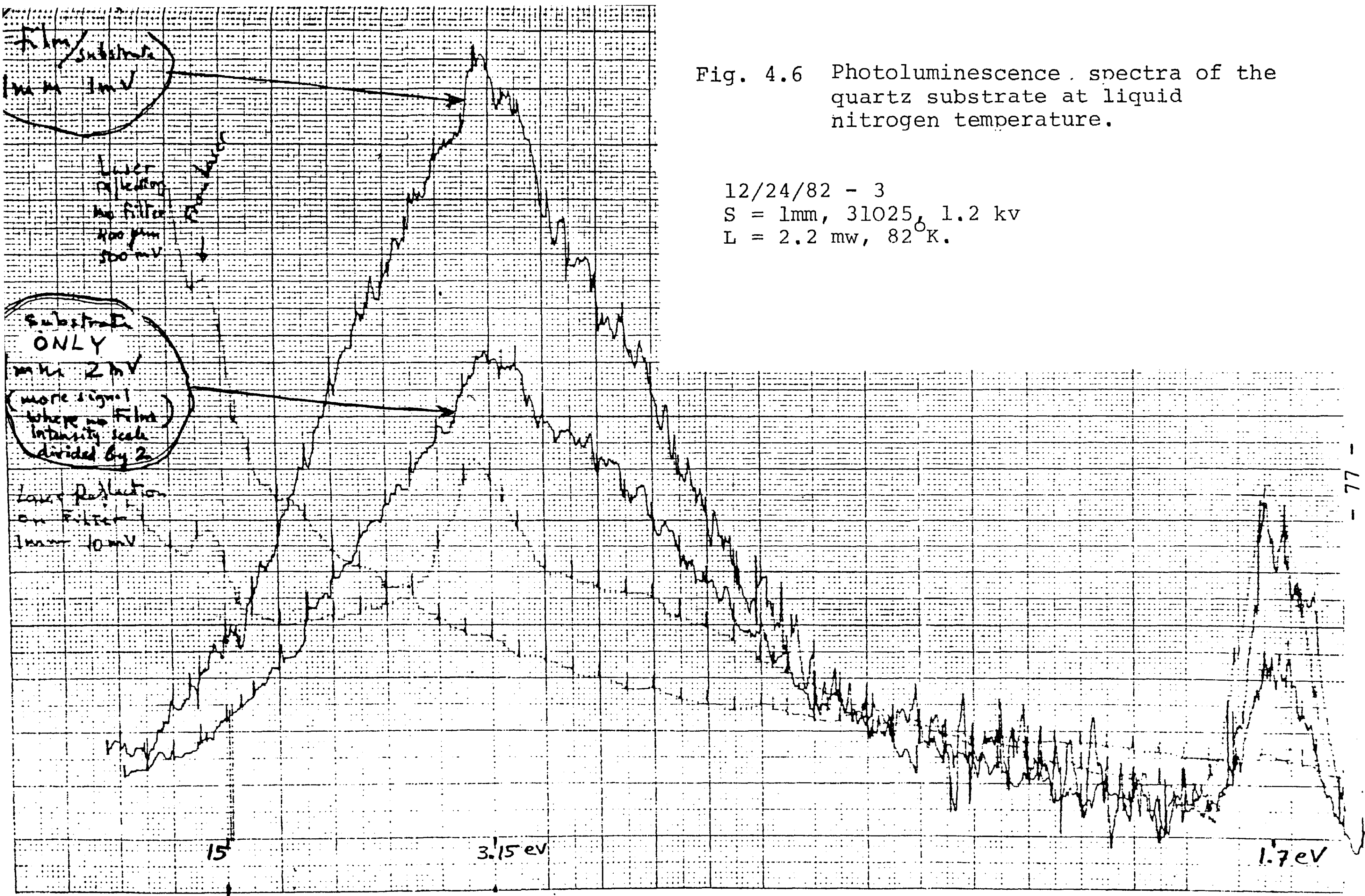

Fig. 4.6 Photoluminescence spectra of the quartz substrate at liquid nitrogen temperature.

correspond with the spectra of known samples of GaN, it was suspected that the films obtained in this run might have not been GaN.

4.12 Potential Problems

Two potential sources of trouble were identified:

A - Residual Oxygen in the vacuum chamber which, because of its high chemical activity relative to the Nitrogen, might have reacted with the Gallium to form Gallium Oxide.

B - Low substrate temperature, which could have been either too low for a reaction between Ga and N_2 to occur, or, too low to produce a crystalline film resulting in the film being amorphous GaN.

4.13 Solutions Employed

Steps were taken to eliminate the above potential problems as follows:

---

*Experimental work by C. Mehta at NJIT during the writing of this thesis has revealed that water vapour in the boron Nitride crucible can cause the boron nitride to decompose at elevated temperatures introducing additional reactive contaminants at the substrate and preventing the deposition of pure gallium. This problem will be discussed further in section 4.20 at the end of this chapter.

Low Substrate Temperature

To increase the substrate temperature beyond 350°C, a new substrate heater was constructed as shown in fig. 4.7 . The quartz substrate was directly mounted on the back side of the lower plate of the heater for efficient heat conduction. With this arrangement, substrate temperatures greater than 500°C (up to 700°C) could be reached.

Residual Oxygen in the Vacuum Chamber:-

Three sources of oxygen contamination to the chamber were possible: *

1. Small Leaks

This of course was the most obvious possible source of O_2 in the vacuum chamber, so it was tested first. A leak detection test was carried out using a mass spectrometer leak detector, model 925-40, made by Varian Vacuum Division. By squirting Helium gas around the chamber and waiting for the mass spectrometer to respond, no leaks could be found even with the leak detector set for the highest sensitivity.

---

*As outlined in the footnote on page 78 , the residual water vapour trapped in the boron nitride crucible can serve to introduce oxygen as the boron nitride reacts with H_2O at elevated temperatures releasing boron oxides which act as reactive contaminants at the substrate. This is discussed further in section 4.20 at the end of this chapter.

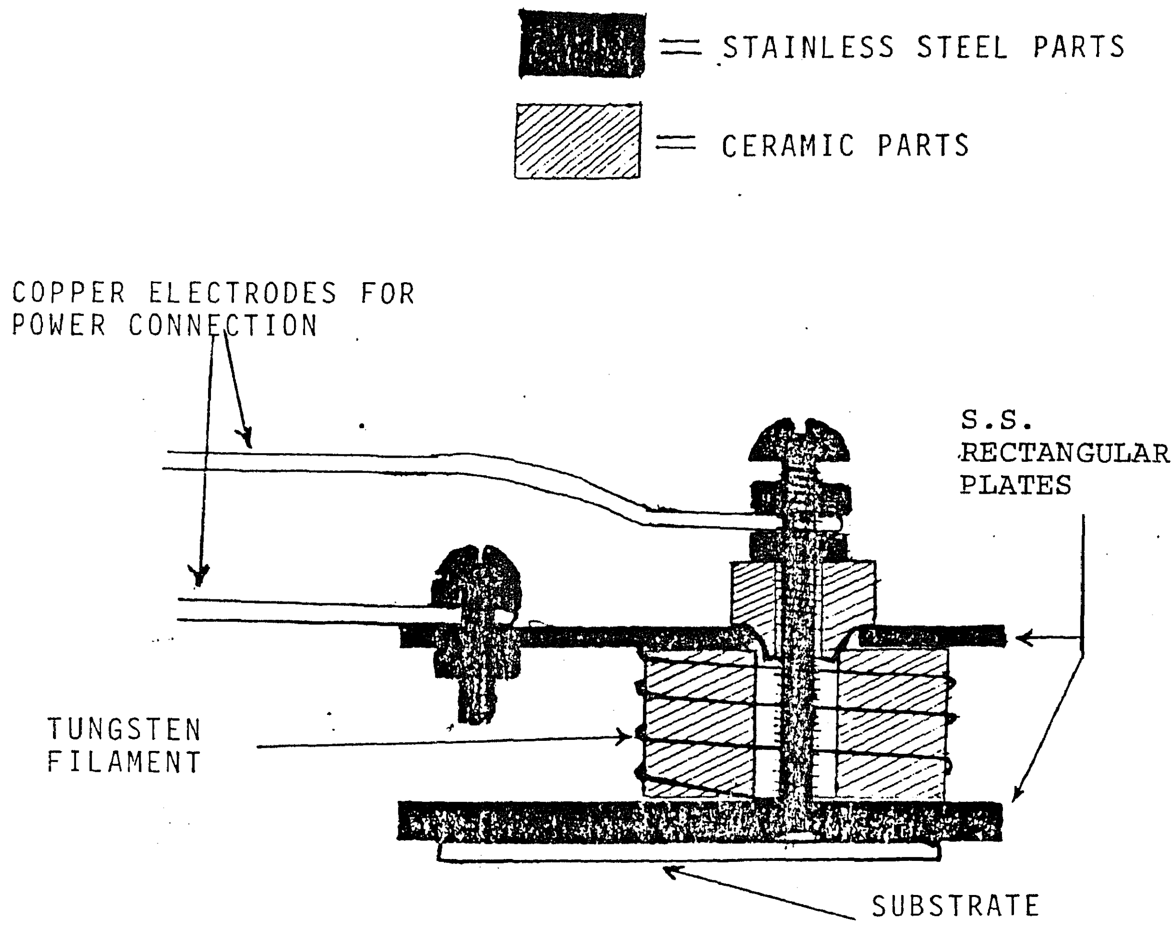

Fig. 4.7 Structure of the substrate heater used for run #7 onwards.

2. Oxygen Contamination from the Nitrogen Tank

To reduce the possibility of introducing small amounts of O_2 present as an unavoidable impurity in the nitrogen tank; it was decided to use a LIQUID nitrogen reservoir as the source for nitrogen vapour. Since the boiling point of O_2 is higher than that of N_2, this would insure that the N_2 vapour is free of O_2, because any residual oxygen that might be present will stay as liquid in the liquid N_2 reservoir[25].

3. Insufficient Pumpdown and Outgassing

To eliminate any residual O_2 in the vacuum chamber due to insufficient pumping down and/or outgassing of residual O_2 trapped on the walls and surfaces, it was decided[6] to pump down to the 10^{-6} torr range overnight (over 14 hours). Then the chamber would be flushed with N_2 and pumped down again to the 10^{-6} torr range. This would be repeated 3 to 4 times to insure that any residual atmosphere in the vacuum chamber will be predominantly nitrogen.

Based on the above considerations, the following procedure was adopted for the runs that were attempted after run No. 6 (i.e. runs No. 7 through 11):

4.14 Start-up Procedure Adopted For Run No.7 Onwards

A . System Preparation

1. The various parts of the system were cleaned with dilute HCl, then trichloroethylene, then blown dry

with helium.

2. The crucible was filled with a fresh load of gallium then the lid was pushed in place and the crucible fitted inside the heater, making sure it is perfectly vertical, with the nozzle pointing towards the substrate. The ionization stage was fitted on top of the nozzle assembly and secured in place.

3. The substrate (Quartz) was cleaned in trichloroethylene for approximately two hours, blown dry with helium, then mounted on the back side of the substrate heater which in turn is secured to the substrate holder as shown in fig. 4.8 . The thermocouple was positioned on one side of the substrate surface.

4. The nitrogen inlet was connected and the line flushed to clear any entrapped air.

B. <u>Start-up Procedure</u>

1. The cooling water lines to the diffusion pump and to the ICB system were turned on.

2. The mechanical (roughing) pump was turned on and used to pump down the diffusion pump for 20 - 25 minutes. Then the diffusion pump was turned on.

3. The vacuum chamber was pumped down with the roughing pump to less than 50 microns of Hg.

4. The diffusion pump was left to warm up while continuously pumping it down with the roughing pump for about 40 - 45 minutes. Then the butterfly valve was

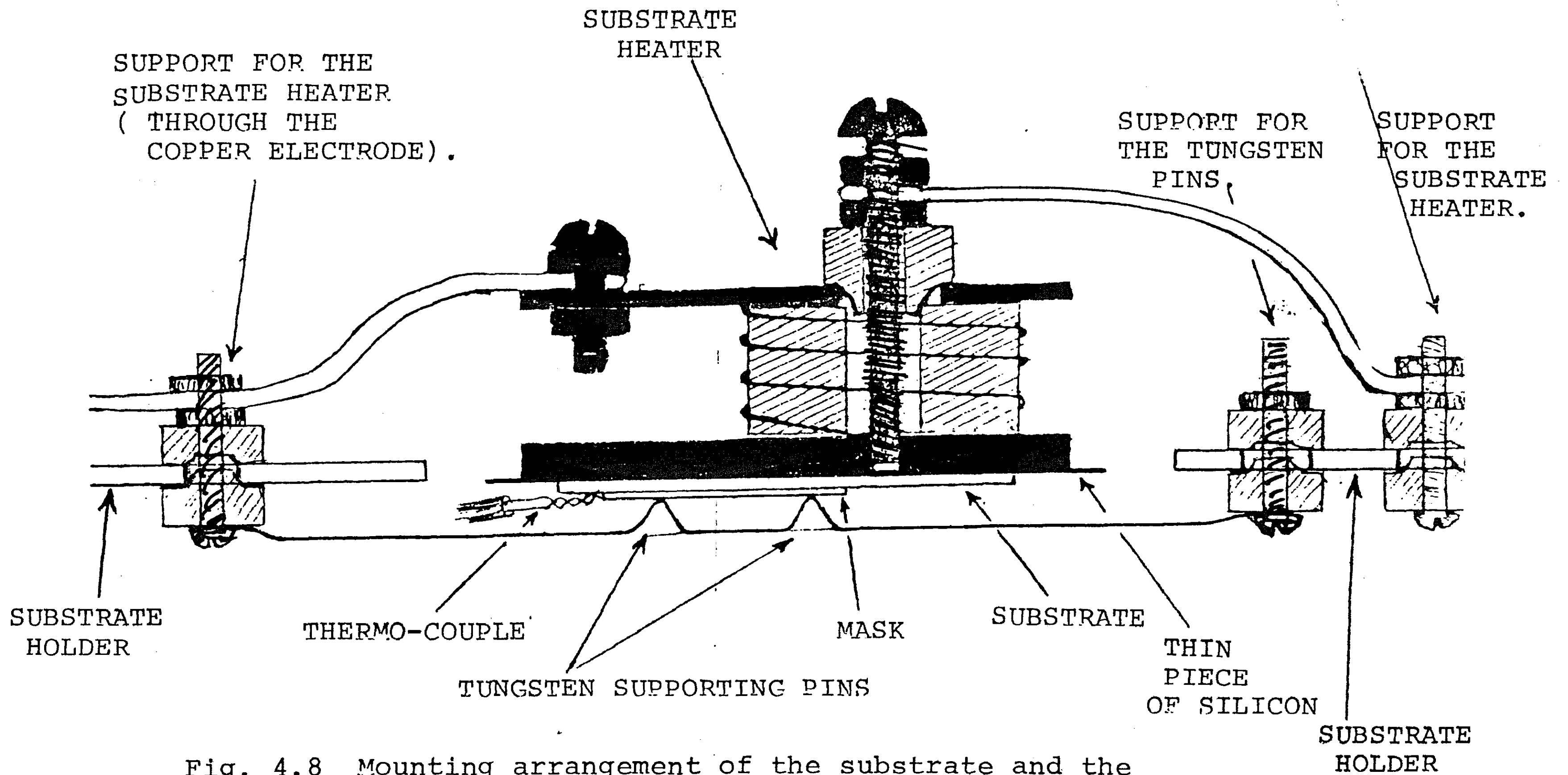

Fig. 4.8 Mounting arrangement of the substrate and the substrate heater on the substrate holder.

opened and the vacuum chamber was pumped down with the diffusion pump. Pumping down in this manner was continued for 12 - 14 hours (overnight) to a base pressure of 1 - 3 x 10^{-6} torr.

5. The vacuum chamber was flushed with nitrogen (obtained from a liquid nitrogen source as described earlier) to a pressure greater than 1 torr, then pumped down again to 1 - 3 x 10^{-6} torr. This was repeated at least 3 times.

6. The nitrogen leak valve was adjusted to get the desired nitrogen pressure in the chamber, i.e., 1 - 5 x 10^{-4} torr.

7. The power supplies were set initially for zero output, then they were plugged in and switched on.

8. The crucible and substrate heaters' voltages were increased slowly in increments of a few volts at a time, letting the system stabilize in two ways before applying the next increment:

   a) Re-establish its equilibrium value of pressure (because the pressure increases slightly when the temperatures of the crucible and the substrate are increased, mainly due to outgassing).

   b) Reach a slow rate of change in both the substrate and the crucible temperatures, say $1^{o}C$ rise in 15 or more seconds.

   Precaution (b) above was found necessary to give enough time for heat conduction from the filaments to the

boron nitride heater and thus avoid excessive local heating of the tungsten filaments which might lead to the breaking of the filaments.

9. Once the desired substrate temperature and crucible temperature were reached, the ionization filament (cathode) voltage was raised slowly up to 14 volts. Then the electron accelerating voltage was applied and both were adjusted to get an electron current for ionization (I_e) of 300 mA with an electron accelerating voltage of at least 100 volts as described in section 3.7 .

10. To begin the deposition, the shutter is moved aside allowing gallium flux to land on the substrate. After depositing for the desired period of time, the run was terminated as follows:-

4.15 Shut Down Procedure Adopted For Run No. 7 Onwards

1. The shutter was returned in place.
2. The electron accelerating voltage was reduced to zero.
3. The ionization filament (cathode) voltage was reduced until the filament was red hot instead of white hot.
4. The crucible and substrate heater filaments' voltages were reduced gradually and,
5. the nitrogen pressure was increased by allowing N_2 into the chamber to a pressure of approximately 150 micron of Hg. The system was kept at this N_2 pressure while continuing (4) above until the filaments were no longer visibly hot.

6. All power supply voltages were reduced to zero.
7. The butterfly valve between the chamber and the diffusion pump was closed and the diffusion pump switched off.
8. The chamber was filled with nitrogen and the system was allowed to cool for at least two hours before it was opened.
9. The cooling water to the ICBD system and to the diffusion pump were turned off.

4.16 Runs No. 7 and No. 8

In both of these attempts, the procedures outlined above were followed to the point of establishing the desired substrate and crucible temperatures; however, in both runs, the substrate heaters were lost (filament broken) before the deposition could begin. In run No. 7, the carbon based ceramic used in the substrate heater disintegrated and fused tiny particles started flashing in the vacuum chamber. For run No. 8, that was replaced by a piece of boron nitride, 1" in diameter. Two turns of 0.019" diam. tungsten wire were used as the heating filament, but this broke (open-circuited at one point) before the substrate temperature could be raised above 450°C, indicating that the filament was not suitable to handle the amount of power required. Therefore it was replaced with 4 turns of 0.023" diam. tungsten wire wrapped around a 1" diam., ½" long, cylindrical boron nitride piece, grooved to accept the filament (for better heat conduction).

4.17 Run No. 9

The conditions for the deposition run were set as follows:-

- Crucible temperature: $990^{o}C \pm 5^{o}C$.
- Electron current for ionization: 350 mA.
- Nitrogen pressure in the chamber: $1 - 2 \times 10^{-4}$ torr.
- Acceleration Voltage: Zero.
- Substrate temperature:

  initial : $618^{o}C$

  final : $667^{o}C$
- Deposition time: 213 minutes.

The following observations were made on the film obtained in this run:-

1. The mask had moved as a result of vibration of the system during the deposition run ; hence the edges were not sharp or well defined.
2. The stainless steel base of the substrate heater which supported the substrate had diffused into the back of the substrate due to the high temperature of the heater.
3. No quantitative thickness measurements were possible on the film, but it could be judged by visual inspection that the film was extremely thin.

Therefore, no further measurements were made on this film and it was decided to:

1. Use a larger nozzle diameter for the crucible (1.5 mm instead of 0.5 mm) to get a higher deposition rate.

2. Use a thin piece of silicon between the quartz substrate and the stainless steel heater base to avoid the diffusion of stainless steel into the back of the substrate.

Both above modifications were made for the subsequent runs (Nos.10 & 11).

4.18 Run No. 10

The conditions for this deposition run were set as follows:-

- Crucible temperature: $995^{o}C \pm 5^{o}C$
- Electron current for ionization: 300 mA $\pm$ 20mA.
- Nitrogen pressure in the chamber: $5 - 6 \times 10^{-4}$ torr.
- Acceleration voltage: Zero.
- Substrate temperature:

  initial : $520^{o}C$

  final : $550^{o}C$
- Deposition time: 4 hours.

After the system was allowed to cool down, the substrate/film was taken out and the following was observed/done:-

1. The back of the substrate was stained with impurities and various spots. These were thought to be diffused silicon at first, but further scrutiny revealed that it must have been impurities or dirt on the silicon surface rather than silicon.
2. The mask edges were sharp and the film was clearly visible; i.e., the constrast was very good.

3. The film was hard, and pressing lightly on it with a pin would not scratch or peel it.

4. The film was not attacked by HCl indicating that it was not gallium metal.

The sample was personally taken to RCA Laboratories on and the following was done/measured.*

1. The film thickness was measured to be about **250** Å. This indicated that the deposition rate under these conditions was approximately 1 Å per minute - a rather low value for ICBD system.

2. Conductivity measurements were attempted, but the film proved to be highly insulating - even with 600 volts applied between 2 points only 1 mm apart.

3. Absorption edge measurements were made but no absorption edge was detected. This however, was thought to be an inconclusive measurement because with such a thin film, the absorption of the band gap must be very high for an absorption edge to be detected with the equipment used.

4. Luminescence tests were made and the results were similar to those obtained for samples R_{61} and R_{62} made in Run No.6

---

*These measurements were supervised by Dr. J.I. Pankove of RCA laboratories, Princeton, N.J.

As for the previous samples, no peaks indicating the band structure of GaN were present and, this time, no peak due to the quartz substrate could be detected either. Instead, all that could be observed was some scattering effects.

4.19 Run No. 11

For this run it was decided to use a thin film of ZnO on quartz as the substrate. The ZnO film was prepared by Dr. J.I. Pankove at RCA Labs. and photoluminescence measurements were made on the ZnO/quartz substrate for later comparison with the spectra of the sample after the deposition run. The substrate was then assembled on a thin piece of clean silicon which in turn was supported on the back of the substrate heater.

Following the procedure described in section 4.14, the deposition parameters were set as follows:-

- Crucible temperature: 1100°C
- Electron current for ionization: 300 mA.
- Nitrogen pressure in the chamber: 1.5×10^{-4} torr.
- Acceleration voltage: Zero.
- Substrate temperature: 590°C.
- Deposition time: 63 minutes.

The film obtained in this run was similar to the films obtained in earlier runs except for one marked difference. This film proved to be highly conductive while all previous films were highly insulating. However, the results of

photoluminescence tests made on this sample were similar to the results obtained from the substrate (ZnO on quartz) before the deposition run, and no peaks characterizing GaN could be observed. Surface analysis of the film was made at RCA labs and the results showed that the film was rich in oron, itrogen and other impurities.

===

4.20 Conclusions and Suggestions for Future Work

A. With regard to the ICBD system:

Although the ICBD system construction was completed and experiments were made using the system, many of the refinements that were contemplated at the early stages were not incorporated in the system due to the extreme budget limitation at the time. Some of the more important improvements that can be suggested for the future are:

1. A safety interlock system is required that will automatically shut off the high voltage power supplies when the vacuum chamber is opened.
2. Substrate heating using a heater directly in contact with the back of the substrate is rather inefficient (because of the bulk heating) and can be a source of impurities and contaminants. Therefore surface heating of the substrate is proposed using infrared lamps focused at the substrate.
3. Although monitoring the crucible and substrate temperatures

with thermocouples can be very accurate, thermocouples raised to these high temperatures can also be a source of trouble and contaminants in the vacuum chamber. Therefore monitoring the temperatures using an optical emission spectrum analyzer would be a preferable alternative.

B. With regard to the deposition of GaN films by R - ICBD:

Our attempts to reproduce the results published to the Takagi research group, as reported in this work, were not successful. All the films obtained were very thin ($\leq$ 250 Å thickness), and the deposition rate of about 1 Å per minute was at least an order of magnitude lower than the typical deposition rates expected of ICBD systems.

The low deposition rate could be attributed to:

- either the small nozzle diameter of the crucible, or
- low crucible (gallium) source temperature.

But since the nozzle diameter was increased from 0.5 mm to 1.5 mm for runs No. 10 and 11 without much improvement in the deposition rate, we must conclude that the crucible temperature must have been lower than that required for efficient gallium vapour (or cluster) ejection. This argument can be further supported by considering the gallium vapour pressure in the crucible for the temperature range under consideration.

Referring to the vapour pressure charts (fig. 4.9), the following data are tabulated for easier reference:-

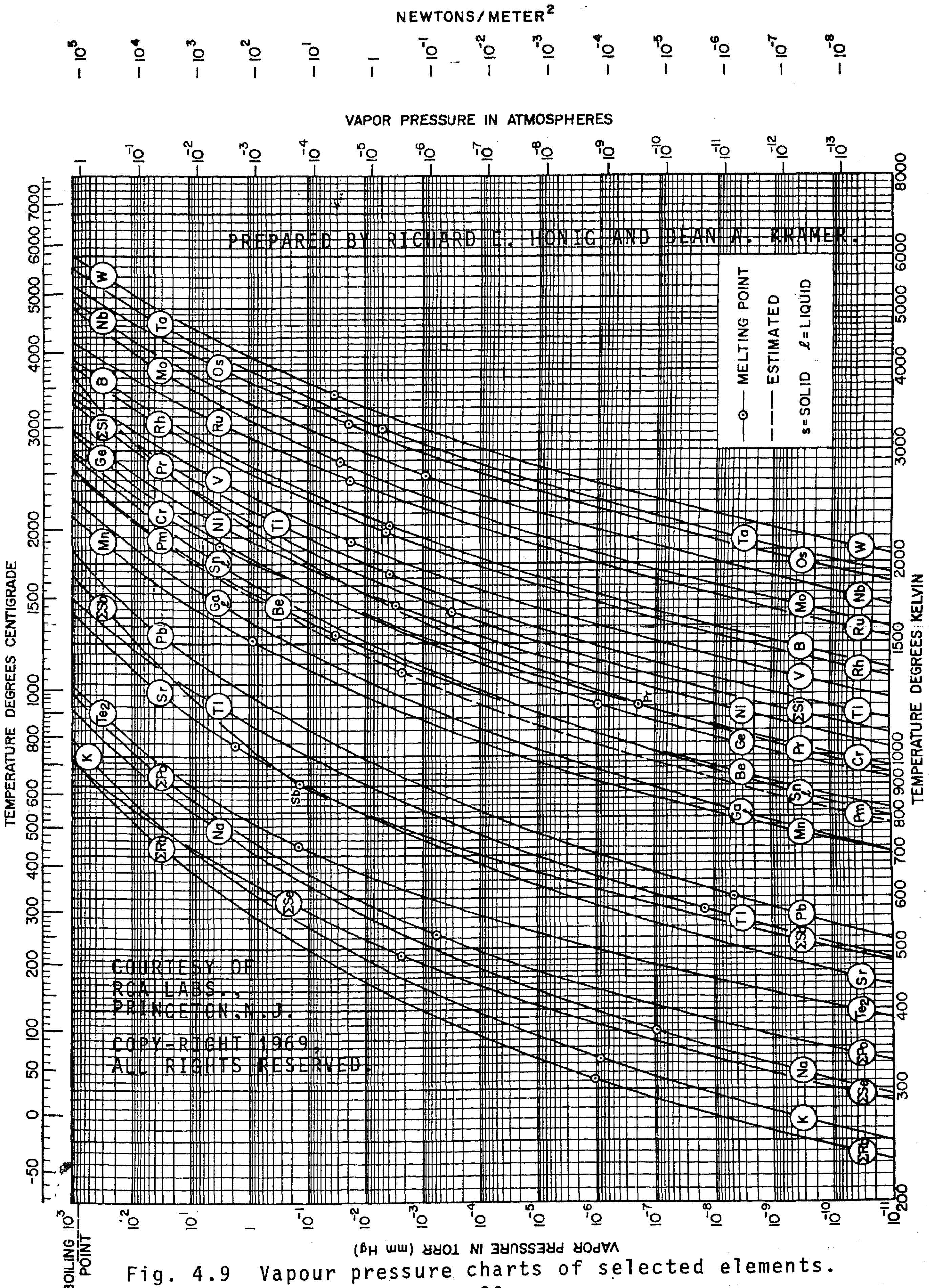

Fig. 4.9 Vapour pressure charts of selected elements.

Temperature (^{o}C)	Vapour Pressure (torr)
900	7×10^{-4}
950	2×10^{-3}
1000	4×10^{-3}
1100	3×10^{-2}
1200	1.5×10^{-1}
1300	5×10^{-1}
1400	2
1500	4
1600	10

Noting the above, the following observations can be made:

1. At $900^{o}C$, the vapour pressure of the gallium in the crucible is only marginally greater than the chamber pressure ($1 - 5 \times 10^{-4}$ torr), so only very little evaporation can be expected.
2. For ICB system, the vapour pressure in the crucible P_o have been reported(55) to be in the range 10^{-2} to 10 torr. This suggests that the crucible temperature should at least be $1100^{o}C$ for gallium nitride deposition.
3. For ICB systems, the ratio of the pressure inside the crucible to that outside the crucible ($p_o/P_{chamber}$) is required to be at least 10^4 to 10^5 as detailed in the earlier part of this thesis.

Since in our experiments (and those reported by Takagi and Matsubara for GaN deposition) the nitrogen pressure in the

chamber was in the 10^{-4} torr range, the gallium vapour pressure required in the crucible would be in the 1 to 10 torr range. This corresponds to a crucible temperature of 1,400°C to 1,600°C.

Based on the above information and the very low deposition rate obtained in the runs that have been attempted so far, we can confidently conclude that a crucible temperature of 900°C is too low for GaN deposition and that future runs should be attempted at higher crucible temperatures, preferably in the range 1,350°C to 1,600°C.

C. The Contamination Problem

Surface analysis of the film obtained in the last run (No. 11) was made at the RCA Laboratories in Princeton, New Jersey. As mentioned earlier, this analysis showed that the film was rich predominantly in boron and nitrogen. Further expermental work by C. Mehta, a graduate NJIT student, during the writing of this thesis revealed that the main source of trouble was water vapour trapped in the boron nitride crucible and heaters. Boron nitride, when exposed to the atmosphere, quickly absorbs moisture present. This trapped water vapour can cause the boron nitride to decompose at elevated temperatures introducing additional reactive contaminants at the substrate and preventing the deposition of pure gallium. The problem can be solved by driving out the water vapour, which can be done in two steps:

- Heating the boron nitride in an oven at 150 - 200°C for approximately four hours to drive most of the water vapour out.
- Then final low temperature (150 - 200°C) annealing in vacuum will drive out the remaining traces of water vapour.

D. Final Remarks

Although our attempts to grow GaN films by the ICB deposition technique at the NJIT Microelectronics Lab. were not yet successful, experimental work is being continued and refinements are constantly introduced based on the wealth of experience gained through the work reported in this thesis. The main objectives of the present work were:

First Stage:-

The deposition of high quality GaN films using the ICB technique and the determination of the optimum values of control parameters (such as Ionization current, I_e; Crucible temperature; Nitrogen Pressure; Substrate temperature ; etc.) that will ensure consistently reproducible results.

Second Stage

Introducing dopants to the GaN films and the fabrication of Metal - Insulator - Semiconductor (MIS) Light

Emitting Diodes (LED's).

Assuming that successful, reliably reproducible results are obtained in the first two stages, work should then be directed to investigating the possibility of commercializing the ICBD method of fabricating GaN LED's and extending the method to the fabrication of multi-colored solid state display units as suggested by Dr. J. I. Pankove[29]. The technique would utilize GaN crystals both as blue light emitting diodes (LED's) and as convenient transparent supports for mounting LED's emitting other colors as discussed in section 4.1 .

A P P E N D I X   A

MACHINE SHOP DRAWINGS FOR THE

PARTS USED IN CONSTRUCTING THE

ICB SYSTEM AT NJIT.

(Figures A.1 through A.13 attached)

BASE

(4) #7 Drill

(4) $\frac{3}{8}$ Drill

5

2.15

1.43

1.81

1.38

5

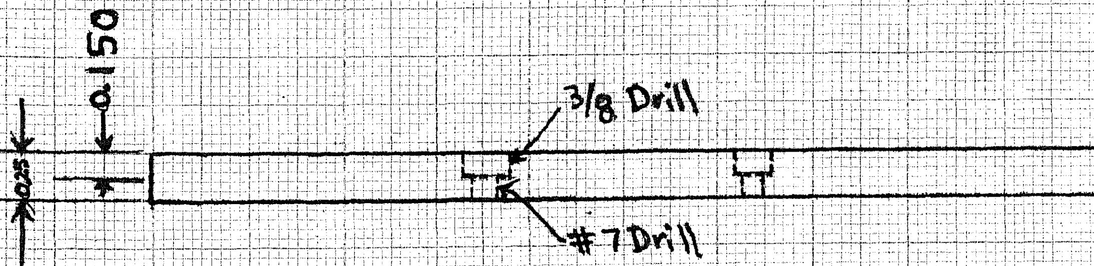

MTL. SS

Fig. A.1 System Base.

Base Plate

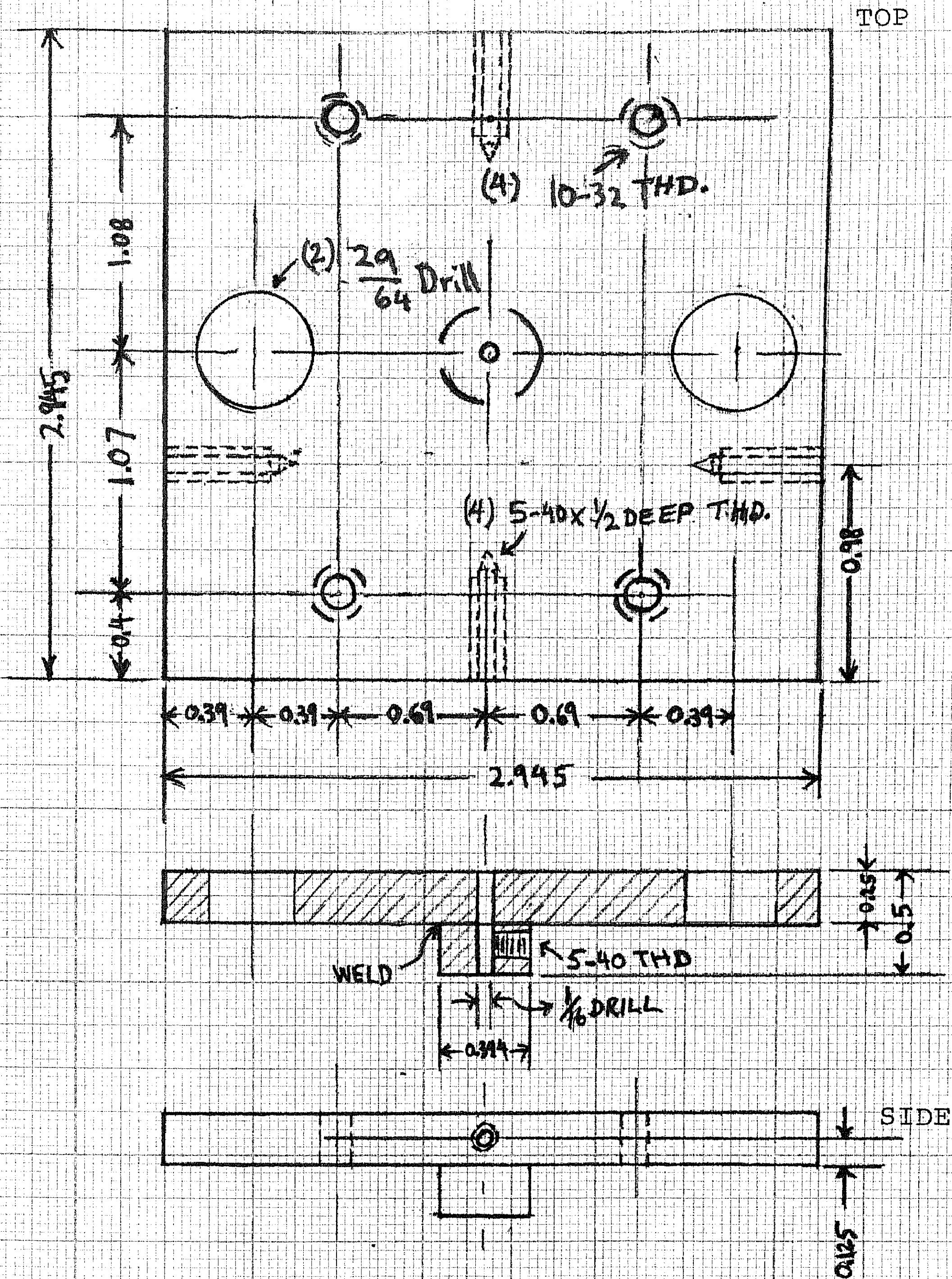

Fig. A.2 Nozzle Assembly Baseplate.

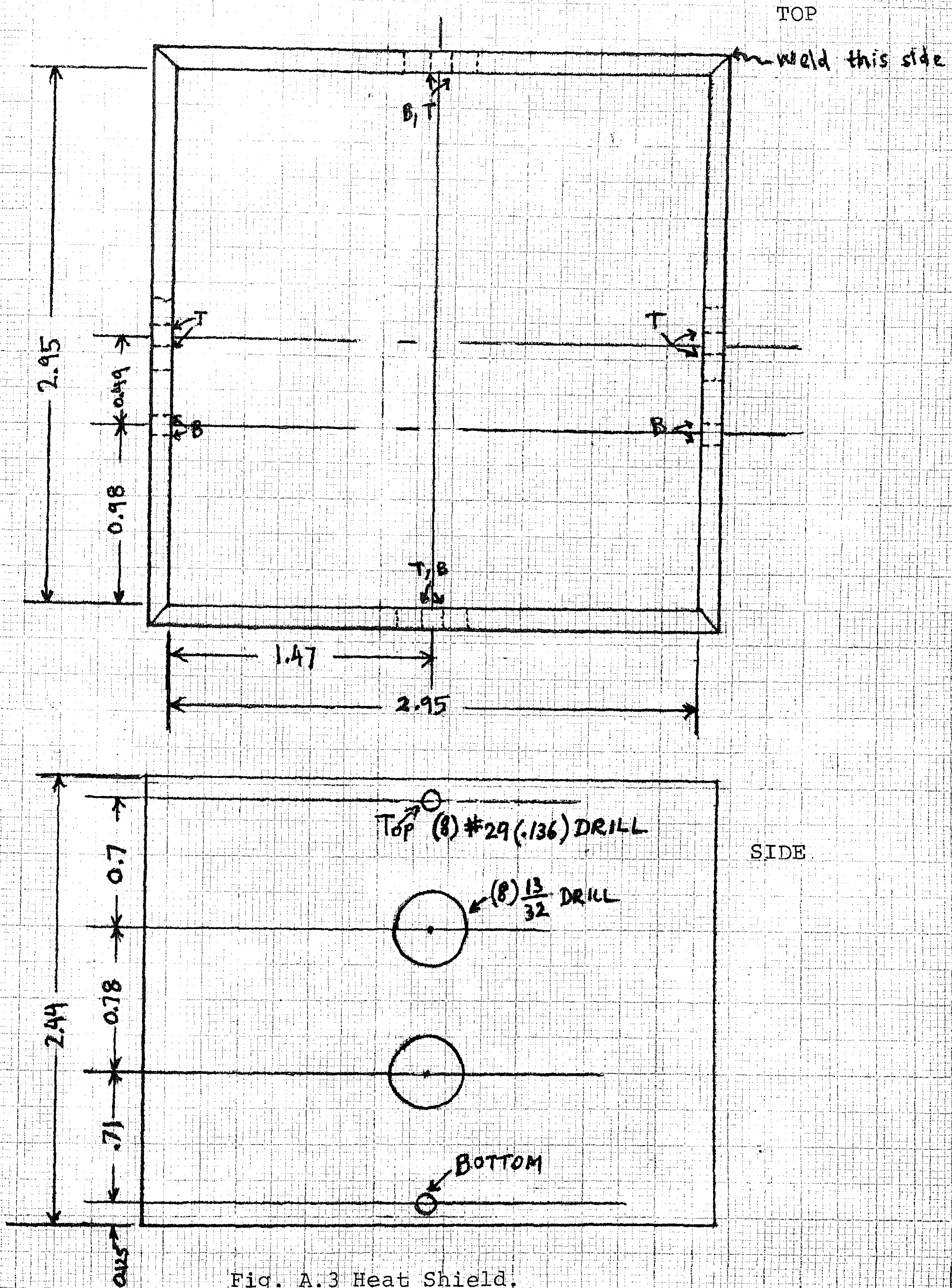

Fig. A.3 Heat Shield.

TOP PLATE

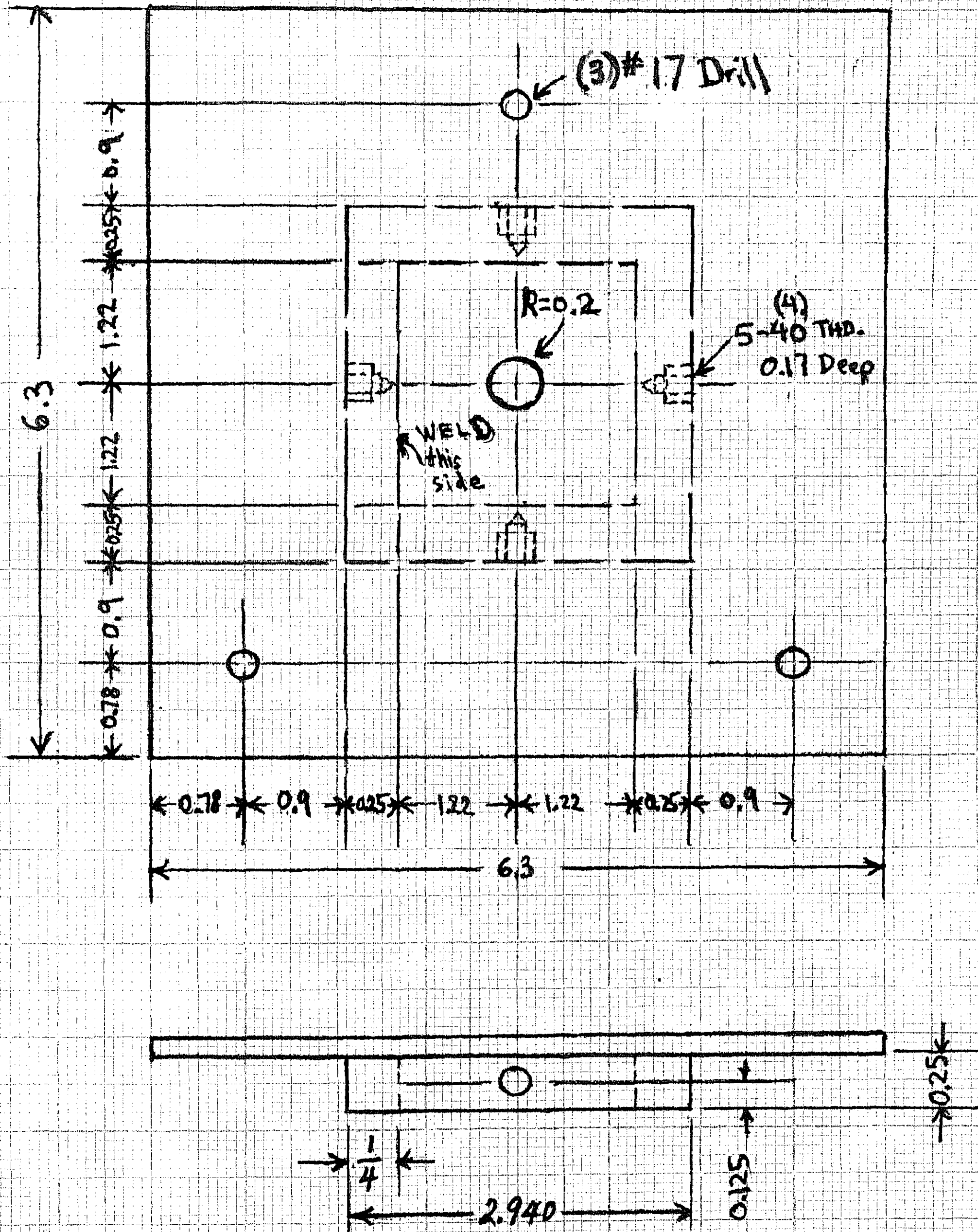

Fig. A.4 Nozzle Assembly Top Plate.

IONIZATION BASE PLATE

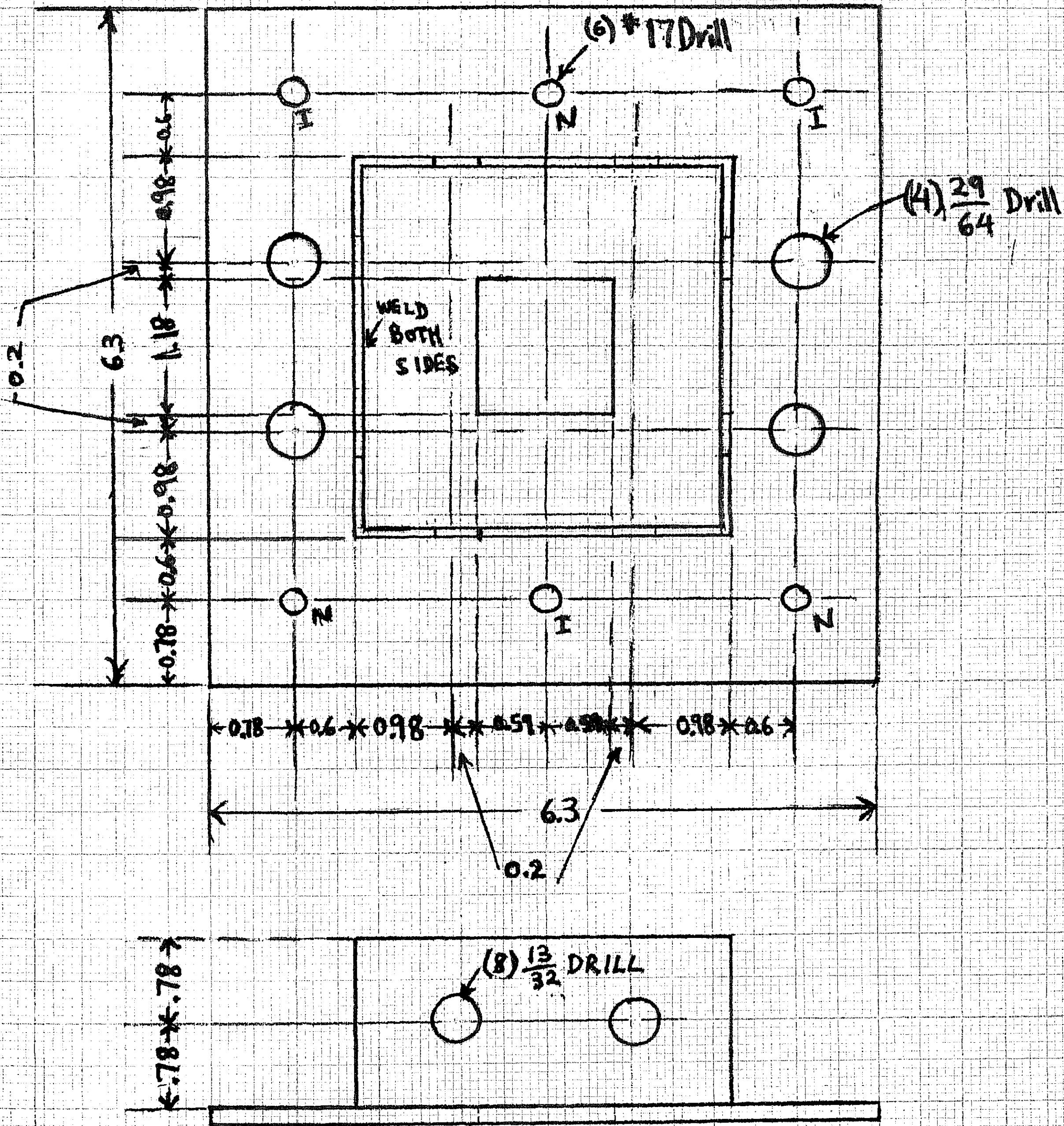

Fig. A.5 Ionization Assembly Baseplate.

ANODE UPPER PLATE

Fig. A.6 Anode upper plate.

ANODE LOWER PLATE

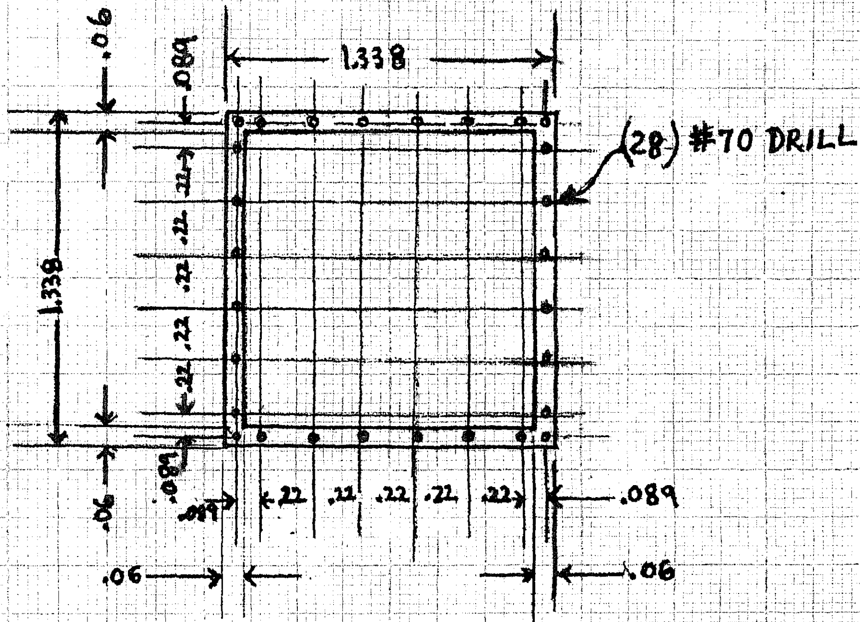

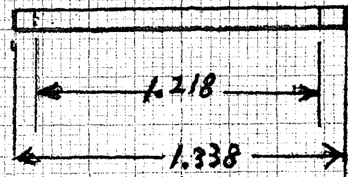

Fig. A.7 Anode Lower Plate.

1- ANODE HOLDER

2- ACCELERATION ELECTRODE

3- SUBSTRATE HOLDER

(3) REQUIRED.

NUB ON ONE PIECE ONLY

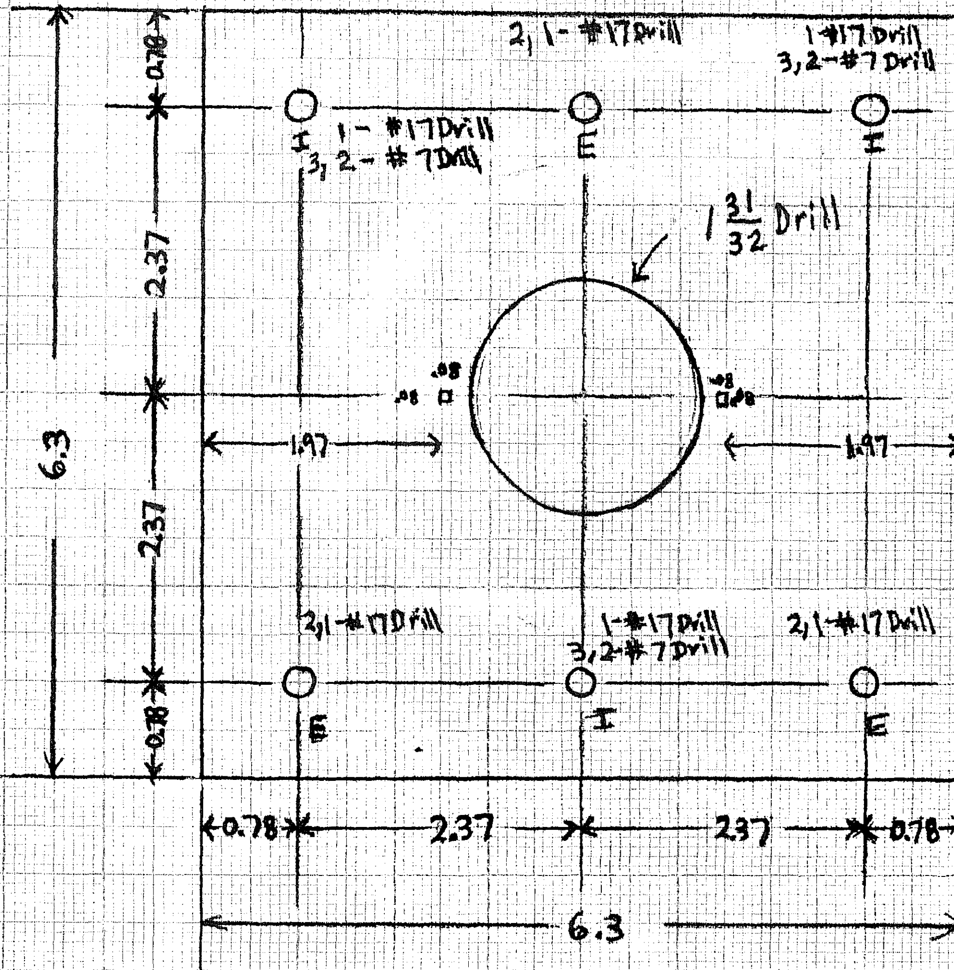

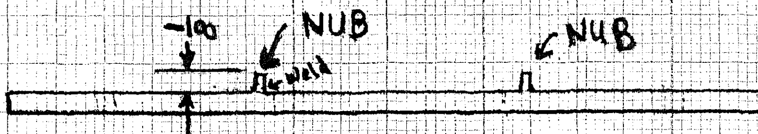

Fig. A.8 Anode Holder, Substrate holder and Acceleration Electrode.

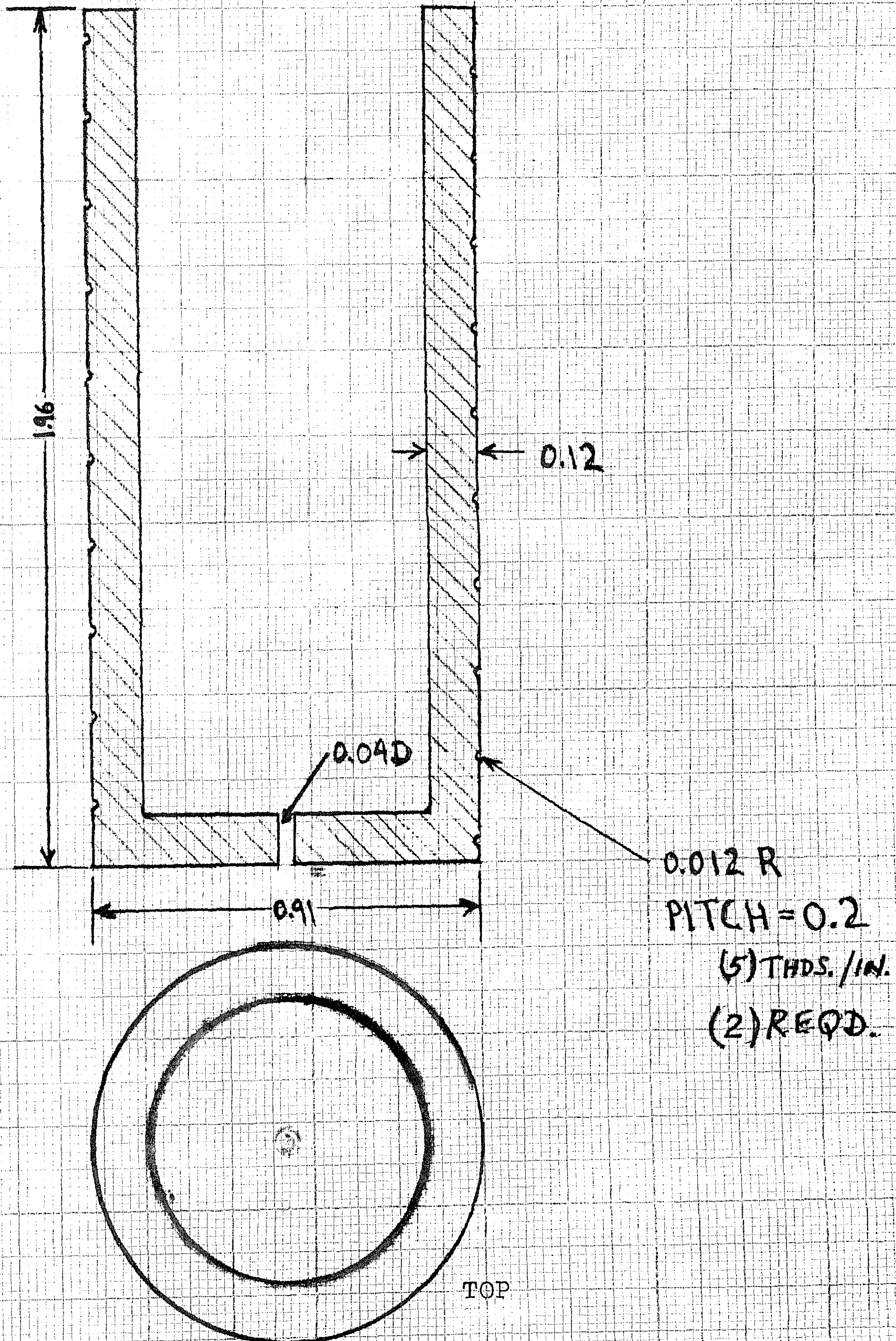

Fig. A.9 Crucible Heater

CRUCIBLE

MATERIAL: BORON NITRIDE

(2) REQD

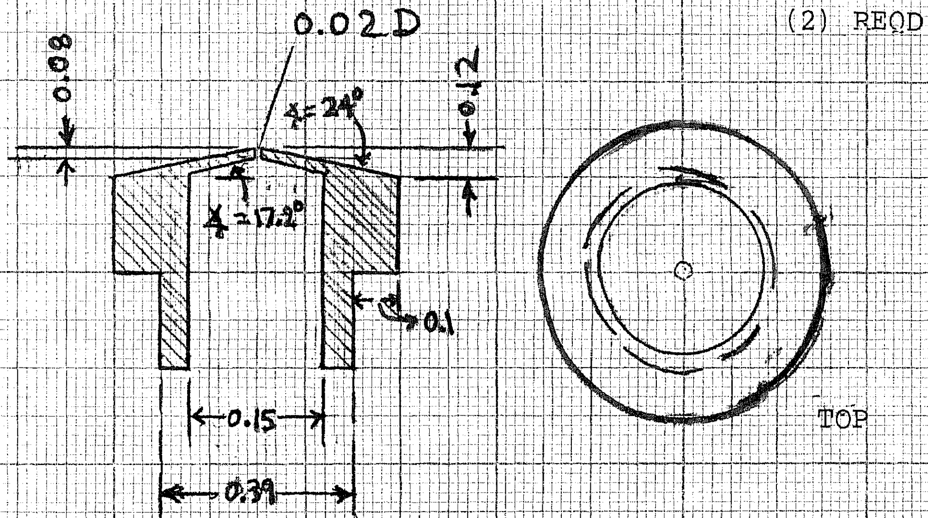

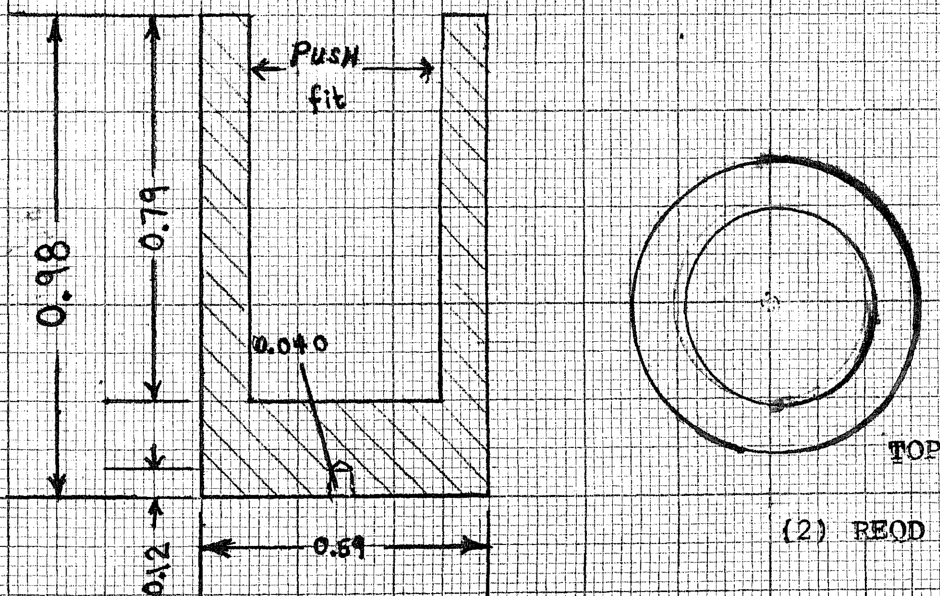

(2) REQD

Fig. A.10 Crucible.

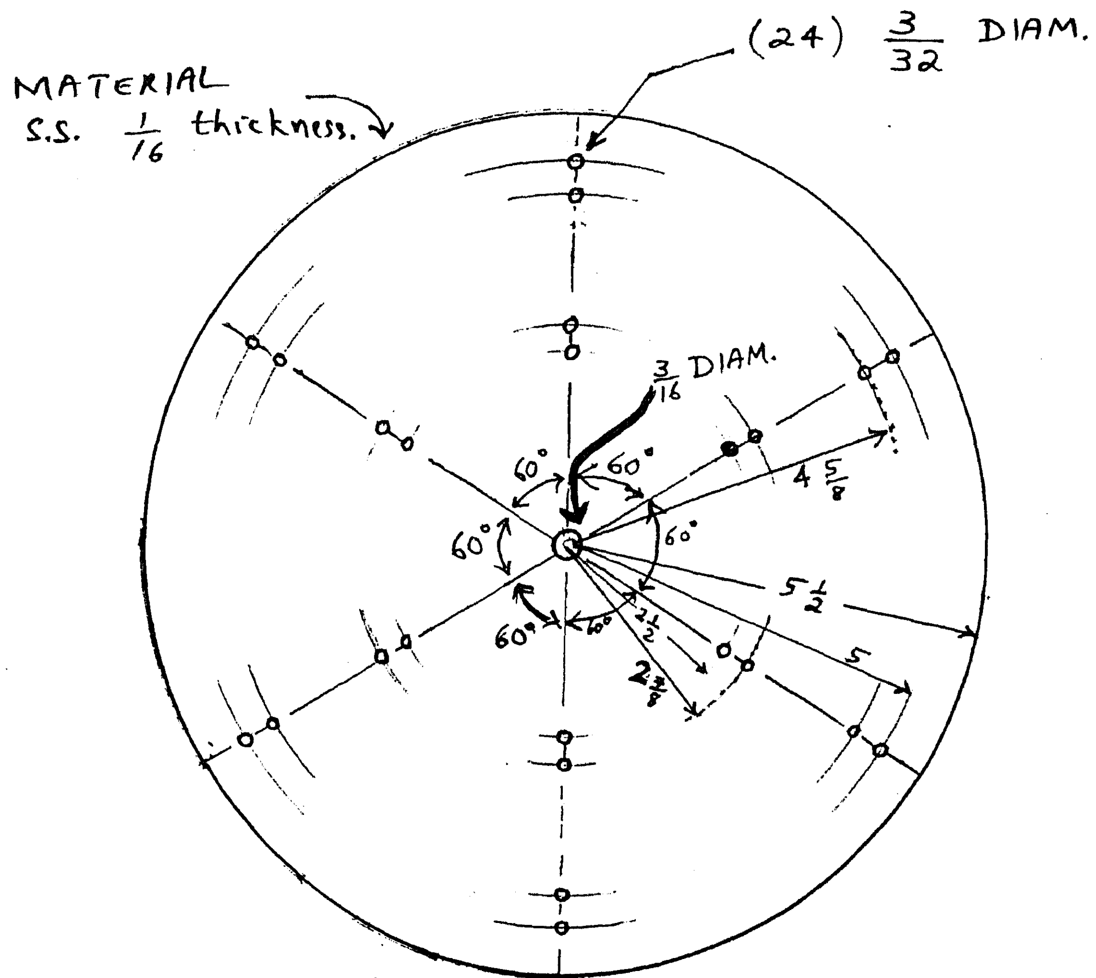

Fig. A.11 Rotating plate of the rotating substrate holder.

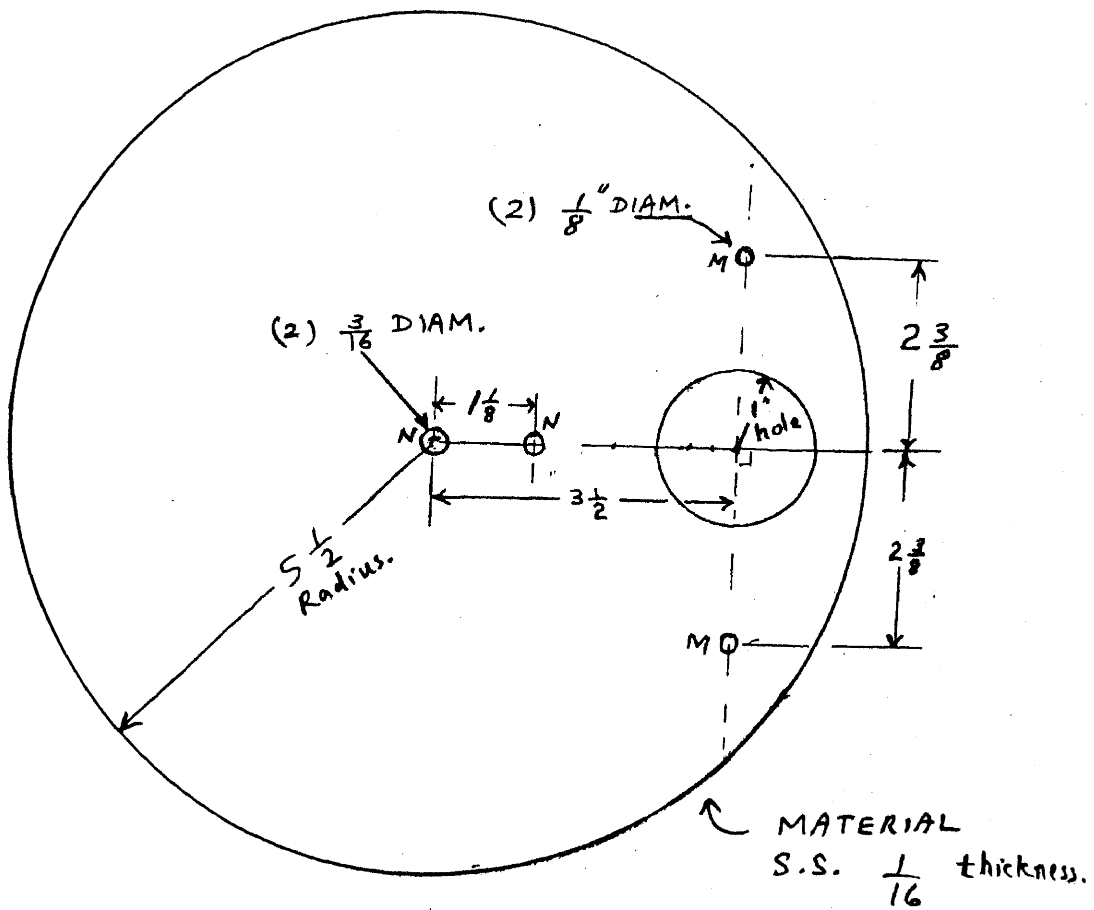

Fig. A.12 Stationary plate of the rotating substrate holder.

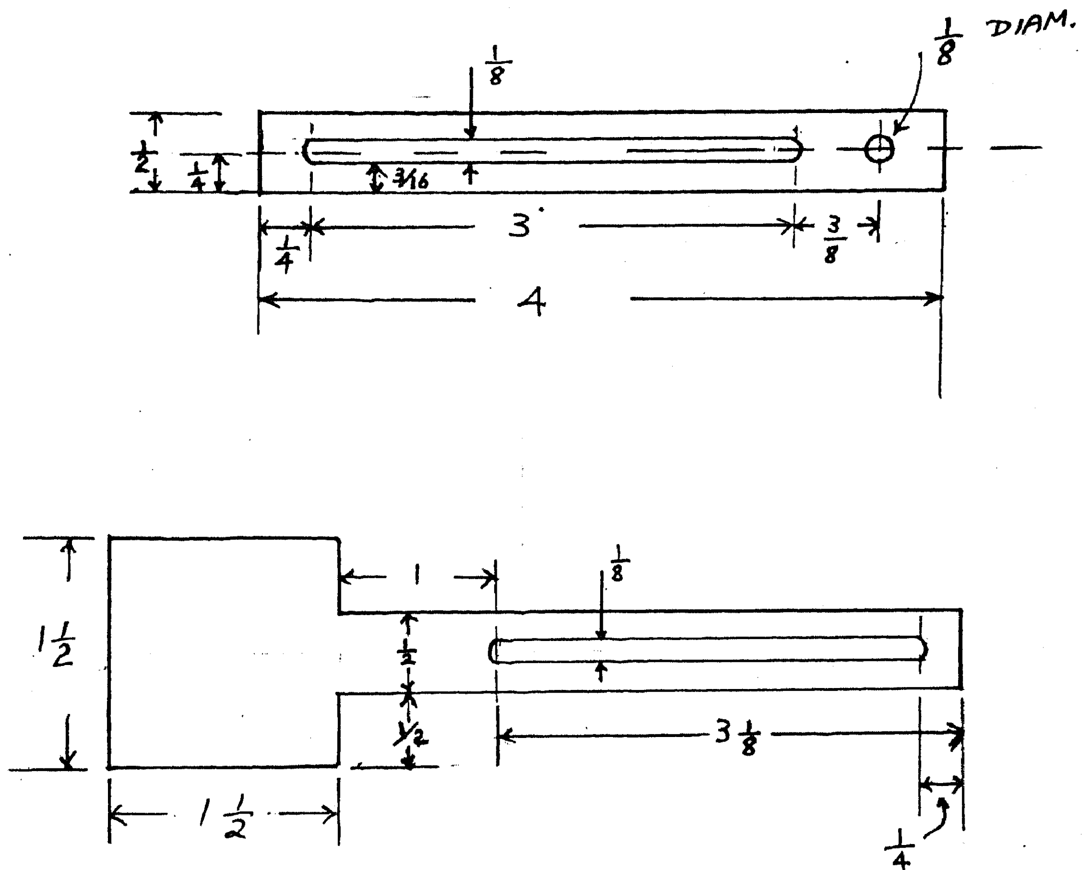

Fig. A.13 Parts for the shield (shutter).

A P P E N D I X   B

INTERNAL WIRING DIAGRAMS FOR THE DC, HIGH VOLTAGE, VARIABLE POWER SUPPLIES USED FOR V_e AND V_a.

(Figures B.1 and B.2 attached)

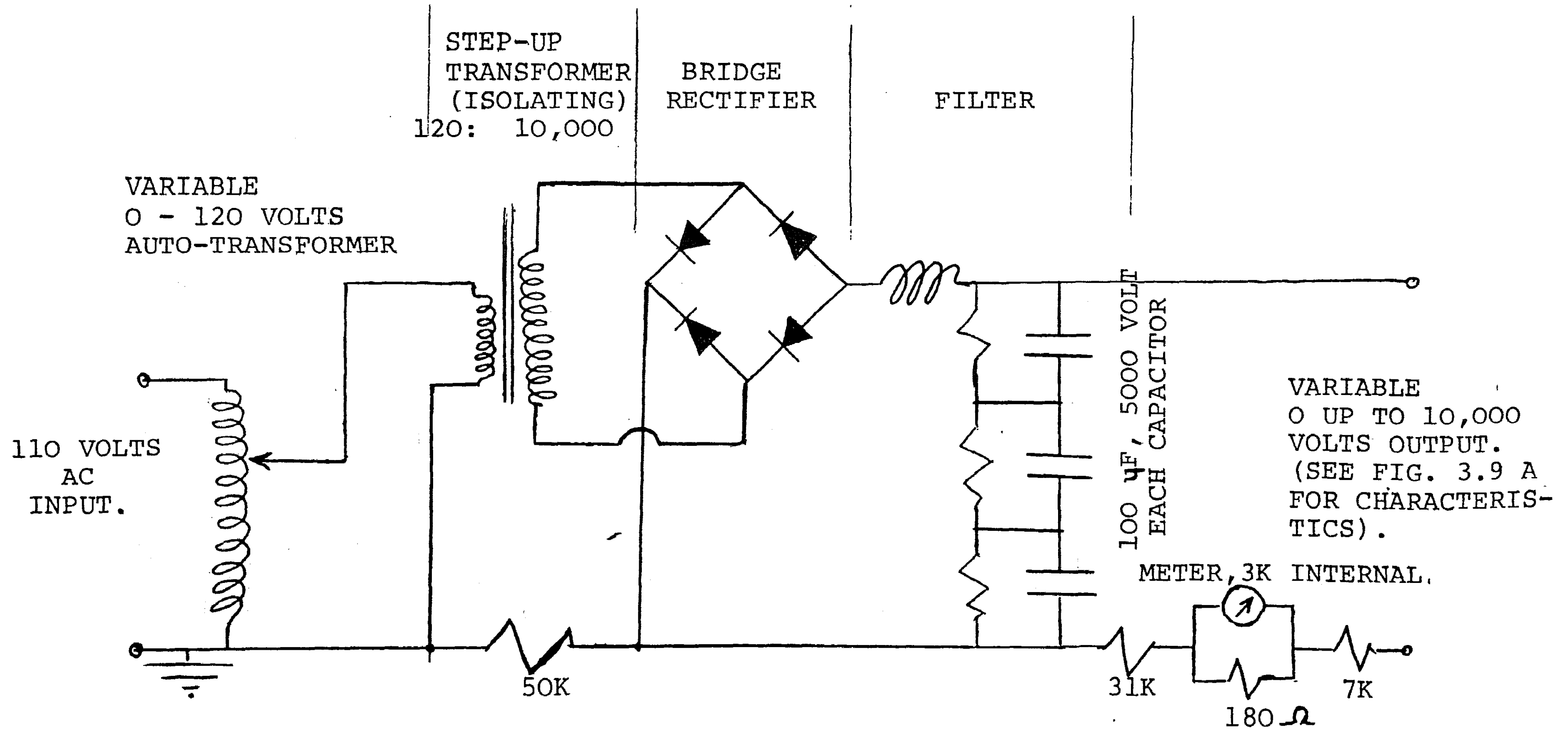

Fig. B.1 Internal wiring diagram for the DC variable power supply used for V_e.

NOTES: - Existing, internally made power supply was utilized.
- Ratings not shown above were not readily available.

PART OF THE CIRCUITS OF AN ELECTRON BEAM POWER SUPPLY (AIRCO MODEL ES6 - 110/210) WAS UTILIZED TO GENERATE THE DC HIGH VOLTAGE, V_a, VARIABLE FROM ZERO TO 10 KV.

THE APPLICABLE WIRING DIAGRAM (AIRCO, CALIFORNIA, DRAWING REFERENCE NO. 2F 6055) IS ATTACHED, AND THE FOLLOWING MODIFICATIONS WERE MADE :-

(1) FUSES F 201, F 202 AND F 203 WERE REMOVED, ISOLATING THE ENTIRE BOTTOM SECTION OF THE DIAGRAM.

(2) THE KEYLOCK SWITCH, S 101 WAS SET IN AN OPEN CIRCUIT POSITION.

(3) AN EXTERNAL CONTROL WIRE WAS CONNECTED TO THE TOP SIDE OF S 101, GIVING 110 VOLT CONTROL VOLTAGE TO ACTIVATE THE STARTING MECHANISM.

(4) TUBE V 201 WAS REMOVED AND REPLACED WITH A SIMPLE LINK.

(5) THE POWER SUPPLY WAS ENERGISED THROUGH A THREE PHASE AUTO TRANSFORMER CAPABLE OF PROVIDING A CONTINUOUSLY VARIABLE OUTPUT (3 PHASE) BETWEEN ZERO AND 208 VOLTS.

(6) TRANSFORMER T 204 WAS UTILIZED AS THE ISOLATING TRANSFORMER I. T. 2 IN FIG. 3.6 . THE INPUT TERMINALS H1 AND H2 WERE BROUGHT OUT AND FED THROUGH A VARIABLE VOLTAGE, 0-240 VOLTS . THE OUTPUT TERMINALS X1 AND X2 WERE EXTENDED OUT USING A HIGH VOLTAGE (15 KV PEAK), HIGH CURRENT (TO 30 AMPS) CABLE.

Fig. B.2. Internal wiring diagram for the high voltage, DC, power supply used for V_a. (Above notes should be read in conjunction with the wiring diagram on page 114 A attached).

R E F E R E N C E S

1. Abraham, F.F., Homogeneous Nucleation Theory, Academic Press, New York, (1974).

2. Anderson, J.B., Gas Dynamics, Vol. 4, Dekker New York, (1974).

3. Anderson J.B., Molecular Beams and Low Density Gas Dynamics, Ed. P.P. Wegener, Dekker, New York, (1974).

4. Chopra, K.L., J. Appl. Phys. Letters 7 (1965) 140.

5. Chopra, K.L., and Randlerr, M.R., J. Appl Phys. 39, (1968), 1874.

6. Cornely, R.H., Personal Communication.

7. Dingle, R., Shaklee, K.L., Leheny, R.F. and Zetterstrom, R.B., "Stimulated Emission and Laser Action in Gallium Nitride," Appl. Phys. Lett., 19, P. 5, (1971).

8. Farges, J., Homogeneous Nucleation in a Free Argon Jet: Observation of Clusters by Electron Diffraction, J. of Cry. Groth 31 (1975 79- 96.

9. Farrow, R.P.C., Cullis, A.G., Grant, A.J. and Jones G.R., Molecular Beam Expitaxy and Field Emission Depositionfor Metal Film Growth on III-V Compound Semiconductors - A Comparative Study : Thin Solid Films, 58 (1979) 189 - 196

10. Grimmeiss, H.G., Groth R., and Maak, J., Naturforsh, Z., 15a, pp. 799, (1960).

11. Hagena, O.F., and Obert, W.: Cluster Formation in Expanding Supersonic Jets : Effect of Pressure, Temperature, Nozzle Size, and Test Gas : The Journal of Chemical Physics, Vol. 56 Number 5, (1972).

12. Itoh, T., Nakamura, T. Muromachi, M., and Sugiyama, T., J. Appl Phys. 16 (1979) 553.

13. Kisicki, B.B., and Kahnag, D., J. Vac. Sci. 5 (1970) 1102.

14. Kuiper, A.E.T., Philips Tech. Note No. 203/75.

15. Martinelli, R.U., and Pankove, J.I., "Secondary Electron Emmission from GaN : C - O Surface," Appl. Phys. Lett., 25, 549 (1974).

16. Maruska, H.P., and Tietjer, J.J., "The Preparation and Properties of Vapor - Deposited Single Crystalline GaN", Appl. Phys. Letters, Vol. 15, P. 327 (1969).

17. Matsubara, K., and Takagi, T., C - 4 - 8 Film Growth of GaN. onto C - axis Oriented ZnO Films using R - ICB Technique and its Application to thin Film Devices, Digest of Tech. Papers, Proc. of the 14th International Conf. On Solid State Devices, Tokyo, (1982).

18. Matsubara, K., Horibe, T., Takaoka, H., and Takagi, T., Electrical Properties of GaN Light - Emitting Diodes Made by the R-ICB Technique, Proc. of the 4th Symposium on Ion Sources and Ion Application, J. of Cry Growth 33 (1976) 77 - 89.

19. Morimoto, K., Watanabe, H. and Itoh, H. : Ionized Cluster Beam Epitaxial Growth of GaP. Films on GaP and SiSubstrates, J. of Cry. Growth 45 (1978) 334 - 339.

20. Namba, Y., and Mori, T., Epitaxial Growth of ZnTe On NaCl By Ion Deposition, Thin Solid Films, 39 (1976) 119-123.

21. Owen, P. L., and Thronhill, C. K., Aeronaut. Res. Council, Gr. Britain, R and M (1948) 2616.

22. Pankove, J. I., "Luminescence in GaN.", J. Luminescence, 7, P. 114, (1973).

23. Pankove, J. I., Schade, H., "Photoemission From GaN.", Appl. Phys. Lett., 25, P.53 (1974).

24. Pankove, J. I., and Norris, P. E., RCA Review 33 (1972) 377.

25. Pankove, J. I., Personal Communication.

26. Pankove, J. I., Bloom, S. and Harbeke, G., Optical Properties of GaN., RCA Review Vol. 36 March (1975).

27. Pankove, J. I., Luminescence in GaN., J. of Luminescence Volume 7, (1973).

28. Pankove, J. I., Blue - Green Numeric Display using Electroluminescent GaN., RCA Review Vol. 34, No. 2 June (1973).

29. Pankove, J. I., Low - Voltage Blue Electroluminescence in GaN., IEEE Transactions on Electron Devices, Vol. ED - 22, No. 9, September(1975).

30. Pankove, J. I., and Lampert, M. A., Model for Electroluminescence in GaN. : Physical Review Letters, Volume 33, No. 6, 5 August (1974).

31. Pankove, J. I., Optical Processes in Semiconductors, Dover Publication, N.Y., New York (1975)- P. 249.

32. Reichelt, K., Transmission Electron Microscopy Study of Cluster Growth of Epitexial and None-pitaxial Copper Film on Musconile MICA, J. of Cry. Growth 33 (1976) 77 - 89.

33. Sedney, R., Gas Dynamics, Vol. I Part II (Dekker, New York, 1970).

34. Stein, Gilbert D., Atoms and Molecules in Small Aggregates - The Fifth State of Matter, Seminar, Yale University (1979).

35. Takagi, T., Yamada, I., Sasaki, A., J. Vac., Sci, Technol., 12 (1975) 1158.

36. Takagi, T., Yamada, I., and Sasaki, A., J. Vac., Sci, Technol., 12 (1975) 1128.

37. Takagi, T., Yamada, I., and Sasaki, A., Conf. On Ion Plating and Allied Techniques, Edinburg (1977).

38. Takagi, T., Yamada, I., and Sasaki, A., Inst. Phys. Conf. Ser. 38 (1978) 229.

39. Takagi, T., Matsubara, K., Takaota, H., and Yamada, I., Proceeding of Int. Conf. on Ion Plating and Allied Technique, (IPAT 1979). (Spectrum Printing Co, Edinburg, 1979) P 194.

40. Takagi, T., Role of Ions in Ion - Based Film Formation, Paper by Ion Beam Engineering Experimental Laboratory Kyoto University.

41. Takagi, T., Yamada, I., Sasaki, A., Itoh, S., Mori, H., Morimoto, H., Kodama, M., Ozawa, M., Photovoltaic Characteristics of Photo - Cells by Ionzed - Cluster Beam Deposition and Epitaxy, Proc. of the 2nd Int. Conf. on Solid State Devices, Tokyo, Japan September 1 - 3 (1976).

42. Takagi, T., Yamada, I., Yanagawa, K., Kunori, M., and Kobiyama S., Proc. of the Sixth Int. Vaccum Congress, Japan March 2-29 (1974).

43. Takagi, T., Yamada, I., Matsubara, K., and Takaoka, H., Ionized - Cluster Beam Epitaxy, J. of Cry. Growth 45 (1978) 318 - 325.

44. Takagi, T., Yamada, I., and Sasaki, A., Ionized - Cluster Beam Deposition and Epitaxy as Fabrication Techniques for Electron Devices. Thin Solid Films 45 (1977) 569 - 576.

45. Takagi, T., Yamada, I., and Sasaki, A., Preparation of Semiconductor Devices by Ionized - Cluster Beam Deposition and Epitaxy, Proc. of the IEEE Int. Electron Devices Meeting, December 6-8 (1976) Washington, D.C. U.S.A.

46. Takagi, T., Yamada, I., and Sasaki, A., The Structure and Properties of Metal and Semiconductor Films Formed by Ionized - Cluster Beam Deposition Technique, Proc. of the Int. Conf. on Metallurgical Coating, April 1976, San Francisco.

47. Takagi, T., Yamada, I.m and Sasaki, A., Ionized - Cluster Beam Deposition, J. Vac. Sci. Technol., Vol. 12, No.6, Nov./Dec. (1975).

48. Takagi, T., Yamada, I., and Kimura, H., Iron Surface Treatment by Boron Implantation, Proc. of the Int. Conf. on Ion Implantation in Semiconductors and other materials, Osaka, Japan, August 26 - 30 (1974).

49. Takagi, T., Yamada, I., Kupori, M., and Kobiyama, S., Vapurized Metal Cluster Ion Source For High Intensity Ion Beam Applications : Proc. of the 2nd Int. Conf. On Ion Sources, CSGAE, Vienna, (1972) P. 790.

50. Takagi, T., Yamada, I., and Sasaki, A., An Evaluation of Metal and Semiconductor Films Formed by Ionized - Cluster Beam Deposition, Thin Solid Films, 39 (1976) 207 - 217.

51. Theeten, J. B., Madar, Mircea, Roussel, Rocher and Laurence, G., J. Cryst. Growth to be Published.

52. Theeten, B., Madar, R., Mircea - Roussel A., Rocher, A., and Laurence, G., J. of Crys. Growth, 37 (1977) 317 - 328.

53. Usui, H., Takaoka, H., Yamada, I., and Takagi, T., Formation of Ionized Cluster Beam, Proc. of the Symp. on Ion Sources and Ion Appl. Technol., Tokyo, (1980), (IEE of Japan , 1980) P. 65.

54. Weissmantel, Chr. Proc. of 7th Intern. Vac. Congr. and 3rd Intern. Conf. on Solid Surf., Vienna, (1977), (F. Berger and Sohne , Vienna, 1977) P. 1553.

55. Yamada, I., Takagi, T., Vapurized - Metal Cluster Formation and Ionized - Cluster Beam Deposition and Epitaxy, 3rd International Conference on Ion and Plasma Assisted Techniques, Netherlands, (1981).

56. Yamada, I., Takaoka, H., Inokawa H., Usui, H., Cheng, S. C. and Takagi, T., Vaporized - Metal Cluster Formation and Effects of Kinetic Energy of Ionized Clusters on Film Formation., Kyoto University, Japan.

57. Yamada, I., Matsubara, K., Kodama, M., Ozawa and Takagi, T., Characteristics of Thin Films Formed by the Ionized - Cluster Beam Technique, J. of Cry. Growth 45 (1978) 326 - 331.

****